ESTABLISHMENT AND MAINTENANCE OF PARASEGMENTAL COMPARTMENTS

by

Sarah Campbell Hughes

A thesis submitted in conformity with the requirements

for the degree of Doctor of Philosophy

Graduate Department of Molecular and Medical Genetics

University of Toronto

Establishment and maintenance of parasegmental compartments. A thesis submitted in conformity with the requiremetns for the degree of Doctor of Philosophy ©2001 by Sarah Campbell Hughes. Grauduate Department of Molecular and Medical Genetics. University of Toronto.

Abstract

Embryos of higher metazoans are divided into repeating compartments early in development. In *Drosophila*, the earliest boundaries are formed by the parasegments, which are coincident with the early expression patterns of two pair-rule genes, *fushi-tarazu* (*ftz)* and *even-skipped* (*eve*). Expression of *ftz* defines the even-numbered parasegments, whereas as *eve* defines the odd-numbered parasegments. I used genetic methods to selectively raise or lower the expression levels of *ftz* and/or *eve,* and the effect on the positioning of parasegment boundaries was determined. I found that the relative levels of *ftz* and *eve*, but not their absolute levels, determined where the borders were positioned. Altered parasegment boundary position produced alternating parasegments of enlarged and reduced sizes. I found that these boundary positions display only a modest ability to revert back to normal widths. Later in development, parasegments enlarged by 30% or more remained enlarged while parasegments that were narrowed by the same amount were lost. Loss of the reduced parasegments occured predominantly by delamination from the epithelial layer followed by cell death.

Acknowledgements

I would like to acknowledge some of the people who made this work possible. First of all my superviosr Dr. Henry Krause for providing a wonderful environment in which I could work and gain the confidence to become an independent researcher. My committee Dr. Derek Van der Kooy and Dr. Brenda Andrews for pushing me and my research to a higher level. I would also like to particularly thank many members of the Krause lab including Andrew Simmonds, Andrzej Nasiadka, Heidi Sampson, and Gilbert dosSantos for everything from being sounding boards for ideas to providing friendship, daily entertainment, and support. These people made the lab a fun place to work. I also thank Angela Pearson and Philippa Bridge-Cook whose friendship and support are most appreciated and treasured. Thanks to Deb Willumsen for her support and for listening to my rants and worries. I also indebted to my family who always supported and believed in me and assisted me when I needed it most. Additionally I thank Bill, Sheila and Ainslie Simmonds for their assistance and support in so many ways. I would also like to thank Dr. Micheal Crump and Dr. Richard Tsang and all the wonderful nursing staff at the Toronto General and Princess Margaret Hospital for helping me to beat cancer and stick around to be able to reach this day.

Lastly and most importantly I want to thank Andrew Simmonds, my best friend , most ardent supporter, cheerleader, proofreader, and MKW for everything.

Table of Contents

List of Figures

List of Appendices

List of Abbreviations

A1	first abdominal segment
A2	second abdominal segment
A3	third abdominal segment
A4	fourth abdominal segment
A5	fifth abdominal segment
A6	sixth abdominal segment
A7	seventh abdominal segment
A8	eighth abdominal segment
A/P	anterior-posterior
AEL	after egg laying
AP	alkaline phosphatase
ATP	adenosine-triphosphate
BCIP	5'bromo-chloro-indol phosphate
BSA	bovine serum albumin
CCD	charge coupled device
CTP	cytosine-triphosphate
CY2	cyanine dye (Absorption 492, Emission 510)
CY3	cyanine dye (Absorption 550, Emission 570)
CY5	cyanine dye (Absorption 650, Emission 670)
DAB	diamino-benzine
DABCO	1,4-Diazabicyclo[2.2.2]Octane
DIG	digoxigenin
DNA	deoxyribonucleic acid

DNAse	deoxyribonuclease
D/V	dorsal/ventral
DTT	dithiothreitol
dNTPs	deoxy-nucleotide-triphosphates
dUTP	deoxy-uracil-triphosphate
EDTA	ethylenediaminetetracetic acid
FISH	fluorescent in situ hybridization
FITC	fluorescein isothiocyanate (Absorption 492, Emission 520)
GAL4	*Gal4* binding domain of yeast
GTP	guanosine-triphosphate
H	heavy chain
hsp70	heat shock 70 promoter
HS	heat shock
HYB	hybridization solution
IgG	immunoglobulin g
kb	kilobase
L	light chain
LiCl	lithium chloride
LSCM	laser scanning confocal microscope
$MgCl_2$	magnesium chloride
ML	multiple labeling
mRNA	messenger ribonucleic acid
NaOH	sodium hydroxide

NBT	nitro-blue tetrazolium
PBS	phosphate buffered saline
PBT	1 X phosphate buffered saline + 0.1% Tween 20
PBTB	1 X phosphate buffered saline + 0.1% Tween 20 + 0.5% skim milk powder
PBTBB	1 X phosphate buffered saline + 0.1% Tween 20 + 0.5% skim milk powder + 0.05% BSA
PCR	polymerase chain reaction
SSC	3M NaCl, 0.3M Sodium Citrate, pH 7.0
T1	first thoracic segment
T2	second thoracic segment
T3	third thoracic segment
Taq	*Thermus aquaticus*
Tris-HCL	tris-hydroxmethyl aminomethane hydrochloride
tRNA	transfer ribonucleic acid
UAS	upstream activation sequence

List of *Drosophila* Genetic Symbols

bcd	*bicoid*
CyO	*Curly of Oster*, second chromosome balancer
en	*engrailed*
eve	*even-skipped*
eve^{ID19}	*even-skipped* hypomorphic temperature sensitive allelle
ftz	*fushi tarazu*
ftz^{5}	*fushi-tarazu* hypomorphic temperature sensitive allele
hh	*hedgehog*
nkd	*naked*
odd	*odd-skipped*
opa	*odd-paired*
prd	*paired*
ptc	*patched*
run	*runt*
slp	*sloppy-paired*
Ubx	*Ultrabithorax*
Ual	*Ultra abdominal-like*
wg	*wingless*

List of Symbols

α	alpha
β	Beta
°C	degree Celsius
μ	micro
g	gram
g	gravitational force
l	litre
m	milli

CHAPTER 1: INTRODUCTION TO DROSOPHILA DEVELOPMENT AND COMPARTMENTS

A fundamental feature of invertebrate and vertebrate embryos is the division of the major body axis into serially repeating groups of cells or segments. This body architecture is very apparent in the external features of invertebrates such as insects, and in the central nervous system and associated structures of vertebrates. Many of these groups of cells can be referred to as compartments and repeated series of such morphological units form the basis of organization, or certain structures within an embryo. An embryo is divided into a specific number of similar (but not identical) units that are arranged in a specific order. A central question of developmental biology is to determine the mechanism(s) by which this division and organization is achieved.

In this thesis, I investigate the process of metameric (use of repeated units) development of the early *Drosophila* embryo through an analysis of the process of the formation of compartments in the early embryo and the effect of changing compartment size. First, I present a brief overview of *Drosophila* development followed by an in depth discussion of the formation and roles of compartmental units. This is followed by a description of the genes *fushi-tarazu* and *even-skipped*, which establish parasegmental compartments. I discuss how these genes are known to regulate each other as well as other compartment-specific genes. Finally, I present previous examples of the effect of changing compartment size and the overall objectives of my thesis.

1.1 Overview of early Drosophila development

The life cycle of Drosophila is divided into a number of distinct stages including embryonic, three larval instars, pupal, and adult (Roberts, 1986). The fertilized embryo undergoes a series of thirteen rapid and synchronous nuclear divisions that occur in the absence of cytokinesis (stage 1-3). This period of nuclear division occurs within the first 2 hours after egg laying (AEL) and is characterized by alternating rounds of DNA synthesis and mitosis with no pausing in G1 or G2. During the telophase of division cycles 8 and 9 (approximately one hour after fertilization at a point when there are approximately 100 nuclei) the nuclei begin to move to the outer edge of the embryo and line up in the cortical region forming a syncytial blastoderm (stage 4; Fig. 1.1A). Once the nuclei reach the outer surface, four more syncytial divisions occur at successively slower rates. Following the thirteenth division (at ~2.25 h AEL) the cell cycle slows and the extended S phase of the fourteenth division begins. Cell membranes then begin to invaginate from the embryo membrane down and around each cortical nucleus, thus forming individual cells. This process is completed by three hours after fertilization resulting in formation of a cellular blastoderm (end of stage 5;Turner and Mahowald, 1976; Foe and Alberts, 1983; Fig 1.1B). The cellular blastoderm establishes a monolayer of about six thousand epithelial cells. Gastrulation then occurs over a twenty-minute period (stages 6 and 7) during which the cephalic furrow is formed, and visible segregation of cells into the presumptive ectoderm, mesoderm, and endoderm occurs (Turner and Mahowald, 1977; Fig 1-1C-D).

Figure 1.1 A series of scanning electron micrographs depicting the embryological development of *Drosophila.* A) A stage 4 syncytial blastoderm embryo. B) A stage 5 cellular blastoderm embryo; the pole cells are beginning to form. C) A stage 6 embryo beginning gastrulation; the cephalic furrow has started to form. D) Stage 7 embryo in which gastrulation is complete. E) Stage 8; germ band elongation. The germ band extends up over the back of the embryo. F) Stage 10; germ band elongation continues. Also the gnathal and clypeolabral lobes form. G) Stage 11; end of germ band elongation; shallow parasegmental grooves are evident and tracheal pits appear. H) Stage 12; the germ band starts to retract. The germ band moves back towards the anterior of the embryo. The surface of the embryo is now marked by segmental furrows, gnathal buds and tracheal pits. I) Stage 13; germ band retraction is complete. At this stage most of the cells of the organ primordia begin to differentiate. At the end of this stage dorsal closure begins. J) Stage 14; head involution begins and dorsal closure continues. K) Stage 15; dorsal closure is complete. L) Stage 16; Cuticle secretion begins. The segmented structures in the larva are labeled as T1-T3 and A1-A8. Micrographs obtained from http://bio.purdue.edu.fly/aimain /images.htm

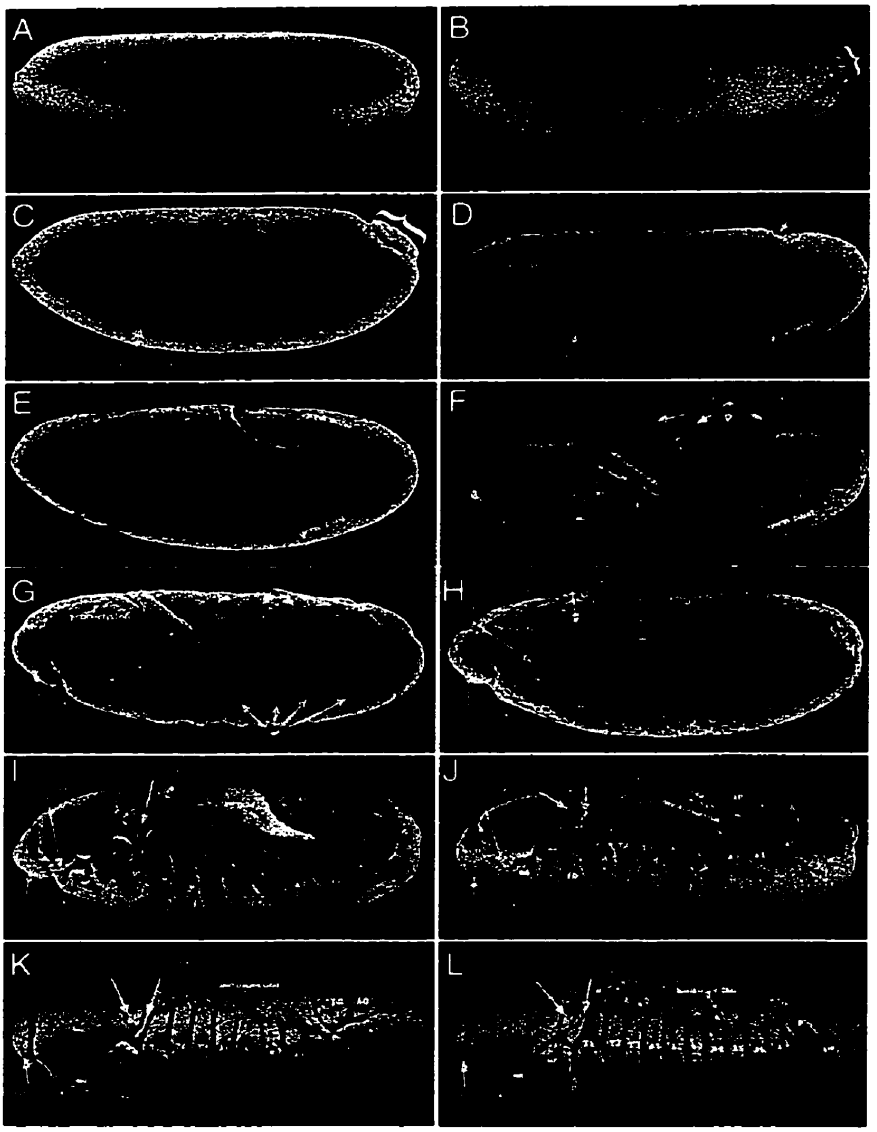
A
B
C
D
E
F
G
H
I
J
K
L

Gastrulation is followed by germ band elongation (stages 8-11; Fig 1.1E, F, G). During mid-germ band elongation (4:20 to 5:20 h; stage 10), shallow grooves marking parasegmental boundaries are formed (Fig. 1.1G). Germ band elongation is completed by the sixth hour of development (stage 11).

After elongation, the germ band retracts (stage 12) such that it reverses its movement and the posterior end of the embryo is no longer located behind the head region (Fig 1.1). The segments are now clearly visible and include the early head segments, three thoracic, eight abdominal and two caudal segments (Turner and Mahowald, 1977; Fig. 1.1H-I). The epithelial ectoderm, neural ectoderm, and mesoderm are all segmented. Following cellularization, only two to three rounds of cell division occur within the entire epithelial ectoderm (at stages 8, 10 and 11; Hartenstein and Campos-Ortega, 1985). Thus, many of the morphological movements within the embryo occur in the absence of cell division.

1.2 Compartments in Animal Development

A fertilized embryo develops quickly from a single cell into a mass of undifferentiated cells. From this stage onward, it will undergo several morphological processes to produce specific and organized structures. At least one major body axis can be defined in all multi-cellular organisms. In *Drosophila*, the anterior-posterior and dorsal-ventral axes of an embryo are established first. Next, cells become allocated to different germ layers: the ectoderm, mesoderm,

and endoderm. Within the different germ layers, groups of cells can be defined as an individual unit based on features such as cell-lineage. Such groups of cells will ultimately acquire specific characteristics dependent upon their location. This process (see below for further description) has been referred to as compartmentalization (Garcia-Bellido et al., 1973; Crick and Lawrence, 1975). Subsequently, embryos undergo dramatic changes in form, a process called morphogenesis. This includes gastrulation, in which the germ layers will sort themselves out, forming the main body plan. During this process, cells on the outside of the embryo may migrate inwards. Concurrent with this process, cell differentiation is also occurring in which either individual cells, or groups of cells will become functionally and/or structurally different from one another. All of these processes are controlled temporally and spatially by differential gene expression.

In higher organisms, the division of the early embryo into repeated units or compartments is a critical component of development. These compartmental divisions provide the framework upon which further differentiation can occur. It is from these compartments that specific body structures including head, abdomen, and appendages will ultimately form. Failure to correctly establish compartments will result in aberrant patterning of the embryo including, for example, the loss of certain structures.

1.2.1 What is a developmental compartment?

Compartments are found in all multi-cellular organisms and can be defined by several basic characteristics. Compartments consist of cells that are descendents of a small group of founder cells, or a polyclone (Crick and Lawrence, 1975). All cells within a compartment preferentially associate with one another and have specific genetic or physical boundaries (Garcia-Bellido et al., 1973; Lewis, 1978). These polyclones retain their boundaries and acquire developmental fates that are different from cells in neigbouring compartments (Garcia-Bellido et al., 1973). Cells within a compartment are thought to associate with one another either through specific mitotic lineage, differential cell adhesion or both (Crick and Lawrence, 1975; Morata and Lawrence, 1975; Morata and Lawrence, 1977).

As cells between compartments are proposed to have different adhesive properties, the boundaries between them are generally very stable and form straight lines (Morata and Lawrence, 1975; Morata and Lawrence, 1977; Lawrence, 1997). This allows cells located along the compartment borders to act as organizing centers, producing signals that guide further patterning of the compartment or even sub-domains of the compartment therein (Morata and Lawrence, 1975; Meinhardt, 1983). In *Drosophila*, there are many examples of such signals (Martinez Arias et al., 1988; Bejsovec and Martinez Arias, 1991; Heemskerk and DiNardo, 1994) reviewed in (Blair, 1995 and Lawrence, 1996 #1281). The stability of the compartment borders are also important for long term patterning. For example, the embryonic anterior/posterior compartment border and associated structures (imaginal discs) are retained through to

adulthood (Wilkins and Gubb, 1991). These basic principles define compartments in both invertebrates and vertebrates.

1.2.2 Models of compartment formation

Historically, many ideas have been put forth as to how such compartments could be established and maintained. One model that has received much attention is the positional information model, which suggests that cells acquire fate based upon their position by responding to a gradient of morphogen-like molecules (Wolpert, 1969; Meinhardt, 1977; Meinhardt, 1983) reviewed in (Lawrence and Struhl, 1996; Wolpert, 1996). A morphogen is a substance (chemical or gene activity) that acts over a distance in a concentration-dependent (or activity-dependent) manner to define multiple cell fates. Thus, a morphogenetic gradient expressed from a defined source can control patterning, polarity and proliferation of cells within a specific field (Lawrence and Struhl, 1996; Wolpert, 1996). This type of system requires that the concentration of the morphogen is different at either end of the gradient and remains different (but constant) such that boundaries would be established at either end. Each cell within the gradient or field must also contain the information necessary to interpret the positional information or morphogen. This can occur by cells interpreting the information present in terms of their position within a morphogenic gradient. Cells can respond to threshold concentrations of morphogenic information, which results in different levels of activity that correlate to different concentrations of a morphogen. This threshold level of activity could

be the amount of a morphogen that is required to bind to a receptor to activate intracellular signaling, or perhaps the concentration of a transcription factor required to regulate specific genes. Three basic features of a morphogen were also predicted. First, the vector or direction of the gradient determined the polarity of the pattern produced (i.e. the direction that the bristles or cuticle extensions face; (Lawrence, 1966; Stumpf, 1966). Second, the scalar concentration of the gradient at different points would provide information to tell each cell where and what it would be (Lawrence, 1966; Stumpf, 1966). Third, the slope or steepness of the gradient would determine the size of the developmental unit (Bohn, 1974; reviewed in Wolpert, 1989; Lawrence and Struhl, 1996; Wolpert, 1996).

Variations on how molecules pattern at a distance have also been proposed. For example, the relay model posits that cells obtain specific identity based upon local interactions with neighbouring cells (Martinez Arias, 1989). As opposed to a morphogen acting over a distance, short-range signals initiate a cascade of short-range secondary signals, which then propagate information across a field (Martinez Arias, 1989). In this way, increasingly complex gene expression patterns are generated gradually from a sequence of local interactions.

Many of these hypotheses have been analyzed and tested in *Drosophila* and other segmented invertebrates such as *Oncopeltus* and *Rhodnius*. These experiments are discussed briefly in the next section. Similar properties may also be applied to patterning decisions in other metameric organisms.

1.2.3 Examples of compartment use to establish a body plan

The concept of the subdivision of a developing organism into repeated units has been around since the nineteenth century (reviewed in Ingham and Martinez Arias, 1992). Early on, these ideas were largely based on outward morphology; more recently there has been a realization that the developmental organization of very different organisms has many common features. Well characterized examples of compartment use include the somites and rhombomeres in vertebrates and parasegments in early *Drosophila melanogaster* embryos (Lumsden, 1990; Lawrence and Morata, 1994). For example, the hindbrain of the developing vertebrate brain is composed of repeated rhombomeres, which are organized as separate compartmental units (Lumsden, 1991; Lumsden and Guthrie, 1991; Fig 1.2A). Cells within a specific rhombomere will mix with each other but not with cells of adjacent rhombomeres. When cells of adjacent rhombomeres (odd and even numbered) are removed and then placed adjacent to each other, new boundaries form, suggesting that differences in cell adhesive properties may be present (Guthrie and Lumsden, 1991). This is further illustrated when cells of the same rhombomere, or tissue from two odd numbered or two even numbered rhombomeres are combined. In this case new boundaries are not formed (Guthrie and Lumsden, 1991).

Figure 1.2: Compartments in mammalian embryos. A) In the mammalian embryo, compartmental divisions include the somites (purple) and rhombomeres (pink) of the hindbrain. B) It has recently been determined that odd-numbered rhombomeres express the Eph receptor tyrosine kinases (Eph) and even-numbered rhombomeres express the corresponding ligand, ephrin. Bi-directional signaling occurs between the Eph receptors and ephrins and is thought to play a role in the establishment and/or maintenance of the rhombomere borders. Figure adapted from (Lumsden, 1990; Dahmann and Basler, 1999).

Compartmentalization in mammalian embryos

A

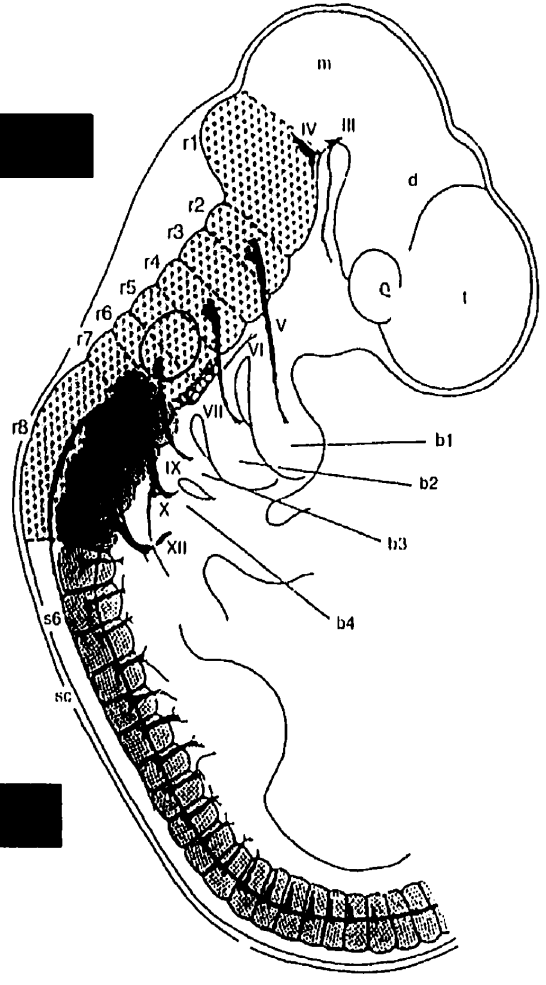

B

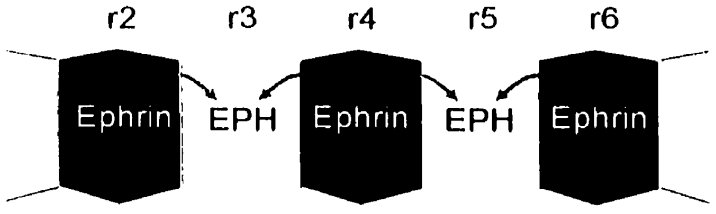

Recently it has been suggested that bi-directional signaling between adjacent cells that express the Eph-receptor tyrosine kinase, and cells that express their ephrin ligands, plays a role in restricting cell intermingling and establishing the rhombomere boundaries (Klein, 1999). Eph receptors and their membrane-bound ligands, ephrins, are expressed in complementary rhombomeres (Fig 1.2B). Xu et al. determined that injection of ectopic ephrin results in the mosaic activation of Eph receptor at the boundaries of odd-numbered rhombomeres, which express the Eph receptor (Xu et al., 1999). On the other hand, injection of Eph receptor results in mosaic activation of the ligand ephrin, and sorting of cells to boundaries of even-numbered rhombomeres. Thus, activation of Eph receptor or ephrin was sufficient to drive cell sorting between adjacent rhombomeres. In zebrafish animal cap assays, cells isolated from two animal caps that were initially injected with either full length Eph receptor or ephrin restricts cells from either animal cap mixing. However, injection of truncated versions of either Eph receptor or ephrin protein was unable to restrict mixing of cells from the two animal caps (Mellitzer et al., 1999). These studies demonstrated that bi-directional Eph receptor-ephrin signalling is sufficient to restrict cell intermingling between rhombomeres, and that this can occur in the absence of differential expression of adhesive molecules. It has also been suggested that Eph receptors and ephrin may regulate the activity of other adhesion molecules (Zisch et al., 1997). Thus, Eph receptors and ephrin may act in parallel or in combination with these cell adhesion molecules to establish the rhombomeres boundaries.

Some of the best characterized examples of compartments are in insects such as the milkweed bug, *Oncopeltus fasciatus*. The abdomen of *Oncopeltus* is clearly segmented with the boundaries of each segment marked by changes in cell shape and in larvae by differences in pigmentation (Lawrence, 1973a; Lawrence, 1973b). As in *Drosophila*, the ectoderm of *Oncopeltus* is composed of a single layer of cells in which the cells of one segment directly abut against the cells of an adjacent segment (Lawrence and Green, 1975). Experiments on this organism have helped to establish the properties of a segment as a compartmental unit and have identified many characteristics that were later found in *Drosophila*. For example, clones of differentially pigmented cells made late in development were never able to cross segment boundaries, whereas clones made very early were able to freely transgress and even straddle segment boundaries (Lawrence, 1971; Lawrence, 1973a; Lawrence, 1973b; Lawrence, 1981). Thus, the *Oncopeltus* segment boundary acts as a lineage restriction and can be defined as a compartment boundary.

Transplantation experiments also showed that the segment boundary itself has specific characteristics and can be regenerated by cells distal to the boundary (Wright and Lawrence, 1981b). For example, when cells taken from the anterior of one segment and the posterior part of the next segment are placed together, a boundary is generated at the point of intercalation (Wright and Lawrence, 1981b). Conversely, if cells are taken from the same position in two different segments, for example the middle region, and are placed together no border is formed (Wright and Lawrence, 1981b). It was concluded that the

segment is a stable structure with specific characteristics that are retained upon transplantation.

Additionally, experiments in *Oncopeltus* provide support for the hypothesis that cell affinity (adhesion) plays a role in maintaining the integrity and linearity of a segment boundary. When the segment border is destroyed by making an incision in the surface of the cuticle, and then all cells surrounding the cut are killed by cauterization, the border can be regenerated by cells that migrate to the wound area (Wright and Lawrence, 1981a). In this experiment, cells from the different segments were differentially marked genetically such that the two populations of cells could be observed. Initially, the migrating cells form a very uneven junction. Over time however, a straight boundary forms. No cells ever crossed over this boundary whether it was regenerated at the original position or at a new position (Wright and Lawrence, 1981a).

Regeneration experiments carried out by Wigglesworth and Locke (reviewed in Locke, 1967) on another segmented insect *Rhodnius*, also demonstrated a link between groups of cells that act as a single developmental unit (compartment) and segments (Ingham and Martinez Arias, 1992). Epidermal pieces of larval cuticle were transplanted to either homologous or heterologous regions of another segment (reviewed in Locke, 1967). Following wound healing, the resulting patterns of differentiated cells were categorized by changes in the adult cuticle surface and associated hairs. Homologous transplants were completely integrated into the new region resulting in normal patterning. However, heterologous transplants were not integrated and new patterns were

established (reviewed in Locke, 1967). It was found that all regions of the *Rhodnius* segments had position specific properties, including the border itself. Cells within the border did not interact with other cells and appeared to be a source or sink of pattern. That is to say, where boundary cells were excised, new boundaries were regenerated (source), whereas new patterns were established at the point of transplantation (sink). Therefore, it was suggested that a gradient of information is present within the segment and is repeated in a segmental pattern with the border itself being the source of the information.

Further to this, other experiments in *Oncopeltus* suggested that the gradient of information was a result of a morphogen that diffused from the segment border (Lawrence, 1966; Stumpf, 1966) and produced a gradient of positional information across a compartment (reviewed in Lawrence, 1992). These initial experiments demonstrated that segmental compartments act as developmental units and that the borders between compartments have specific characteristics.

1.2.4 Examples of compartments in Drosophila melanogaster

There are many different examples of compartments in *Drosophila*. The initial identification of compartments was in imaginal discs, the tissues set-aside during embryogenesis that ultimately form structures such as the adult wing, leg, head and body tissues. A technique combining mitotic recombination and specific markers of mutant cells allowed the analysis of imaginal disc cell lineages in development. One of the markers used, the *Minute* mutation, causes

cells to grow and divide more slowly (Morata and Ripoll, 1975). When clones (a group of cells arising from the same progenitor by mitosis) of *Minute*$^{+}$ cells are made by mitotic recombination in heterozygous *Minute* animals, the differences in growth rates between wild type and heterozygous mutant cells allows the *Minute*$^{+}$ clones (also marked by the cuticular cell markers *multiple wing hairs* and *jagged vein*) to grow rapidly relative to their heterozygous neighbours. However, despite this considerable growth advantage these clones never cross the anterior-posterior compartment borders of wing discs (Garcia-Bellido et al., 1973).

It was initially suggested that the *Drosophila* embryo is composed of a series of segmental primordia and that these divisions are based upon the visible morphological divisions observed in larvae and adults (Fig 1.3D,E; Martinez-Arias and Lawrence, 1985). This type of organization is what is observed in *Oncopeltus* and *Rhodnius*. However, subsequent, clonal analysis established that, at the cellular blastoderm stage, ectodermal cells are divided into anterior and posterior polyclones (group of cells descendent from a small group of founder cells), a subset of which give rise to anterior and posterior sub-compartments (Fig. 1.3B; Garcia-Bellido et al., 1973; Crick and Lawrence, 1975; Lawrence, 1981). Additionally, in imaginal disc-related structures such as the legs and wings, these boundaries end up passing through the middle of the segments, dividing the appendages in two. The compartment boundaries therefore did not coincide with segmental boundaries as suggested by the visible

Figure 1.3: (A) Parasegments are first defined by the expression of *eve* (in blue) and *ftz* (in brown). (B) The expression of *en* divides the parasegment into anterior (a) and posterior (p) compartments. The borders of the parasegments are offset from the segmental boundaries, such that each segment is composed of the anterior compartment of one parasegment and the posterior compartment of the adjacent parasegment. (C) Late embryo, (D) larval cuticle (shown in dark-field) and (E) adult structures are also shown. The registries of embryonic parasegments with larval and adult segmental structures are illustrated. T1, T2, and T3 stand for the first, second and third thoracic segments. A1-A8 represents the eight abdominal segments. Proper establishment of the embryonic parasegments is required to produce wild type larvae and adults. Figure adapted from Wolpert, 1999.

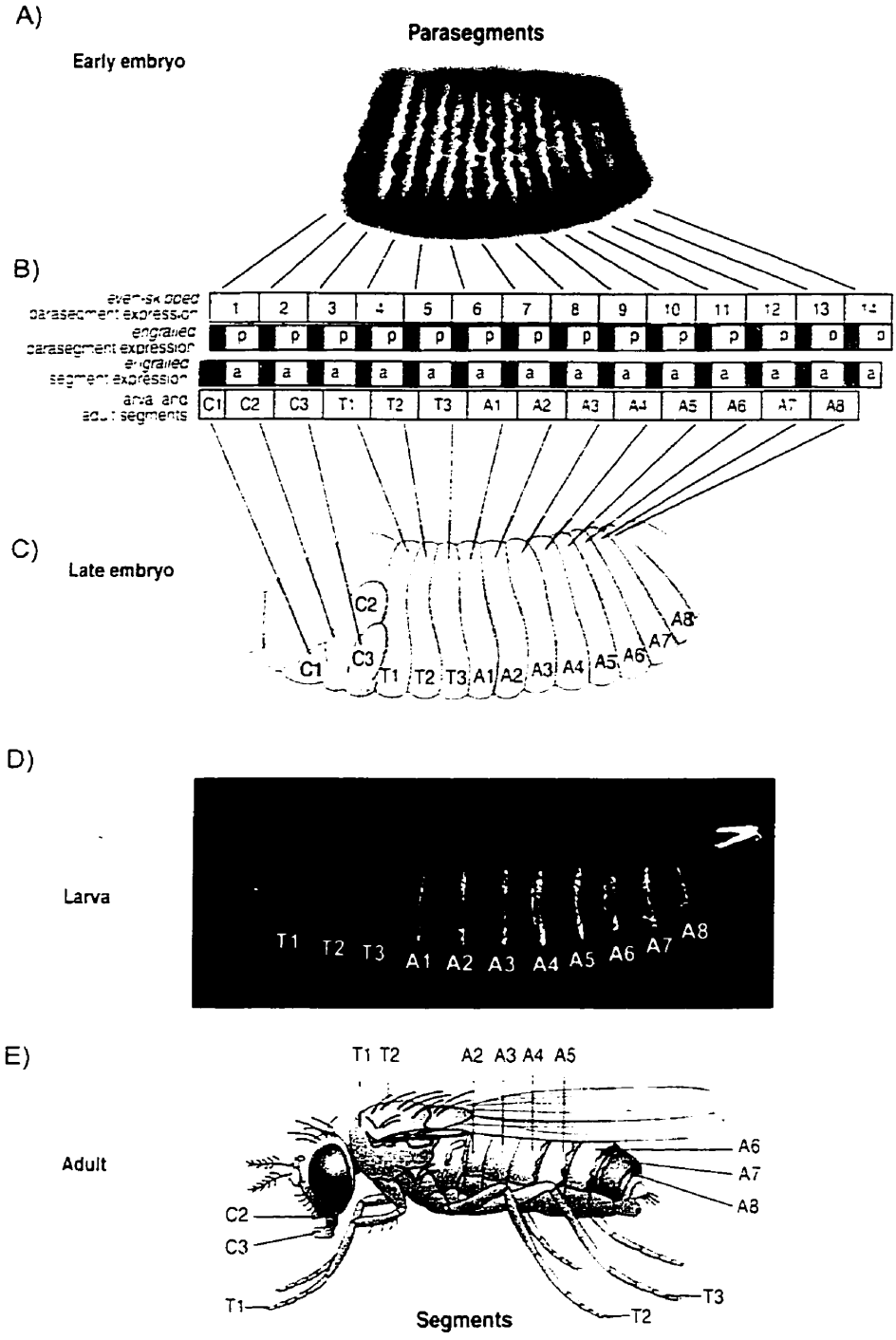
A)
Parasegments
Early embryo
B)
even-skipped parasegment expression
engrailed parasegment expression
engrailed segment expression
anal and adult segments
1 2 3 4 5 6 7 8 9 10 11 12 13 14
p p p p p p p p p p p p p p
a a a a a a a a a a a a a a
C1 C2 C3 T1 T2 T3 A1 A2 A3 A4 A5 A6 A7 A8
C)
Late embryo
C2
C3
C1
T1 T2 T3 A1 A2 A3 A4 A5 A6 A7 A8
D)
Larva
T1 T2 T3 A1 A2 A3 A4 A5 A6 A7 A8
E)
Adult
T1 T2 A2 A3 A4 A5
A6
A7
A8
C2
C3
T1
T3
T2
Segments

segmental grooves in the larva. Thus, these observations suggested that the initial compartments do not correspond with segments but are slightly out of register and were thus called parasegments (Fig. 1.3A,B; Martinez-Arias and Lawrence, 1985). In *Oncopeltus* and *Rhodnius* the existence of parasegmental compartments is unclear and experiments discussed previously dealt specifically with the segmental regions (Lawrence, 1973a). Additionally, the developmental ages at which these experiments were carried out was subsequent to when segments were already physically visible.

Several lines of evidence support the existence of the parasegmental compartment. For example, the borders of expression of genes in the bithorax complex are not delimited by the borders of the morphologically visible segments, but rather are confined within parasegmental boundaries (Morata and Kerridge, 1981; Minana and Garcia-Bellido, 1982; Hayes et al., 1984; Struhl, 1984). Additionally, parasegment borders coincide with anterior-posterior compartment boundaries in both embryonic and adult tissues (Garcia-Bellido et al., 1973; Vincent and O'Farrell, 1992). Thus, the parasegment itself fulfills the definition of a compartment. The parasegment appears to be the first and basic unit of organization within the early *Drosophila* embryo (Martinez-Arias and Lawrence, 1985; Lawrence, 1988; Fig 1-3A).

As mentioned above, it was thought initially that segments, which are visually apparent at stage 11, are the basic unit of organization within the embryo (Lawrence, 1988). Segments are defined structurally by the positions where longitudinal muscles attach to the body wall. These attachments cause deep

indentations within the ectoderm (Martinez-Arias and Lawrence, 1985). Parasegments are out of register with these later arising segmental compartments (stage 11) such that each parasegment will contain the posterior compartment of one segment, and the anterior compartment of the adjacent segment (Fig 1.3B). Shallow parasegmental grooves are visible in both the ectoderm and mesoderm at stage 10, before the formation of segmental furrows. Although parasegments are defined in both the ectoderm and underlying mesoderm, further division into anterior and posterior sub-compartments occurs in the ectoderm only (Lawrence, 1988). These parasegmental boundaries are maintained throughout all remaining developmental stages. Current theories of *Drosophila* development focus upon the parasegment as the basic metameric unit within the embryo.

1.3 *A hierarchy of interacting maternal and zygotically active genes establish parasegments*

An early *Drosophila* embryo consists of a multinucleate syncytium. However, by two to three hours after fertilization, the embryo is composed of about 6000 cells. These cells are organized by specific patterns of gene expression, which ultimately provide each row of cells along the anterior-posterior axis with a unique identity. In several ethyl methane sulfonate (EMS) mutagenesis screens, most of the zygotic genes (activated following fertilization) that affect early embryonic development were identified (Nusslein-Volhard and Wieschaus, 1980; Jurgens et al., 1984; Nusslein-Volhard et al., 1984; Wiechaus

et al., 1984). Zygotic embryonic lethal phenotypes were followed by the cuticular phenotypes of late stage embryos.

The cuticle is a hard exoskeleton that is secreted by the embryo just prior to hatching (see Fig. 1.1D). Along the ventral surface of the embryo, cuticular extensions organized in bands of hairs called denticle belts are required for locomotion. The structure and organization of the denticle belts can be used to identify specific segments. A second series of EMS screens identified maternal effect mutations (mutations within the maternal products deposited in the oocyte) that also affect segmental patterning (Schupbach and Wiechaus, 1986). The maternally active genes establish the major axes of the embryo (anterior-posterior, dorsal-ventral, terminal regions), while the zygotically active genes act to divide these regions into parasegmental units. The hierarchical interactions between these different classes of genes are described further below.

1.3.1 *Maternal contribution to embryonic body plan formation*

During oogenesis, associated nurse cells (helper cells) export large amounts of maternal mRNA and protein products into the oocyte. A number of different mRNAs are localized to specific areas of the oocyte such as the anterior tip (*bicoid*); posterior pole (*nanos*) while others are present throughout (*hunchback*; Fig. 1.4). Specific localization or degradation elements within the mRNA, which bind to other maternal gene products or cellular structures (e.g. actin cytoskeleton), control positioning of the mRNA within the oocyte/embryo

Figure 1.4: The *Drosophila* body plan is established through a series of hierarchical gene interactions that divide the embryo into smaller and smaller regions. Many maternal genes express gradients of proteins. These are interpreted by the gap genes, which define broad regions along the anterior-posterior axis of the embryo. Next the majority of the pair-rule genes are expressed in a periodic pattern, in parts of every other segment, establishing smaller regions of division. The segment polarity genes subsequently divide the embryo into finer divisions and are expressed in parts of every segment. Expression of specific homeotic genes provides different segmental regions with unique identities.

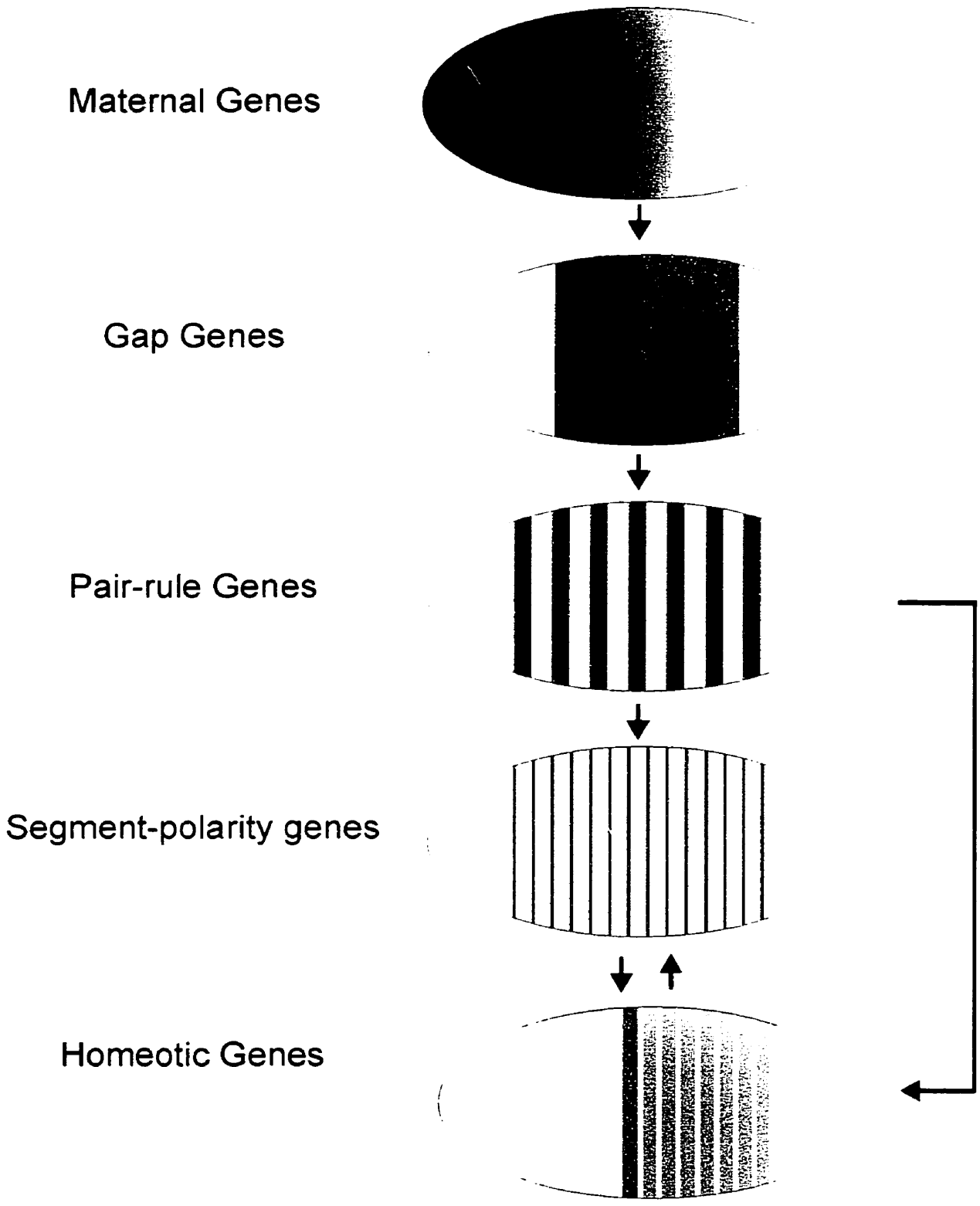
Maternal Genes
Gap Genes
Pair-rule Genes
Segment-polarity genes
Homeotic Genes

(Mlodzik and Gehring, 1987; Macdonald and Struhl, 1988; Dubnau and Struhl, 1996); reviewed in (Cooperstock and Lipshitz, 1997; Bashirullah et al., 1998). As a result, gradients of maternal protein are produced that act as morphogens along the anterior-posterior, and dorsal-ventral axes of the embryo. Zygotic transcription begins by about two hours of development (early syncytial blastoderm stage). By the cellular blastoderm stage, just one hour later, the identity of most cells in the ectoderm, with regards to the anterior-posterior and dorsal-ventral axes has been established (reviewed in St Johnston and Nusslein-Volhard, 1992)).

1.3.2 Zygotically active segmentation genes establish the body plan

The transition from maternal to zygotic transcriptional control occurs at about 2.5 hours of development (Edgar and O'Farrell, 1989). The gap genes are the first set of genes to be activated zygotically by the maternal, anterior-posterior coordinate genes that act in a concentration-dependent manner. Gap genes encode transcription factors that act to define large blocks of cells along the anterior-posterior axis of the embryo (Fig. 1.4). Mutations in gap gene products result in defects in contiguous sets of segments in the larval cuticle. Combinatorial activities of gap genes control the activation of the next class in the gene hierarchy, the pair-rule genes.

Pair-rule genes are transcriptionally activated about thirty minutes after activation of the gap genes (Edgar and O'Farrell, 1989). Pair-rule gene products, again mainly transcription factors, further divide the embryo into repeated

domains, and thus are the first genes to be expressed in a repeated periodic pattern. Each pair-rule gene is initially expressed in a pattern of seven repetitive stripes (Nusslein-Volhard and Wieschaus, 1980); Fig. 1.4). Mutations in pair-rule genes result in defects within alternating segments. The pair-rule genes, often acting in combination, are required for the regulation of the segment-polarity genes.

Segment-polarity genes define sub-domains within each segment (Nusslein-Volhard and Wieschaus, 1980). Acting at the bottom of the segmentation hierarchy, segment-polarity genes, as the name implies, are thought to be involved in establishing the fate of cell types (e.g. determination of polarity and naked cell fate versus production of denticle hairs) within each segment (Martinez Arias et al., 1988). Mutations of segment-polarity gene products result in defects within each segment of the developing embryo.

Many segmentation genes (including the gap genes and pair-rule genes) are required to activate the homeotic selector genes (Duncan, 1986; Ingham and Martinez-Arias, 1986; Martinez Arias et al., 1988; Irish et al., 1989; Tremml and Bienz, 1989). Homeotic genes are activated after the embryo has been divided into repeating units (Lewis, 1978; Struhl, 1982). It is the activity of the homeotic selector genes that ultimately provides each segmental unit of the embryo with a unique identity (Lewis, 1978; Struhl, 1982; Akam, 1987). The majority of homeotic genes are organized into two complexes called the Antennapedia complex (contains genes *labial*, *postbithorax*, *Deformed*, *Sex combs reduced* and *Antennapedia*) and the bithorax complex (contains genes *Ultrabithorax*,

abdominal-A, and *Abdominal-B*) that are expressed co-linearly with the order of genes along the chromosomes (Duncan, 1986; Morata, 1993; Lawrence and Morata, 1994; Simon, 1995; Duncan, 1996). As with most other segmentation genes, homeotic genes encode transcription factors that regulate the expression of other genes (reviewed in McGinnis and Krumlauf, 1992)). Thus, segmentation is controlled by an elaborate hierarchy of gene products, the majority of which are transcription factors, which act to successively subdivide a homogenous syncytium into repeating metameres, each with its own unique identity.

1.4 How are parasegments established?

Two pair-rule genes *even-skipped* (*eve*) and *fushi-tarazu* (*ftz*) are expressed in patterns that correlate with alternate parasegmental compartments (Hafen et al., 1984; Carroll and Scott, 1985; Macdonald et al., 1986). *ftz* is expressed in the even-numbered parasegments and *eve* is expressed in the odd-numbered parasegments. The expression of *ftz* and *eve* then resolves (explained further below) such that there are high levels of expression within cells at the anterior edge of each parasegment, with low levels in the posterior cells. This results in a pattern with sharp anterior boundaries of *ftz* and *eve* expression. It was suggested that both the high levels and sharp anterior boundaries of *ftz* and *eve* expression are required to define the alternating parasegmental boundaries (Lawrence et al., 1987; Lawrence and Johnston, 1989). Thus, in this model, it is the boundary between *ftz* expressing and *ftz* non-expressing cells and the *eve* expressing and *eve* non-expressing cells that will delimit the

parasegmental boundaries. *ftz* and *eve* expression is also coincident with the expression of other genes within a parasegment, such as the homeotic genes (Lawrence et al., 1987; Lawrence and Johnston, 1989). It was proposed that *ftz* and *eve* expression are required to delimit the parasegmental boundaries.

1.4.1 The expression pattern of *eve*

The importance of the role of *eve* in segmentation is exemplified by the fact that in strong *eve* mutants, embryos lack all segmental divisions and the larval cuticle is a non-segmented surface, completely covered in denticles (Nusslein-Volhard et al., 1985). However, *eve* hypomorphic alleles (expression levels are lower than wild type) produce larval cuticles in which alternate segments (the even-numbered abdominal segments) are deleted (Nusslein-Volhard et al., 1985). Thus, *eve* is primarily required to establish the odd-numbered parasegment primordia, but also plays a role in the establishment of all parasegmental boundaries (Macdonald et al., 1986; Manoukian and Krause, 1992; Fujioka et al., 1995). This is unlike any other pair-rule gene.

Early experiments show that initial *eve* transcript activation prior to cellularization appears to be in a concentration gradient with high levels at the anterior end of the embryo and lower levels posteriorly (Macdonald et al., 1986). This gradient is maintained until just subsequent to the 13th nuclear division, and then resolves into seven transverse stripes (Macdonald et al., 1986). The first *eve* stripe is located over the cephalic furrow (Macdonald et al., 1986).

At cellularization, each stripe of *eve* expression is four cells wide (with a four cell gap), and then further narrows to approximately three cells wide,

separated by five cell-wide gaps (reviewed in Harding et al., 1986). After gastrulation, eve stripes narrow to one to two cells in width and a second set of weak stripes (the minor stripes) appear in between, resulting in a pattern of fourteen evenly spaced stripes. These fourteen *eve* stripes are present for only a short period following gastrulation (Macdonald et al., 1986). The minor eve stripes are only one to two cells in width and are located at the anterior edge of the even-numbered (ftz-dependent) parasegments. The minor *eve* stripes appear at about the same time and in the same cells as the initial activation of *en* in the *ftz* domain (DiNardo et al., 1985; Kornberg et al., 1985; Macdonald et al., 1986; Frasch and Levine, 1987).

eve protein is also expressed in a broad pattern across the trunk region of the early embryo, which initially suggested that to obtain a pattern of seven stripes, selective repression of the interstripe regions must occur (Frasch and Levine, 1987). The boundaries of protein expression are refined as cellularization occurs. It was later determined that discrete portions of the eve promoter could activate different subsets of eve stripes, suggesting that this was important in the specification of boundaries (discussed further below; Howard and Ingham, 1986; Goto et al., 1989; Harding et al., 1989; Howard and Struhl, 1990; Small et al., 1992; Small et al., 1996; Fujioka et al., 1999).

eve expression within the germband is gradually lost during germband elongation and by 5 hours of development is completely undetectable (Macdonald et al., 1986). *eve* function is required for proper extension of the germband (Irvine and Wieschaus, 1994). *eve* is again detected in certain subsets

of cells within the developing ventral nerve cord between 7 and 10 hours of development (Carroll and Scott, 1985; Macdonald et al., 1986). For example, *eve* is required to determine the identity of specific neurons including the RP2 and a/pCC neurons (Doe et al., 1988). Additionally, *eve* is thought to be required for proper development of the hindgut (Gorfinkiel et al., 1999).

1.4.2 Regulation of eve expression

Analysis of the *eve* promoter region has identified several cis-regulatory enhancer elements. Separable portions of the *eve* promoter are able to activate discrete *eve* stripes. Individual elements were identified for the early stripes 2 and 3 and a single element for all 7 of the late (minor) stripes (Goto et al., 1989; Harding et al., 1989; Small et al., 1992; Small et al., 1996). Additionally, early stripe 7 expression can be driven by a region including either the stripe 2 or stripe 3 elements (Small et al., 1996). Gap genes control the early stripes of *eve* expression directly. For example, stripe 2 activation requires both the maternal gene *bicoid (bcd)* and the gap gene *hunchback* (*hb*) for activation while the anterior and posterior borders of *eve* are established by the repressive activities of the gap genes *giant* and *Kruppel*, respectively (Stanojevic et al., 1989; Small et al., 1991; Small et al., 1992; Wu et al., 1998). Stripes 3 and 7 are activated by ubiquitously distributed factors of the JAK-Stat pathway (Small et al., 1996). The JAK- tyrosine kinase *Hopscotch* acts through the STAT protein Marelle to activate the stripes (Binari and Perrimon, 1994; Small et al., 1996; Yan et al., 1996). The borders of stripe 3 and 7 are defined by the repressive activities of *Knirps* and *hb* (Stanojevic et al., 1989; Small et al., 1996). *hb* protein is

responsible for establishing the anterior border of stripe 3 and the posterior border of stripe 7 whereas *Knirps* expression defines the posterior border of stripe 3 and the anterior border of stripe 7 (Small et al., 1996). *eve* stripes 1 and 5, and stripes 4 and 6 are controlled by two separate elements (Fujioka et al., 1999). The boundaries of stripe 5 are controlled by the expression of *Kruppel* and *giant* (Fujioka et al., 1999). The anterior border of stripe 4 and the posterior border of stripe 6 are controlled by *hb*, while the intervening boundaries are established by the repressive activity of *knirps* (Fujioka et al., 1999). Once activated by gap genes the expression of *eve* may be refined by the activity of other pair-rule genes such as *runt (run)* and *odd-skipped (odd,)* which have been demonstrated to act as repressors of *eve* expression (Fig. 1.5B; Manoukian and Krause, 1992; Saulier-Le Drean et al., 1998).

The expression of the later minor *eve* stripes is controlled by a single upstream element (the late element), which is regulated by *paired (prd)*, *run* and early *eve* expression (Goto et al., 1989; Harding et al., 1989; Fujioka et al., 1995; Fujioka et al., 1996a; Fujioka et al., 1996b). It has been proposed that the early broad stripes of *eve* act in a concentration-dependent manner to repress the normal activator *prd* as well as repressors of the late stripes (*run* and *odd*; Fig. 1.5B). These late *eve* stripe repressors are affected by lower levels of *eve*, and thus generate a narrow zone at the edge of each early *eve* stripe where a late *eve* stripe can then be activated (Fujioka et al., 1995). The presence of high

Figure 1.5: Schematic diagram of the inter-regulation between *ftz* and *eve* and regulation by other pair-rule genes (A) prior to cellularization (stage 5) and (B) at the beginning of gastrulation (stage 6). Some of the interactions have been determined directly by kinetic experiments and others are inferred by genetic interactions. A blunt ended line (in red) indicates a gene that represses another gene. A solid line arrow (in green) indicates a gene that activates another.

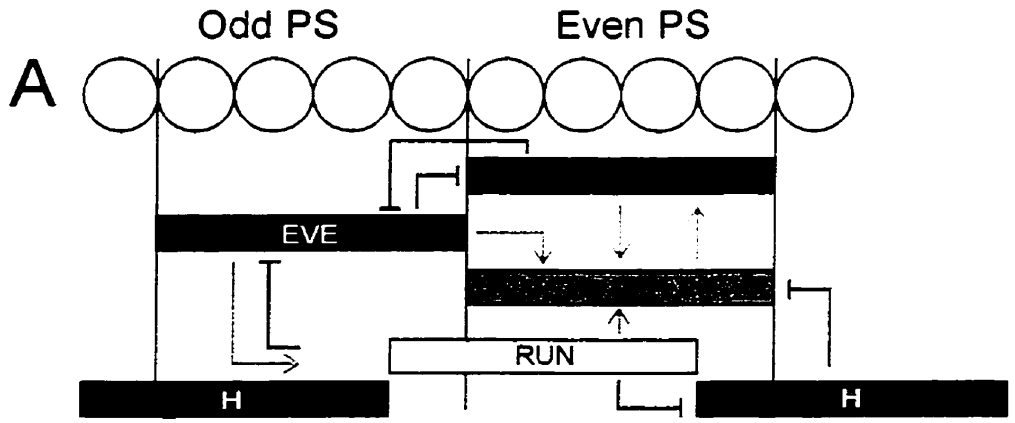
A
Odd PS
Even PS
EVE
RUN
H
H

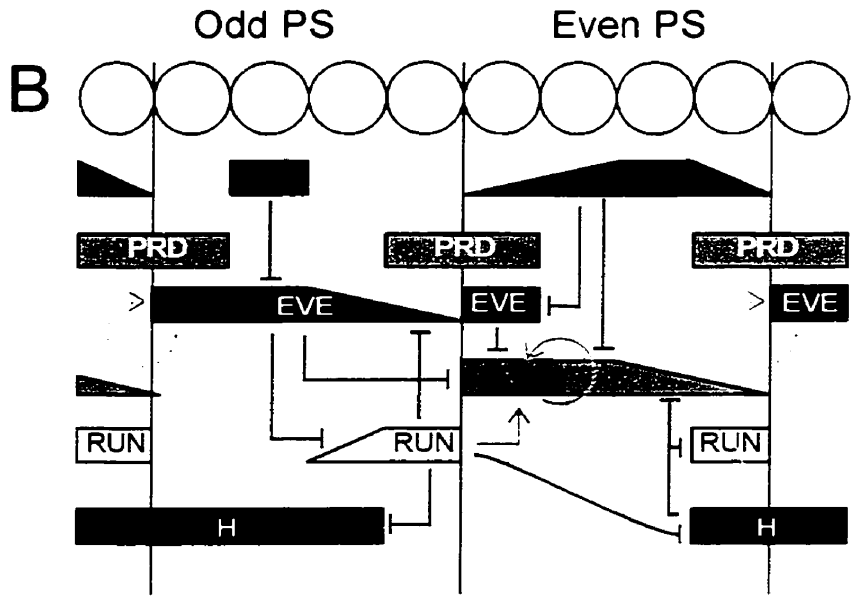
B
Odd PS
Even PS
PRD
PRD
PRD
EVE
EVE
EVE
RUN
RUN
RUN
H
H

affinity EVE binding sites within the *eve* promoter suggests that *eve* may be able to autoregulate its own expression (Hoey and Levine, 1988; Jiang et al., 1991). However, kinetic experiments show that *eve* autoregulation may be indirect and occur via inactivation of an *eve* repressor (Manoukian and Krause, 1992). The *runt* and *odd* genes may play a role in eve repression since the *runt* and *odd* gene products can function as direct repressors of *eve* activation (Fig. 1.5B; Manoukian and Krause, 1992; Saulier-Le Drean et al., 1998). In this context, kinetic experiments refer to those in which a brief pulse of gene expression (using a heat shock promoter) is induced and the time required for target genes to respond is measured. If responses occur within approximately 18 minutes of the heat shock it is indicative of a direct interaction between the genes (Manoukian and Krause, 1992; Saulier-Le Drean et al., 1998; Nasiadka and Krause, 1999). A longer interval between heat shock and response would indicate an indirect interaction between the genes.

It was initially suggested that *eve* is somehow required for the maintenance of the *ftz* expression pattern, but not for initiation or resolution (Carroll and Scott, 1986; Harding et al., 1986). However, based on subsequent kinetic and genetic experiments, it appears that *eve* also plays a role in the initiation of *ftz* expression (Manoukian and Krause, 1992; Fujioka et al., 1995). Prior to cellularization, *eve* can activate *ftz* transcription (Fig. 1.5B; Manoukian and Krause, 1992) and it is the early wide stripes of *eve* that are most important for *ftz* activation and function (Fujioka et al., 1995).

1.4.3 The expression pattern of ftz

Embryos homozygous for *ftz* die late in embryogenesis and form cuticles in which only half of the normal number of segments are present (Wakimoto and Kaufman, 1981; Wakimoto et al., 1984). The resulting mutant cuticles are described as containing abnormally wide segments with only one set of denticle bands, which are most similar to that of the most anterior segments, as opposed to a fusion of the two denticle bands (Hafen et al., 1984; Wakimoto et al., 1984; Weiner et al., 1984).

Transcription of *ftz* begins at approximately 2 hours after fertilization, during the syncytial blastoderm stage (nuclear cycle 12), in two broad bands within the trunk region that correspond to the regions of the future stripes 1 and 5 (Yu and Pick, 1995). On top of this broad pattern, individual stripes of *ftz* transcript appear. *ftz* stripes do not arise in a linear fashion (anterior to posterior), and they also appear to form initially ventrally and then spread dorsally to circumvent the embryo (Krause et al., 1988; Yu and Pick, 1995). As the process of cellularization begins (stage 5; marked by the invagination of nuclear membranes) transcript levels of future stripes 1 and 2 appear as a single band that then separate (Yu and Pick, 1995). Future stripe 5 and 3 also appear individually at this point, with future stripes 6 and 7 appearing as a broad band that subsequently separates. Stripe 4 is the last to appear (Yu and Pick, 1995). At the same time the expression of transcript in the inter-stripe regions fade to undetectable levels (Yu and Pick, 1995). By the completion of cellularization (at 3 hours; stage 6) *ftz* transcript levels are at their highest level, and each stripe is

3 to 4 cells wide, the approximate width of a parasegment (Carroll and Scott, 1985; Yu and Pick, 1995). Expression of ftz transcript coincides with even-numbered parasegments. During gastrulation (stages 6-7) the anterior edge of each *ftz* stripe increases in intensity while the width narrows to 1 to 2 cells (Yu and Pick, 1995). By the end of germ band extension (stage 8), expression of all *ftz* transcripts is lost (Yu and Pick, 1995).

ftz protein is initially present within the embryo between 3 and 5 hours (stages 5-10) of development (Carroll and Scott, 1985; Krause et al., 1988). The order and appearance of *ftz* protein stripes is the same as that of the *ftz* transcript (Krause et al., 1988; Karr and Kornberg, 1989; Yu and Pick, 1995). Loss of transcript in the inter-stripe regions may be due to the short half-life of *ftz* transcripts and protein (six to seven minutes) with continued synthesis of *ftz* transcripts in the stripe regions only (Edgar et al., 1986a; Edgar et al., 1987). Instability elements in the *ftz* transcript have been mapped to a 201-nucleotide element within the 3' untranslated region (*ftz* instability element), and a second element in the 5' third of the coding region (Riedl and Jacobs-Lorena, 1996). Although instability elements have not been functionally mapped in the *ftz* protein, there are PEST (P=proline, E=lysine, S=serine, T=threonine) regions, which are characteristically found in many proteins that are degraded rapidly (Krause et al., 1988). As *ftz* acts in combination with other pair-rule genes, rapid degradation of transcript and protein in the inter-stripe regions may be important for ensuring that the protein is restricted to only certain cells at particular developmental stages (Edgar et al., 1986b; Edgar et al., 1987). The importance

of the "on" and "off" states of *ftz* expression is substantiated by two *ftz* missense mutations ftz^{UAL} and ftz^{Rpl} which produce a more stable protein product, relative to wild type resulting in anti-*ftz* segmentation defects (retain segments normally lost in *ftz* mutant) and homeotic transformations (Kellerman et al., 1990). Additionally, by placing the *ftz* transcript under control of the *hsp70* promoter, transcript is expressed throughout the embryo and again an "anti-*ftz*" phenotype is produced (Struhl, 1985).

Similar to *eve*, *ftz* protein is expressed once again at later stages in a subset of nuclei in each segment of the developing central nervous system (6 to 10 hrs AEL) as well as in the hindgut (12-14 hrs AEL; Carroll and Scott, 1985; Doe et al., 1988; Krause et al., 1988). *ftz* is required to determine neural identity in some of the cells in which it is expressed (Doe et al., 1988). For example, *ftz* is required for differentiation of the neurons referred to as RP2 neurons (Doe et al., 1988). The requirement of *ftz* within the hindgut is unknown at this point (Krause et al., 1988).

It was initially suggested that FTZ had no effect on *eve* expression (Carroll and Scott, 1986; Howard and Ingham, 1986; Ingham et al., 1988; Pankratz and Jackle, 1990). However, more recent genetic analysis suggests that *eve* might in fact be a target of FTZ (Kellerman et al., 1990; Klingler and Gergen, 1993). Another study uses kinetic analysis to show that FTZ does not directly regulate *eve* (Nasiadka and Krause, 1999). Thus, FTZ likely has no direct effect on *eve* expression. Rather, FTZ may indirectly affect *eve* by activating *odd* early (prior

to cellularization), leading to the repression of *eve* (Saulier-Le Drean et al., 1998; Nasiadka and Krause, 1999).

1.4.4 Regulation of ftz expression

The 6.1 kb upstream promoter region of the *ftz* gene contains three functional regions, the upstream enhancer, the zebra element, and the neurogenic element, that are required for the various expression patterns observed. *ftz* transcription requires cooperative activity between the zebra and upstream elements (Hiromi et al., 1985). Sequences within the upstream enhancer are required for *ftz* autoregulation as well as interaction with various gap gene proteins, which act as activators and repressors (Hiromi et al., 1985; Hiromi and Gehring, 1987). The neurogenic element is required for the late stage neuronal expression of *ftz* (Hiromi et al., 1985). The zebra element is composed of a mixture of activator and repressor binding sites that in combination are primarily responsible for the 7-stripe expression pattern of ftz (Dearolf et al., 1989a; Dearolf et al., 1989b).

Although the exact combination of genes that regulate *ftz* expression is unknown, several pair-rule, gap, and maternal genes are known to affect *ftz* expression. These genes include *Kruppel*, *knirps*, *hunchback (hb)*, *giant*, *caudal*, *hairy (h)*, *run*, *odd*, and *eve* (Carroll and Scott, 1986; DiNardo and O'Farrell, 1987; Carroll and Vavra, 1989; Dearolf et al., 1989a; Saulier-Le Drean et al., 1998). For example, expression of the maternal gene *caudal* is required for proper *ftz* expression in the posterior end of the embryo. In the absence of

caudal, expression of *ftz* stripes 5, 6, and 7 are greatly reduced or absent (Macdonald and Struhl, 1986). The *ftz* promoter contains binding sites (fDE1; 32 base pairs in length) for *h* protein and H acts as a repressor of *ftz* transcription (Hooper et al., 1989; Tsai and Gergen, 1995). Products of several gap genes such as *Kruppel*, *knirps* and *hb* regulate expression of *h* and therefore these gap genes may act indirectly on *ftz* through *h* (Carroll et al., 1988b).

In general, *h* transcripts are initially expressed throughout the syncytial blastoderm (Ingham et al., 1985). Transcripts are then localized into a periodic pattern in a pattern that partially overlaps *ftz* transcripts (Ingham et al., 1985). *h* is predominantly expressed in the odd-numbered parasegments and overlaps the anterior parasegment boundaries by one cell (Fig. 1.5B). In *h* mutant embryos the expression of *ftz* is greatly expanded (Carroll and Scott, 1985; Howard and Ingham, 1986), and ectopic expression of *h* completely eliminates *ftz* expression (Carroll and Scott, 1986; Howard and Ingham, 1986; Ish-Horowicz and Pinchin, 1987; Parkhurst and Ish-Horowicz, 1991).

The expression of another pair-rule gene, *run*, also affects *ftz* expression. Initially, *run* is expressed in seven stripes that overlap odd-numbered parasegments by one cell and the anterior half of the even-numbered parasegments (Kania et al., 1990). The expression of *run* is complementary to that of *h*. In *run* mutants, *ftz* stripes initiate but then decay rapidly. Thus, *run* may be acting as an activator of *ftz* transcription (Ingham and Gergen, 1988). This suggests that *run* may be acting on *ftz* indirectly through its ability to repress *h*. The effects of *run* on *ftz* have been shown to act primarily through the same

binding element (fDE1), as does *h* protein (Tsai and Gergen, 1995). Prior to cellularization *run* is able to activate *ftz* expression most likely indirectly through the repression of *eve* (Fig. 1.5A; Manoukian and Krause, 1993).

In an *eve* mutant, *ftz* expression is initiated in an essentially wild type pattern, but by gastrulation (3 hours AEL) expression of *ftz* is lost (Harding et al., 1986). Prior to the completion of cellularization, *eve* directly activates both *ftz* and *run* expression (Fig. 1.5A; Manoukian and Krause, 1992). However, during gastrulation intermediate levels of *eve* now directly repress the expression of *ftz* and *run* (Fig. 1.5B; Manoukian and Krause, 1992). Thus, the expression of the pair-rule genes *h* and *run* are predominantly required for the refinement of *ftz* expression, but not for direct initiation as expression of *ftz* in any of these mutants is lost only after cellularization (Yu and Pick, 1995). Additionally, the expression of *eve* also plays a role in the refinement of *ftz* stripes, but it is not essential.

Using kinetic experiments it has also been demonstrated that *ftz* and *odd* proteins are able to directly activate one another's expression prior to the end of cellularization. This may be important for the initiation of *ftz* expression (Fig. 1.5A; Saulier-Le Drean et al., 1998; Nasiadka and Krause, 1999). During gastrulation, *odd* switches activities from an activator to a repressor of *ftz* expression. This results in further refinement of the ftz stripes within the even-numbered parasegments (Fig. 1.5B; Saulier-Le Drean et al., 1998).

1.4.5 FTZ and EVE establish where parasegmental boundaries are positioned

Within the early embryo, the positions of parasegmental boundaries are colinear with the anterior boundaries of *ftz* and *eve* expression (Lawrence et al., 1987; Lawrence and Johnston, 1989). *ftz* and *eve* are both expressed during the syncytial blastoderm stage in alternating broad stripes that have the appearance of bell-shaped gradients (Frasch and Levine, 1987; Ingham and Martinez Arias, 1992; Fig. 1.6A). *ftz* and *eve* are expressed in alternating parasegments, such that *eve* expression establishes the odd-numbered parasegments, while *ftz* expression establishes the even-numbered parasegments (Fig. 1.6; Lawrence et al., 1987; Lawrence and Johnston, 1989). The expression patterns of ftz and eve are complementary and at this stage there is overlap at the edges of each expression domain. Where the two expression domains overlap correspond to the positions where parasegmental boundaries will later be formed (Fig. 1.6A). By gastrulation the stripes of *ftz* and *eve* have narrowed to sharp stripes, of two to three cells in width, which have very distinct anterior boundaries and less distinct posterior boundaries (Fig. 1.6B; Hafen et al., 1984; Carroll and Scott, 1985; Macdonald et al., 1986). The boundaries of the parasegments correspond to the anterior stripe boundaries of *ftz* and *eve* expression (Lawrence et al., 1987; Lawrence and Johnston, 1989). This prompted the theory that it is these sharp anterior stripe boundaries and the high levels of *ftz* and *eve* expression that determine where and when parasegment borders are established.

ftz and *eve* are transcription factors that activate parasegment-specific genes, including numerous segment-polarity and homeotic genes

Figure 1.6: *eve* and *ftz* are expressed in alternating parasegments. *eve* expression establishes the odd-numbered parasegments and *ftz* establishes the even-numbered parasegments. The vertical dashed lines mark the parasegmental boundaries. A) In the syncytial blastoderm *ftz* and *eve* are expressed in bell-shaped gradients. *ftz* and *eve* are expressed in complementary patterns with overlap at the edges of each expression pattern. B) By gastrulation, cells have been formed and the expression of *ftz* and *eve* has been refined. *ftz* and *eve* are now expressed most highly in the anterior-most cells of each parasegment, while the expression in the more posterior cells is gradually lost. Resolution of *ftz* and *eve* out of the posterior-most cells allows expression of the segment-polarity gene *wingless* (*wg*). Retention of *ftz* and *eve* expression in the anterior-most cells allows activation of the segment-polarity gene *engrailed* (*en*).

A)
Pre-cellularization
B)
Gastrulation
eve
wg
1
2
3
4
5
6
7
8
9
10
11
12
13
14

(Ingham and Martinez-Arias, 1986; Lawrence et al., 1987; Carroll et al., 1988a; Ingham et al., 1988; Irish et al., 1989; Peifer and Bejsovec, 1992). Expression of the segment polarity gene *engrailed* (*en*) in the anterior cell of each parasegment (Fig. 1.6B) is dependent upon the expression of *ftz* and *eve* as well as other pair-rule genes such as *odd* and *prd* (Carroll and Scott, 1986; Harding et al., 1986; Howard and Ingham, 1986; Macdonald et al., 1986; Lawrence et al., 1987; Carroll et al., 1988a; Ingham et al., 1988). Within thirty minutes of establishment of the periodic pattern of *ftz* and *eve* during cellularization, *en* protein is detectable (DiNardo et al., 1985; Fjose et al., 1985; Kornberg et al., 1985). The *en* protein (EN) is later required to establish the posterior sub-compartment of each parasegment (Morata and Lawrence, 1975; Kornberg et al., 1985). EN is a homeodomain-containing protein that is required to activate the expression of *hedgehog* (*hh*) in *en*-expressing cells (Heemskerk and DiNardo, 1994). *hh* encodes a secreted signaling molecule (morphogen) which is a novel, self-processing cholesterol anchored protein that mediates many patterning processes in vertebrates and invertebrates (Hammerschmidt et al., 1997).

A second segment polarity gene, *wingless* (*wg*) is expressed in the most posterior cells of each parasegment (Fig. 1.6B), partly as a result of negative regulation by *ftz* and *eve* (Baker, 1987; Ingham et al., 1988). *wg* encodes a signaling molecule and is a member of the large family of WNT proteins (Rijsewijk et al., 1987). WG acts as a morphogen and is required embryonically to establish cell fate and polarity within the parasegment (Cabrera et al., 1987; DiNardo et al., 1988; Martinez Arias et al., 1988; Bejsovec and Martinez Arias,

1991; Ingham and Martinez Arias, 1992; Noordermeer et al., 1992; Peifer and Bejsovec, 1992; Vincent and O'Farrell, 1992; Struhl and Basler, 1993; Zecca et al., 1996).

wg and *en/hh* expressing cells are juxtaposed on either side of the parasegmental boundary (Fig. 1.6B) and as such provide markers for boundary position. It has been shown that between 4 and 5.5 hours of development, reciprocal signaling between the *wg* and *en/hh* expressing cells is required for stabilization of their expression and thus consolidation and maintenance of the parasegmental borders (DiNardo et al., 1988; Martinez Arias et al., 1988; Poole and Kornberg, 1988; Bejsovec and Martinez Arias, 1991; Heemskerk et al., 1991; Lee et al., 1992; Vincent and O'Farrell, 1992; Ingham, 1993). Through the remainder of embryogenesis, *wg* and *en/hh* expression become independent of one another and each gene acts to determine specific cell fates within the parasegment (Dougan and DiNardo, 1992; Bejsovec and Wieschaus, 1993; Gritzan et al., 1999).

Initial expression of the homeotic genes, which provide each parasegment with a unique identity, is also coincident with parasegmental boundaries (Duncan, 1986; Ingham and Martinez-Arias, 1986; Carroll et al., 1988a; Muller and Bienz, 1992). Gap genes provide region specific pattern, while pair-rule genes provide parasegment specific pattern. For example, *ftz* protein is a direct transcriptional activator of the homeotic gene *Ultrabithorax* (*Ubx*) in parasegment 6, the main domain of *Ubx* function (Muller and Bienz, 1992). Within the *Ubx* promoter there are *ftz* DNA binding sites that are adjacent to or overlap with *hb*

binding sites. HB, a gap protein, is a repressor of *Ubx* activity. It is proposed that competition between FTZ and HB for these binding sites, or overcoming the repressive effects of HB are the likely mechanisms that results in the formation of the sharp anterior boundary of *Ubx* expression in parasegment 6 (Muller and Bienz, 1992).

The expression of *Ubx* is also coincident with parasegment borders as defined by expression of *ftz*-lacZ in parasegment 6 and *eve*-lacZ in parasegment 5 (Lawrence, 1988). *ftz* is also required for the activation of other homeotic genes in the *Antennapedia* and *bithorax* complexes (such as *Sex combs reduced* and *Antennapedia)* in the proper pattern and parasegment (Ingham and Martinez-Arias, 1986). Thus, *ftz* and *eve* expression not only determine where parasegmental boundaries are formed, but also activate gene whose products are required to maintain parasegmental boundaries. Through the subsequent activation of specific homeotic genes, *ftz* and *eve* also provide parasegments with their specific identities.

1.4.6 Previously proposed mechanisms for how ftz and eve establish en and wg expression

It was suggested initially that a gradient of FTZ or EVE, within a stripe, highest at the anterior and lower at the posterior, might be interpreted directly by *en* (Ingham et al., 1988; Lawrence and Johnston, 1989). In this model, the peak in expression at the anterior edge, means that *en* would be activated above a certain threshold of *eve* or *ftz* expression (Ingham et al., 1988; Lawrence and

Johnston, 1989). Recent evidence suggests that, at least for *ftz,* this does not occur as the *ftz* stripe is not a gradient. Rather, each cell contains similar amounts of FTZ except at the posterior edge of the stripe where expression is dropping off (Krause et al., 1988; Lawrence and Pick, 1998). It was also demonstrated that *ftz* expression could be lowered by EVE and *en* expression would still initiate in the correct cells (Manoukian and Krause, 1992). Additionally, when the number of copies of the *ftz* gene are artificially increased from one to four, antibody staining shows an overall increase in the amount of FTZ within all cells in the stripe. If a threshold effect were occurring, *en* activation should now occur earlier and in broader stripes (Lawrence and Pick, 1998). This was not observed, suggesting that, after cellularization, FTZ activity does not depend on its expression being in a gradient. However, there is evidence that *eve* may function by a different mechanism to activate *en* and that there does appear to be a gradient of EVE within each stripe (Frasch et al., 1988; Warrior and Levine, 1990).

In an alternative model, EVE activates *en* indirectly within the *ftz*-dependent parasegment, perhaps through direct repression of *odd* (Fig. 1.7; Manoukian and Krause, 1992). EVE represses both *ftz* and *odd* directly, however *odd* is more sensitive to lower levels of EVE than *ftz*. *odd* and *ftz* expression are completely overlapping at the anterior edge at syncytial blastoderm, but *odd* expression disappears from the anterior cells of the even-numbered parasegment during gastrulation (Manoukian and Krause, 1992; Fujioka et al., 1995); Fig. 1.7). This loss of *odd* expression begins in the stripes

Figure 1.7: A schematic of the expression patterns of several pair-rule genes at gastrulation that are involved in the regulation of the segment-polarity genes *en* and *wg*. Two parasegments are illustrated; a *eve* –dependent odd-numbered parasegment and a *ftz*-dependent even-numbered parasegment. Some of the interactions have been determined directly by kinetic experiments and others are inferred by genetic interactions. A blunt ended line (in red) indicates a gene that represses another gene. A solid line (in green) arrow indicates a gene that activates another.

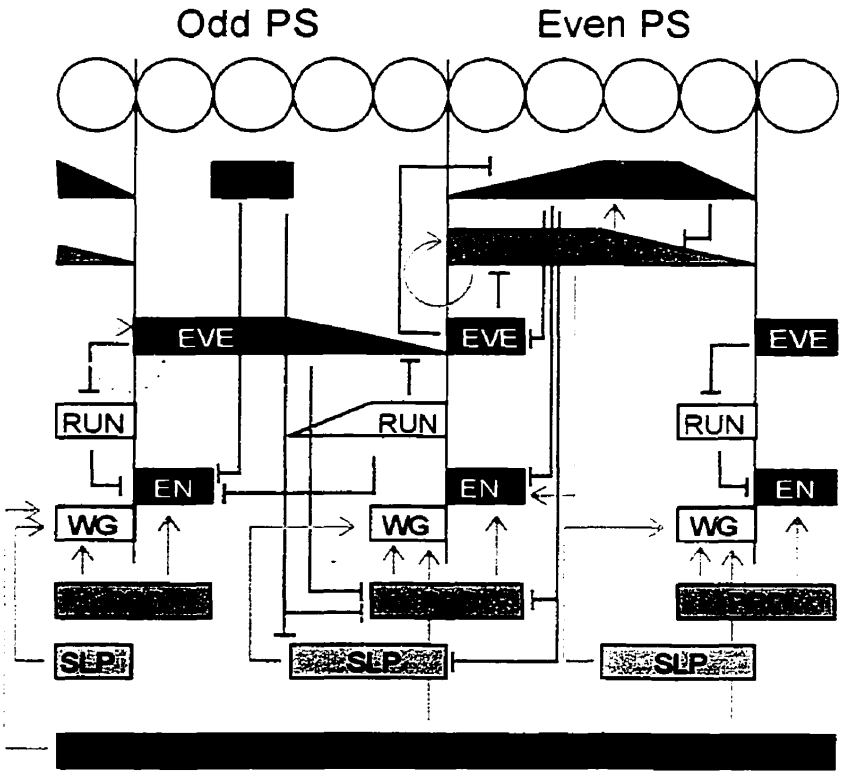

slp = odd-placed

out = odd-staggered

at the anterior of the embryo just before the *en* stripes appear. In *eve* null embryos, the expression of *ftz* and *odd* remain completely overlapping and *en* fails to be activated (DiNardo and O'Farrell, 1987). In embryos null for both *eve* and *odd*, expression of *en* re-appears within the *ftz*-dependent parasegments (DiNardo and O'Farrell, 1987). Although *en* expression is not quite the same as wild type (*en* stripes are wider and not equivalently spaced), the reappearance of *en* expression suggests that *eve* and *odd* play a role in the establishment of the correct width and placement of the even-numbered (*ftz*-dependent) *en* stripes (DiNardo and O'Farrell, 1987). FTZ is able to directly activate *en* expression, most likely once *odd* is repressed by EVE (Nasiadka and Krause, 1999). Additionally during gastrulation, *eve* is expressed weakly in the *ftz*-dependent parasegments (Harding et al., 1986; Macdonald et al., 1986). It is proposed that this low level of EVE in the *ftz*-dependent parasegment is also sufficient to repress *odd* but not *ftz* (Fig. 1.7; Manoukian and Krause, 1992). However, there are some inconsistencies with this hypothesis. The repression of some *odd* stripes occurs at cellular blastoderm, which is prior to when the late minor *eve* stripes appear (Fujioka et al., 1995). Thus, Fujioka et al., conclude that the minor *eve* stripes are not required for *eve* regulation in the *ftz* domain (Fujioka et al., 1995). They suggest that the posterior trailing edges of the early *eve* stripes in the *eve*-dependent parasegments are sufficient for mediating the effects on *ftz* and *odd* (Fujioka et al., 1995). However, other studies suggest that the late minor *eve* stripes are also likely to contribute to the level of expression and maintenance of the odd-numbered *en* stripes (Manoukian and Krause, 1992). It

appears that *eve* will interact with different combinations of pair-rule genes as well as in a concentration dependent manner (Manoukian and Krause, 1992; Fujioka et al., 1995). Thus, EVE activates the even-numbered (*ftz*-dependent) *en* stripes indirectly by repressing *odd*.

The odd-numbered *en* stripes are most likely activated by a combination of *eve* and another pair-rule gene, *prd* (Fig 1.7). These *en* stripes initiate at the posterior edges of the early *prd* stripes where they overlap with the anterior edges of the early *eve* stripes (Scott and O'Farrell, 1986; DiNardo and O'Farrell, 1987; Ingham et al., 1988). *prd* is initially expressed in seven stripes that overlap the even-numbered parasegments (Kilchherr et al., 1986; Ingham et al., 1988; Baumgartner and Noll, 1990). The broad stripes lose expression in the middle of each parasegment resulting in fourteen stripes that overlap each parasegment boundary (Frigerio et al., 1986; Kilchherr et al., 1986; Ingham et al., 1988; Baumgartner and Noll, 1990). These stripes of *en* are missing in either *eve* or *prd* mutants (DiNardo and O'Farrell, 1987; Ingham et al., 1988). Conversely, ectopic expression of *prd* results in the posterior expansion of odd-numbered *en* stripes (Morrissey et al., 1991). Thus, initial activation of odd-numbered *en* stripes requires both *eve* and *prd*.

Restriction of the anterior boundaries of these *en* stripes in the odd-numbered parasegment may be controlled, in part, by the late expression of *run*. Initially, *run* expression in seven stripes overlaps the posterior half of each *eve* stripe and the anterior half of each *ftz* stripe (Fig. 1.7; Kania et al., 1990). By gastrulation *run* expression is expressed in 14 stripes in the posterior portion of

each parasegment (Manoukian and Krause, 1992). RUN can directly repress odd-numbered *en* stripes (Fig. 1.7; Manoukian and Krause, 1992). In turn, run is repressed by lower concentrations of EVE than is prd which allows the activation of *en* in cells that express *prd* but not *run* (Fig. 1.7). *en* stripes are of normal size but have slightly altered spacing in *run* mutants. The odd-numbered (*eve*-dependent) *en* stripes are expanded, but are then subsequently repressed in the middle thus producing fourteen stripes (Manoukian and Krause, 1992). The even-numbered (*ftz*-dependent) *en* stripes are lost (Manoukian and Krause, 1992). Thus, it has been suggested that the even-numbered *en* stripes in *run* mutants are ectopic *en* stripes activated by *eve* and not by *ftz* (Manoukian and Krause, 1992).

Other genes that may be acting on the *en* stripes are the products of the genes *sloppy-paired* (*slp*) and *odd* (Fig. 1.7; Fujioka et al., 1995; Saulier-Le Drean et al., 1998). *slp* is also repressed by EVE in a concentration-dependent manner. *slp* is repressed at lower concentrations of EVE than is *prd* and thus may act in a similar manner to *run* on *en* expression, in that SLP may be repressing the anterior boundary of the *en* stripes. Like RUN, ectopic SLP abolishes all *en* expression (Cadigan et al., 1994). ODD stripes in even-numbered parasegments, as well as the later arising ODD stripes in the odd-numbered parasegments, repress the expression of *en* both directly and indirectly (Fig. 1.7; Saulier-Le Drean et al., 1998). ODD acts indirectly on *en* by repressing the *en* activators *ftz*, *prd*, *eve* and *slp* (Fig. 1.7; Saulier-Le Drean et al., 1998). ODD also directly represses *en* expression (Saulier-Le Drean et al.,

1998). This repression of *en* is removed when EVE directly represses *odd*, thus allowing the activation of *en* by FTZ or PRD.

FTZ and EVE repress the activity of *wg*, such that *wg* is only expressed in a single row of cells at the posterior edge of each parasegment after FTZ and EVE have resolved out of these cells (Ingham et al., 1988; Fig. 1.6B and Fig. 1.7). In *ftz* or *eve* mutants *wg* is activated ectopically, in effect filling in the regions between stripes where *ftz* or *eve* are missing (Ingham et al., 1988).

In the absence of *prd*, or *odd-paired* (*opa*; expressed ubiquitously in the embryo) *wg* expression is lost in alternating segments (Fig. 1.7; Ingham et al., 1988). Thus, *prd* and *opa* may be required to activate the expression of *wg* in the cells that first lose *ftz* and *eve* expression. The activity of *slp* is also required for the activation of *wg* expression in all parasegments (Cadigan et al., 1994). Ectopic expression of *slp* results in a nearly ubiquitous expression of *wg* (Cadigan et al., 1994). The expression of *wg* is repressed directly by *odd* in all parasegments (Saulier-Le Drean et al., 1998). *odd* also represses the expression of *prd* and *slp*, which normally activate *wg* (Fig. 1.7; Saulier-Le Drean et al., 1998). This is consistent with the fact that in *odd* mutant embryos, *wg* stripes are expanded (Mullen and DiNardo, 1995).

In summary, the correct expression of *en* within the anterior most cell of each parasegment and *wg* in the most posterior cell are dependent upon *ftz* and *eve* as well as the combinatorial activities of several other pair-rule genes. Inter-regulation between *eve*, *run*, *odd* and *slp* denote the anterior and posterior boundaries of *en* stripes, while *ftz*, *eve*, and *prd* are involved in activation. Inter-

regulation between odd and slp restricts the widening of *wg* stripes when the stripes of *ftz* and *eve* narrow, while *prd* and *opa* may also be involved in *wg* activation.

1.5 What happens when compartment size is altered during embryogenesis?

An interesting property of compartments is that they appear capable of sensing and modulating their size in response to improper specification. In *Drosophila* embryos, an experiment that addressed the effects of changing parasegment compartment size used genetic manipulation of the maternal gene *bicoid (bcd)*. *bcd* establishes the primary anterior-posterior patterning and acts in a concentration-dependent manner (Frohnhofer and Nusslein-Volhard, 1986; Nusslein-Volhard et al., 1987; Berleth et al., 1988; Driever and Nusslein-Volhard, 1988a). When the number of copies of the *bcd* gene are increased or decreased, corresponding shifts in the anterior-posterior fate map occur. For example, an anterior morphological marker, the cephalic furrow, is normally located at 65% egg length just behind the region that forms the head. When one copy of the *bcd* gene is removed, the cephalic furrow shifts anteriorly by 16% (Driever and Nusslein-Volhard, 1988a). Conversely, increasing the number of copies of the gene to three or four shifts the cephalic furrow posteriorly by 6% and 9%, respectively (Driever and Nusslein-Volhard, 1988a). Because of the increase in size of the anterior parasegments, some of the posterior compartment sizes are correspondingly reduced. This was shown by observing

the expression of *eve* (Driever and Nusslein-Volhard, 1988a). Thus, a link was established between the number of copies of the *bcd* gene, changes in the size of the expression domains of various segmentation genes, and changes in parasegment size (Struhl, 1989; Cohen and Jurgens, 1990; Eldon and Pirrotta, 1991; Kraut and Levine, 1991). Nevertheless, despite these early changes in parasegment size, wild type larvae and adults were obtained (Frohnhofer and Nusslein-Volhard, 1986; Berleth et al., 1988; Driever and Nusslein-Volhard, 1988a). Therefore, it was concluded that the altered parasegments must be capable of sensing and correcting their size later in development.

Subsequent studies showed that many of the embryos in which *bcd* copy number was manipulated did not survive. One study, for example, examined the effects of mothers carrying seven copies of the *bcd* gene (Busturia and Lawrence, 1994). This appears to be the maximum number of copies of the *bcd* gene that can be introduced. As expected, the head regions were greatly enlarged, while parasegments in the trunk region were compressed in size (Busturia and Lawrence, 1994). The majority of these embryos developed with minor segmental defects and only 25% were able to hatch. Fewer cells were present in all parasegments and the numbers of cells were not corrected by adulthood as determined by bristle number (each cell produces one bristle) (Busturia and Lawrence, 1994). Parasegment 8 (corresponding to abdominal segment 3; A3) was the most severely affected with 85% of cuticles showing defects. Thus, this study demonstrated that although the embryo does retain

some ability to correct to wild type, compartments that are significantly altered in size are increasingly less able to do so.

Another study confirmed that embryos from mothers containing one or two copies of *bcd* produced wild type larvae despite initial decreases in the size of the anterior anlagen (Namba et al., 1997). However, approximately 15% of embryos from mothers with four copies of *bcd* exhibited very minor cuticular phenotypes consisting of one missing denticle band or a fused set of denticle bands (Namba et al., 1997). Embryos from mothers with six copies of *bcd* showed various defects with only 30% of the larvae exhibiting completely wild type cuticles. The majority of larvae had defects that ranged from a mild fusion or lack of single denticle belts (25%), to malformed denticle belts in more than two segments (21%), to a complete lack of segmentation (24%; Namba et al., 1997). Interestingly, it was found that repair of the expanded compartments resulted from excess apoptosis, whereas the compressed compartments exhibited a reduction in the levels of apoptosis (Namba et al., 1997).

As described earlier, parasegmental boundaries are dependent upon the activities of *ftz* and *eve,* which act downstream of the genes (such as *bcd*) that initially establish the anterior-posterior pattern. Are parasegmental compartments able to respond to changes in size as a result of changes in *ftz* and *eve* gene expression? The results obtained from changing *bcd* gene copy number are somewhat conflicting and the extent to which parasegmental compartments can be altered and still revert to wild type size is unclear. This relates to the question of exactly how and when parasegmental boundaries are

positioned and what happens when altered boundaries are returned or fail to return to their proper positions. For example, if reduced parasegments are not removed by increased rates of apoptosis, how are they deleted? How do *ftz* and *eve* pair-rule phenotypes arise? Prevalent theories are conflicting and incomplete on these questions.

1.6 Overview of thesis

The first metameric units within the *Drosophila* embryo are the parasegments, which are defined by the expression of *ftz* and *eve.* In Chapter 2, I investigate the role of *ftz* and *eve* in the establishment of parasegmental boundaries. By specifically altering the expression levels of *ftz* and/or *eve*, the positioning of parasegmental boundaries can be changed. The improper placement of parasegmental boundaries results in parasegmental compartments of altered sizes. In Chapter 3, I examine what happens to parasegmental compartments that have been altered in size. Compartments that are changed in size by more than 30% or more are unable to correct back to wild type. This suggests that parasegmental compartments are plastic, with an ability to tolerate small changes in size. Additionally, the *ftz* and *eve* pair-rule mutant phenotypes are not due to a simple deletion of every other segment, but rather to a complex process involving cell respecification, cell movement, and cell death. Finally I discuss these results, how they relate to segmentation within metazoans in general, and suggest possible future experiments. Three appendices are also included which describe the fluorescent in situ hybridization approach developed to facilitate these studies.

CHAPTER 2: THE RELATIVE LEVELS OF FTZ AND EVE EXPRESSION POSITION THE PARASEGMENTAL BOUNDARIES EARLY IN EMBRYOGENESIS

This chapter comprises half of a similar report submitted to Development by Sarah Hughes and Henry M. Krause (2000)

2.1 Abstract

Parasegments are initially defined by alternating stripes of expression of *ftz* and *eve*. However, the mechanism and timing of *ftz* and *eve*-mediated establishment of parasegment boundaries remain unclear. In this chapter, I show that parasegment widths are defined early in development by the relative levels of *ftz* and *eve* at stripe junctions. Changing these levels resulted in alternating widened and narrowed parasegments as marked by the shifted stripes of *en*, which continue to mark parasegmental boundaries. If the relative levels of *ftz* and *eve* were changed equivalently, wild type spacing of the parasegmental boundaries was re-established.

2.2 Introduction

The *Drosophila* embryo is divided into fourteen parasegmental compartments; the basic units of organization within the early embryo (Martinez-Arias and Lawrence, 1985; Lawrence, 1988). As described in Chapter 1, parasegmental compartments are established through a hierarchy of interacting maternal and zygotic genes that divide the embryo initially into broad domains and then into successively finer domains. The expression of *ftz* and *eve* are proposed to establish the sub-division of the embryo into parasegments (Lawrence et al., 1987; Lawrence and Johnston, 1989). *ftz* and *eve* are expressed during late syncytial blastoderm in seven broad stripes. By gastrulation, the expression pattern of each gene has resolved into narrow stripes with sharp anterior boundaries (Harding et al., 1986; Frasch and Levine,

1987). The boundaries of the parasegments correspond exactly to the distinct anterior edges of each *ftz* and *eve* stripe (Lawrence et al., 1987; Ingham et al., 1988; Lawrence and Johnston, 1989). *eve* expression establishes the odd-numbered parasegments, whereas *ftz* expression establishes the even-numbered parasegments. FTZ and EVE have been shown to regulate a number of genes, which are specifically expressed within the boundaries of a parasegment. Well characterized examples include the segment-polarity genes *en* and *wg,* as well as the homeotic gene *Ubx* (Ingham and Martinez-Arias, 1986; Macdonald et al., 1986; Baker, 1987; Lawrence et al., 1987; Carroll et al., 1988a; Ingham et al., 1988; Irish et al., 1989; Muller and Bienz, 1992; Peifer and Bejsovec, 1992).

Although it is clear from previous studies that *ftz* and *eve* define parasegmental boundaries, exactly how and when they do so has been a subject of debate. The earliest models suggested that *ftz* and *eve* position the parasegmental borders after gastrulation, about an hour after the two genes are first expressed (Lawrence et al., 1987; Lawrence and Johnston, 1989). This assumption was based on three observations; first, the borders of *ftz* and *eve* stripes are diffuse and overlapping before this time (Frasch and Levine, 1987; Kellerman et al., 1990; Ingham and Martinez Arias, 1992). Second, induction of the downstream target gene *engrailed* (*en*) coincides temporally and spatially with the resolution and intensification of anterior *ftz* and *eve* stripe borders (Lawrence et al., 1987; Ingham et al., 1988; Kellerman et al., 1990). Third, in some of the first pair-rule phenotypes to be characterized, the anterior borders of

ftz and *eve* stripes failed to intensify and sharpen (Howard and Ingham, 1986; Frasch and Levine, 1987; Carroll et al., 1988b; Carroll and Vavra, 1989). For example, in *eve* mutants, *ftz* stripes remain broad and symmetric, and do not sharpen at the anterior edge (Carroll and Scott, 1985; Harding et al., 1986; Frasch and Levine, 1987; Frasch et al., 1988; Lawrence and Johnston, 1989). In *eve* mutants, metamerization does not occur and no *en* stripes are activated (Nusslein-Volhard et al., 1984; Harding et al., 1986; Frasch et al., 1988). The lack of metamerization was interpreted to be a result of the lack of the sharp anterior boundaries of *ftz* expression, which somehow renders *ftz* unable to activate *en* (Lawrence and Johnston, 1989). Subsequent studies, however, have shown that parasegmental borders can still form when the levels (or activities) of *ftz* and *eve* are altered and when their anterior stripe borders fail to sharpen (DiNardo and O'Farrell, 1987; Frasch et al., 1988; Kellerman et al., 1990; Lawrence and Pick, 1998; Nasiadka and Krause, 1999). However, in general, it was thought that the expression pattern of *ftz* and *eve* at gastrulation, specifically the high expression in the cells at the anterior of the parasegment, was important in demarcating parasegmental boundaries. *ftz* and *eve* expression in the remaining posterior portions of the parasegment was proposed to be non-essential (Lawrence et al., 1987).

This chapter focuses on how parasegmental boundaries are positioned. My results show that parasegmental widths are first defined well before the completion of cellularization by the relative levels of *ftz* and *eve* expression. Changing these levels in pre-cellularized embryos resulted in major changes in

parasegment widths, producing enlarged and reduced parasegments. However, *ftz* and *eve* expression levels could be changed quite dramatically with no effects on parasegmental boundaries so long as the relative levels were kept in balance.

2.3 Materials and Methods

2.3.1 Drosophila stocks

Stocks were maintained on a basic cornmeal, agar, molasses, sugar mix at 25°C. Several stocks were used to address how altering the relative levels of *ftz* and *eve* affect embryonic development. The *eve* hypomorphic allele, $cn^1 eve^{ID19} bw^1 sp^1$/CyO (obtained from the Bloomington Stock Centre) is a temperature sensitive allele (amino acid 121 changed from an arginine to a histadine within the homeodomain) that expresses progressively lower levels of *eve* within the embryo as the temperature is increased (Frasch et al., 1988). Normal levels of *eve* are present at 18°C, however at 29°C there is almost no *eve* present within the embryo (Frasch et al., 1988). Another temperature sensitive allele, ftz^{54B}/TM3, generated by ethyl methanesulfonate, was used to lower the level of *ftz* within the embryo (obtained from Bloomington Stock Centre). This line expresses normal levels of *ftz* at 18°C that become reduced as the temperature is raised (Wakimoto et al., 1984).

A transgenic line *HSFtz* (*hsf2*), which contains the *hsp70* promoter gene attached to the *ftz* gene, was used to raise levels of *ftz* within the embryo (Struhl, 1985). *HSFtz* is a homozygous viable line inserted on the second chromosome. A second *HSFtz* construct (*hsf245A*), homozygous viable on the third chromosome, was also used where required for specific genetic combinations (Fitzpatrick et al., 1992). Both *HSFtz* lines produce similar phenotypes under similar heat shock conditions. The cellular levels of *ftz* produced from the *HSFtz* transgene following an 8 minute heat shock are lower than endogenous levels of

FTZ (Struhl, 1985; Fitzpatrick et al., 1992; Nasiadka and Krause, 1999). Shorter heat shocks were used here.

A transgenic line with the *eve* gene under the control of the *hsp70* promoter (*HSEve*; obtained from Gary Struhl), is homozygous on the second chromosome, and was used to raise the expression levels of *eve* within the embryo.

Oregon R stocks were used as wild type controls. All other stocks used were prepared from these original lines. Where required, mutant second chromosomes were balanced over a CyO balancer marked with a *hunchback lacZ* reporter gene to mark homozygous embryos (Driever at al., 1989). To analyze the expression history of *ftz* and *eve,* a lacZ reporter attached downstream to either the *ftz* or *eve* promoter was used. A *ftzlacZ* transgenic construct balanced over a TM3 balancer (Hiromi et al., 1985) and an *evelacZ* transgenic insertion on a SM6 balancer (Pazdera et al., 1998) were used in combination with eve^{ID19} or *HSFtz* and *HSEve* lines.

2.3.2 Embryo collections

Embryos were collected on apple juice-agar plates that were applied with a fresh yeast paste. Pre-collections of at least one hour were used to ensure proper timing of embryos. Embryo collections of thirty minutes were aged at 25°C until the required embryonic age. Stages of embryogenesis were assigned as described in (Campos-Ortega and Hartenstein, 1985). All heat shocks were carried out in a 36.5°C water-bath by complete immersion for the specified

amount of time. Embryos were dechorionated and fixed in 5% EM grade formaldehyde as described in Lehmann and Tautz (Lehmann and Tautz, 1994). Cuticles were prepared from 24-hour-old embryos as described in Saulier-Le Drean et al (1998).

2.3.3 DNA probes for in situ hybridization (probe preparation and protocol)

DNA probes were prepared by PCR as adapted from the Boehringer Mannheim protocol by Patel and Goodman (1992). Initially, a template was prepared using two primers (T3 and T7; Promega) to amplify the cDNA portion of the *en* gene from the plasmid *pBSen* (from S. DiNardo). PCR reaction conditions consisted of 30 cycles at 94°C for 1 minute, 53°C for 45 seconds, 72°C for 1.5 minutes. The template was then used directly in the labeling reaction using DIG DNA Labeling Mix (Boehringer Mannheim) and a single primer (T3) to produce a run-off anti-sense probe using PCR. The same PCR reaction conditions described above were used in the labeling reaction. To reduce the overall size of the probe, it was boiled for 3-5 hours. For hybridization, 5 µl of boiled probe was added to 95 µl of DNA hybridization solution, heated for 5 minutes, cooled on ice and added to approximately 50 µl of settled embryos. Hybridization and post-hybridization washes were carried out as described previously (Saulier-Le Drean et al., 1998). Immunohistochemistry for antibody detection was also carried out as described in (Saulier-Le Drean et al., 1998). A DAB substrate kit (Pierce) was used to develop horseradish peroxidase signals. An EN monoclonal antibody (4D9; from

T. Kornberg and the Developmental Hybridoma Bank) and anti-βgal (Promega) antibody were used singly or simultaneously.

2.3.4 Double fluorescent antibody labeling

Embryos for immunofluorescence were collected and fixed as described above. Embryos were rinsed two times in methanol, then twice in PBTBB (1X PBS + 0.1% Tween 20 + 0.5% skim milk powder + 0.05% BSA). Blocking in PBTBB was carried out at room temperature for at least 2 hours. Primary antibodies [mouse α–*en* 4D9 (1:1000), mouse α–*wg* 4D4 (1:10) (Developmental Hybridoma Bank), rabbit α–spectrin (1:1000; Obtained from D. Branton)] were diluted in PBTBB and incubated with embryos overnight at 4°C. After washing, appropriate secondary antibodies [α-mouse CY3 (1:1000), α-mouse CY2 (1:1000), α-rabbit CY3 (1:1500); α-sheep CY3 (1:1000) all obtained from Jackson ImmunoResearch Laboratories Inc., or α-rabbit FITC (1:500; obtained from KPL Laboratories] were diluted in PBTBB and incubated with the embryos for two hours. If two primary antibodies from the same species were used, one antibody was added first and then blocked with unconjugated sheep-α-mouse or sheep-α-rabbit antibodies (1:200; Jackson ImmunoResearch Laboratories Inc) as per manufacturer's instructions. After incubation with secondary antibodies, embryos were washed in PBTBB. Alternatively, embryos were incubated in biotinylated α-mouse antibody (Vector Labs; 1:300) for two hours, washed for 2 hours in PBTBB, and then incubated with Streptavidin Texas Red (Amersham; 1:200) for 2 hours. After incubation with secondary antibodies, washes in

PBTBB were carried out until background levels were sufficiently reduced. Embryos were resuspended in 2.5% DABCO (1,4-Diazabicyclo [2.2.2.] Octane) in glycerol, mounted on slides and imaged using a Leica TCSNT confocal microscope.

2.3.5 Temperature shifts

eve^{ID19} and *HSFtz* embryos were collected at 25°C as described previously. For *eve*^{ID19} embryos, the apple juice-agar plates were then placed at the specific temperatures in a series from 18°C to 30°C in two-degree increments and aged until 4 to 4.5 hours after egg laying (AEL). Appropriate alterations were made to accommodate the rate of aging at each temperature. Embryos were then fixed and analyzed by *in situ* hybridization for the expression of *en*. *HSFtz* embryos were collected and aged at 25°C. At 2.5-3 hours AEL, a heat shock was administered in a timed series extending from no heat shock to a 6 minute heat shock. At 4 to 4.5 hours AEL the embryos were fixed and analyzed by *in situ* hybridization for the expression of *en*.

2.3.6 Survival studies

Embryos were collected for 30 minutes, aged at 25°C until 2.5–3 hours AEL and then heat shocked for 4 minutes. Approximately 300 to 600 embryos for each genetic background were collected and then transferred to food vials and allowed to develop at 25°C. The food vials were cut off at the level of the food such that embryos could be placed directly on the food subsequent to heat

shock with minimal manipulation. The percentage of larvae that hatched and the percentage of adults that eclosed were counted. Reported larval hatchings were adjusted to approximate homozygous numbers based on predicted mendelian genetic fractions. Homozygous adult survivors were scored using phenotypic markers.

2.4 Results

2.4.1 Altering the relative expression levels of ftz and eve alters the position of parasegment boundary formation

Changing the relative levels of *ftz* and *eve* expression within the early embryo produces very specific and reproducible segmental phenotypes (Fig. 2.1). The expression/activity levels (simplified to "levels" hereafter) of *ftz* and *eve* were altered within the embryo using either heat shock-inducible transgenes (Fig. 2.1C; *HSFtz*, Fig. 2.1D; *HSEve*) or temperature-sensitive alleles (Fig. 2.1B; eve^{ID19}, Fig. 2.1E; ftz^{54B}). Decreasing the level of *eve* (Fig. 2.1B), or increasing the level of *ftz* (Fig. 2.1C), early in development, produced a pattern in which the even-numbered abdominal segments (A2, A4, A6, A8) were absent (Fig2.1A). Alternately, when the level of *eve* was increased (Fig. 2.1D) or the level of *ftz* was decreased (Fig. 2.1E), the odd numbered abdominal segments (A1, A3, A5, A7) were absent. This absence of alternate cuticle segments is characteristic of pair-rule gene phenotypes (Nusslein-Volhard and Wieschaus, 1980). However, this pattern contrasts with what was observed earlier in embryogenesis. In stage 9 embryos, all fourteen parasegments were present, albeit altered in size (Fig. 2.1G-J). The stripes of *en*-expressing cells, which mark the parasegmental boundaries, were out of register as compared to wild type embryos (Fig. 2.1F).

Figure 2.1: Changing the relative levels of *ftz* and *eve* within embryos early in embryogenesis produces specific cuticular and embryonic phenotypes. A) A wild type cuticle. B) Cuticle produced by embryos heterozygous for an *eve* temperature sensitive (eve^{ID19}) allele. C) Cuticle phenotype observed when *ftz* levels are artificially elevated using heat shock *HSFtz*. D) Cuticle pattern observed when the levels of *eve* are artificially raised using heat shock *HSEve*. E) Cuticles produced from a heterozygous *ftz* hypomorph (ftz^{54B}) allele. Early in embryogenesis, all parasegments are present albeit altered in size. F) A stage 9 wild type whole mount embryo with fourteen equally sized parasegments as marked by the expression of the *en* gene. G) A similarly aged eve^{ID19} embryo in which the position of *en* stripes have been shifted. H) A stage 9 *HSFtz* embryo showing the same phenotype of coupled *en* stripes as in the eve^{ID19} embryo. I) The opposite pattern of shifted *en* stripes is seen in a stage 9 *HSEve* embryo. J) A stage 9, ftz^{54B} embryo that exhibits the same pattern of coupled *en* stripes as seen in the *HSEve* embryo.

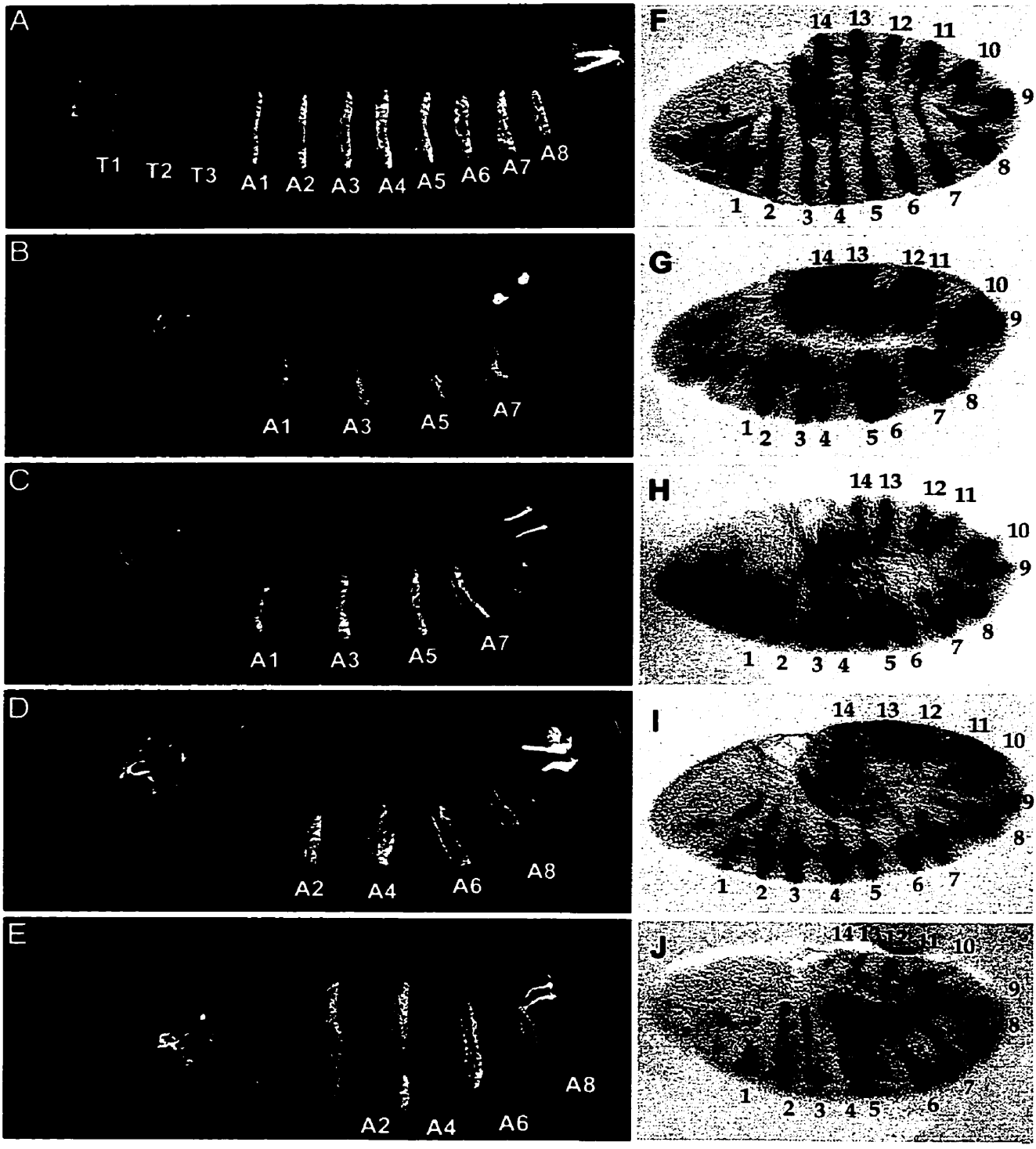
A
T1
T2
T3
A1
A2
A3
A4
A5
A6
A7
A8
B
A1
A3
A5
A7
C
A1
A3
A5
A7
D
A2
A4
A6
A8
E
A2
A4
A6
A8
F
14 13 12 11 10 9 8 7 6 5 4 3 2 1
G
14 13 12 11 10 9 8 7 6 5 4 3 2 1
H
14 13 12 11 10 9 8 7 6 5 4 3 2 1
I
14 13 12 11 10 9 8 7 6 5 4 3 2 1
J
14 13 12 11 10 9 8 7 6 5 4 3 2 1

When the level of *eve* was lowered (Fig. 2.1G) or *ftz* was increased (Fig. 2.1H) there was an increase in the size of the *ftz*-dependent parasegments at the apparent expense of the *eve*–dependent parasegments. As seen in the cuticular phenotypes, the opposite pattern was observed when the level of *eve* was increased (Fig. 2.1I), or the level of *ftz* was reduced (Fig. 2.1J). In this case, there was an increase in the size of the *eve*-dependent parasegments at the expense of the *ftz*-dependent parasegments. These results agree with previous studies on the patterns of *en*-expressing cells in eve^{ID19}, *ftz* hypermorphic, *HSFtz*, and *HSEve* embryos (DiNardo and O'Farrell, 1987; Kellerman et al., 1990; Manoukian and Krause, 1992; Nasiadka and Krause, 1999).

2.4.2 Coupled stripes of en expressing cells denote parasegments of altered sizes.

Parasegments are initially defined by the expression patterns of *ftz* and *eve*. Subsequently, several segment-polarity genes (e.g. *en*) and homeotic genes (e.g. *Ubx*) are activated within or coincident with the boundaries of the parasegment and can be used to identify a parasegmental region (Lawrence et al., 1987; Lawrence, 1988; Lawrence and Johnston, 1989). To confirm that the altered stripes of *en* expressing cells still mark the parasegmental boundaries I analyzed the expression of *ftz*, *eve* or UBX in the enlarged and reduced parasegments.

ftz- and *eve-lacZ* reporters were used to follow the expression of *ftz* and *eve*, as β-galactosidase protein is very stable thereby providing a history of its expression. In stage 12 wild type embryos, the expression of

ftz-lacZ was detected within each *ftz*-dependent parasegment (Fig. 2.2A). In *HSFtz* embryos the enlarged parasegments were marked by expanded expression of *ftz-lacZ*, which was expressed coincidentally with the even-numbered stripes of *en*- expressing cells (Fig. 2.2B). Ubx protein is normally activated to high levels throughout the sixth parasegment and within the anterior portions of the remaining abdominal parasegments in stage 10 wild type embryos (Fig. 2.2C). In *HSFtz* embryos, Ubx protein was present throughout the expanded *ftz*-dependent parasegment six and its anterior expression was coincident with the *en* stripes (Fig. 2.2D). In stage 12 wild type embryos, *eve-lacZ* expression was within the domain of each *eve*–dependent parasegment (Fig. 2.2E). In *HSEve* embryos, expression of the *eve-lacZ* transgene expanded within the boundaries of the enlarged *eve*-dependent parasegments (Fig. 2.2F). Expression of Ubx protein begins in parasegment 6, as was seen in wild type embryos, and this anterior-most stripe ass now much narrower, coincident with the reduced parasegmental widths (Fig. 2.2H). The expression patterns of *eve-lacZ* in *HSFtz*, *ftz–lacZ* in *HSEve*, and all combinations in eve^{ID19} have been analyzed and similar results to those described above were obtained (data not shown). In all cases, the expression patterns described indicated that, while stripes of *en* expression have shifted in position, they continued to mark parasegmental compartment borders.

Figure 2.2: Coupled stripes of *en* expression denote altered parasegment sizes. Embryos double-labeled for En (in red) and either *ftz*-lacZ, or *eve*-lacZ expression (in green) demonstrates that the altered parasegmental borders marked by the *en* expressing cells continue to represent parasegmental boundaries. The wild type expression of *ftz*-lacZ and *eve*-lacZ are illustrated in panels A and E respectively. The expression of either *ftz*-lacZ (B) or *eve*-lacZ (F) follows the apparent movement of the parasegmental border in *HSFtz* and *HSEve* embryos respectively. The expression of a downstream target, *Ubx*, also follows the change in position of the parasegmental boundaries. The wild type expression of Ubx protein (in green) is illustrated in stage 10 embryos (C and G). UBX is expressed at low levels in parasegment 5 and at higher levels in parasegment 6 in a stage 10, *HSFtz* embryo (D) and *HSEve* embryo (H). In either *HSFtz* or *HSEve* embryos, the expression of UBX is coincident with the altered positions of the *en* stripes.

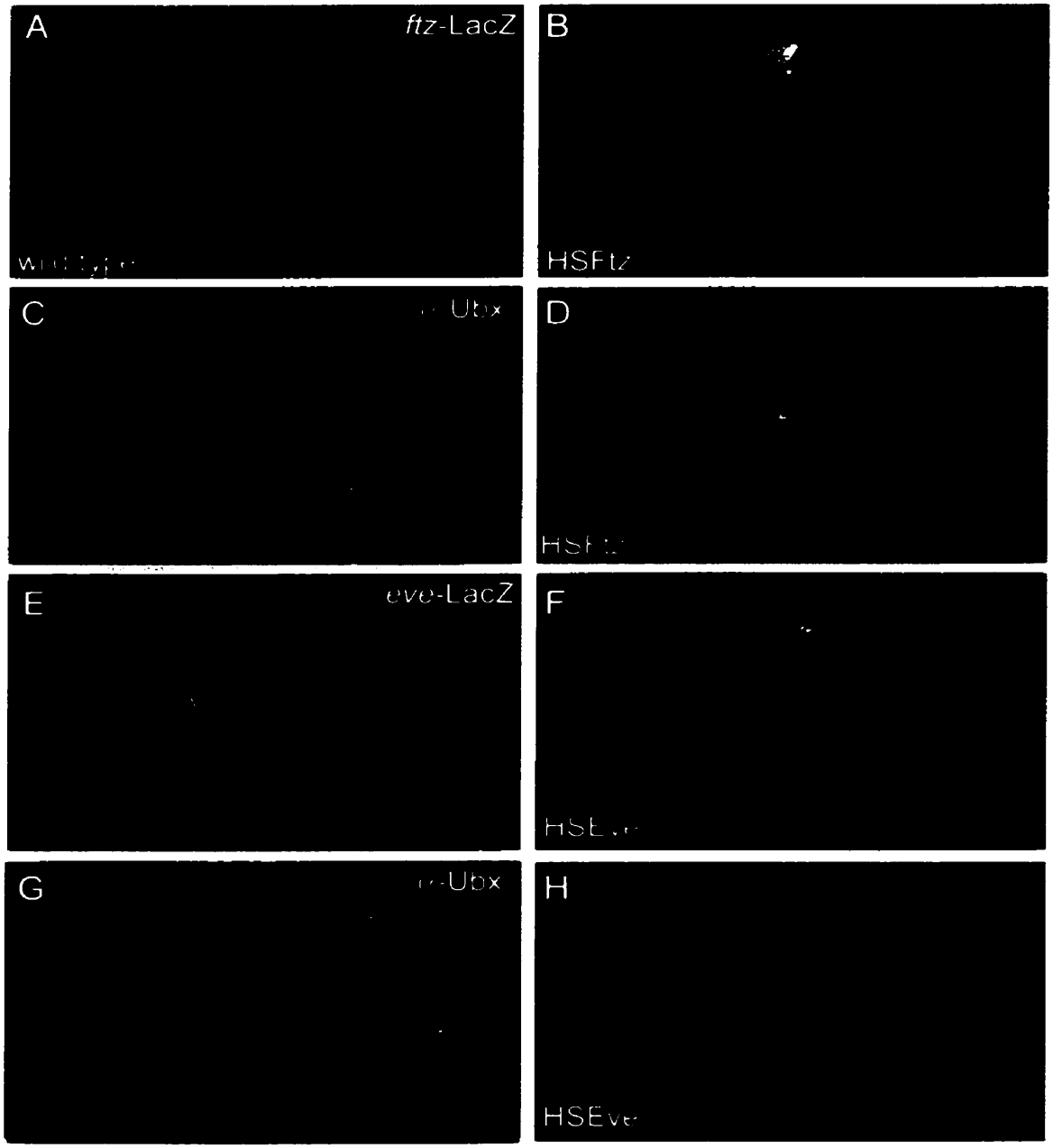
A
ftz-LacZ
B
HSFtz
C
Ubx
D
E
eve-LacZ
F
G
Ubx
H
HSEve

2.4.3 Relative levels of ftz and eve position the parasegmental boundaries

My research suggests (see Figure 2.1) that the relative levels of *ftz* and *eve* expression and activity determined the widths of alternate parasegments. To test this model further, I altered the levels of *ftz* and *eve* using various combinations of *ftz* and *eve* alleles that increase and decrease expression (see Materials and Methods for details). Embryos, 2.5-3hr AEL were subjected to a brief 4-minute heat pulse at 36.5°C. The effect of altering relative *ftz* and *eve* levels was analyzed by monitoring *en* expression, which marks the positions of the parasegmental borders.

The graph in Figure 2.3 shows the percentage of stage 9 (4-4.5 hours AEL) embryos that show either a normal (black), coupled (grey) or severe (white; partial stripe fusing) change in parasegmental border position. Wild type embryos exhibited an equally spaced pattern of *en* stripes. When wild type embryos were heat shocked for 4 minutes, there are a small number of both the altered *en* stripe patterns (3% and 4%). This provided a control for the effect of heat shock alone. When *eve* or *ftz* levels were lowered or raised, the majority of embryos exhibited a coupled pattern (Fig. 2.3). eve^{ID19} (eve ↓) embryos exhibited an increase in the number of coupled and severe *en* stripe patterns (75% and 20% respectively; Fig. 2.3). *HSEve* (eve↑) embryos appear to be somewhat more sensitive to the heat shock as a larger number had severe patterns

Figure 2.3: Relative levels of *eve* and *ftz* are important in establishing parasegmental border position. Levels of *eve* and *ftz* were genetically altered alone and in combination, and the effects on *en*--expression patterns monitored. Values on the graph denote the percentages at which normal (black bars), coupled (grey bars) and severe (white bars) changes in *en* expression patterns were observed. Values are given for heat-treated wild-type control, eve^{lD19}, (eve↓), $HSEve^{19B}$ (eve↑), *hsf2* (ftz ↑), eve^{lD19}; *hsf245A* (eve↓ ftz ↑), and *hsf2*; $HSEve^{19B}$ (eve↑ ftz↑) embryos. Note the dramatic increase in the percentage of severe patterns that are observed when *eve* expression levels are lowered while *ftz* expression levels are raised. In contrast, increasing the levels of *eve* and *ftz* at the same time returns most of the observed patterns back to normal. Error bars represent standard deviation.

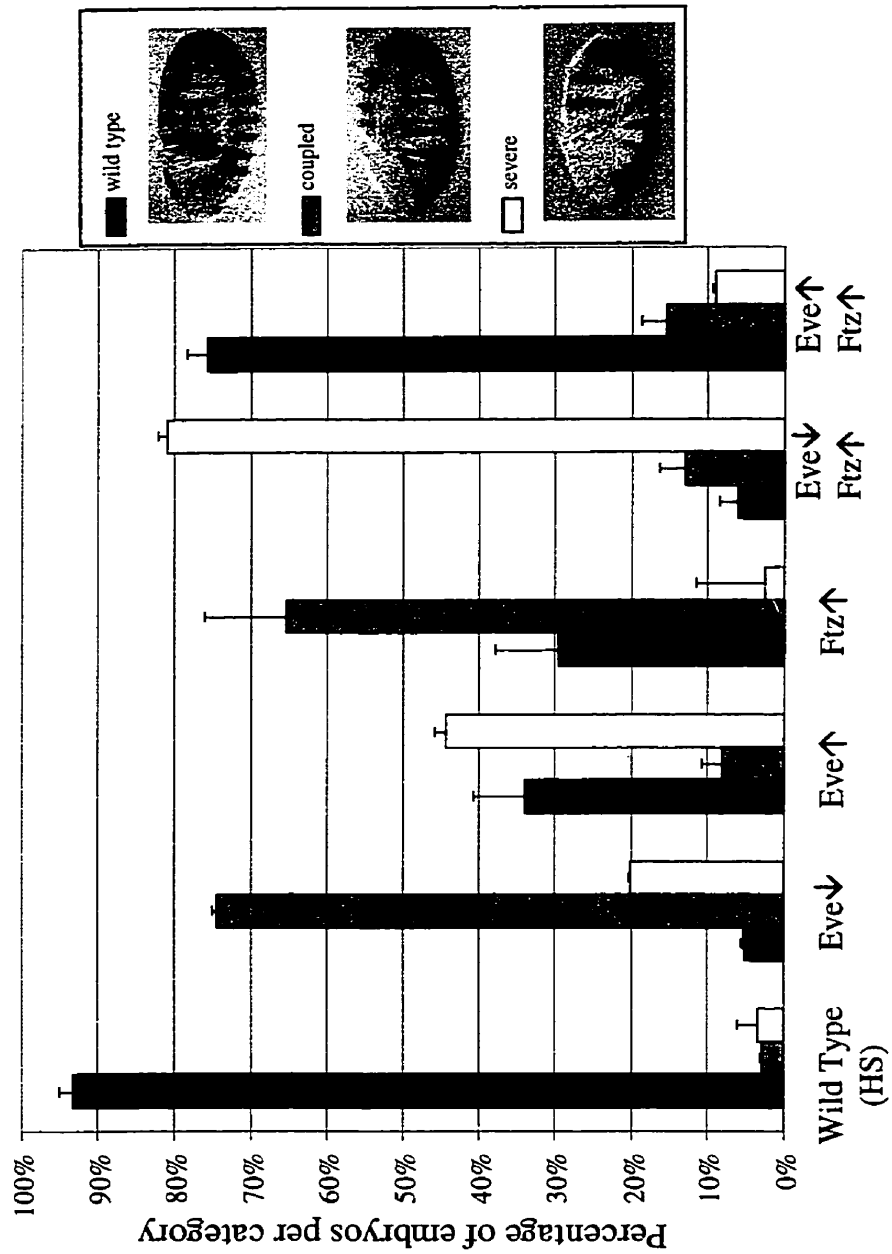
Percentage of embryos per category
100%
90%
80%
70%
60%
50%
40%
30%
20%
10%
0%
wild type
coupled
severe
Wild Type (HS)
Eve↓
Eve↑
Ftz↑
Eve↓ Ftz↑
Eve↑ Ftz↑

of *en* stripes (44%). When *HSFtz* (ftz↑) embryos were given a 4 minute heat shock, the majority exhibited a moderately coupled (65%) pattern of *en* stripe movement, while 3% had a severe pattern (Fig. 2.3).
In each case, altering the levels of *ftz* or *eve* alone caused a distinct increase in the number of embryos with altered parasegmental boundaries. However, when the levels of *eve* were lowered and the levels of *ftz* were increased at the same time (eve↓ ftz ↑), there is a major shift from coupled (13%) to more severe patterns (81%; Fig. 2.3) of *en* expression. Conversely, when relative levels of *ftz* and *eve* were both increased at the same time (eve↑ ftz↑; both transgenes under control of the hsp70 promoter) the majority of the embryos reverted back from coupled (15%) and severe (9%) *en* patterns to normal stripe spacing (76%; Fig. 2.3). A similar trend was observed when *ftz* and *eve* were both lowered at the same time (data not shown). Thus, absolute levels of *ftz* and *eve*, within the ranges tested, appear to be unimportant so long as the relative levels are kept in balance.

The *ftz* and *eve* genes are also required for many functions in addition to the proper positioning of *en* stripes. Therefore, the question remained; does restoration of wild type spacing of the parasegmental boundaries lead to restoration of normal development? Figure 2.4 shows that under my experimental conditions, 93% of the wild type embryos hatched to larvae and 88% eclosed as adults. Control embryos were also immersed in a room temperature water bath to ensure that this method of administering heat shock

Figure 2.4: Coordinate alterations in *ftz* and *eve* expression have little effect on viability. Expression levels of *ftz* and *eve* were altered as described in Figure 2.3, and the embryos allowed to develop. Black bars indicate the percentage of embryos that hatched as first instar larvae. Grey bars indicate the percentage that eclosed as adult flies. Combinations of *ftz* and *eve* under- and over-expressing lines are designated as in Figure 2. Altering the relative level of *ftz* or *eve* expression separately results in decreased viability in both embryos and adults. When the relative expression levels of *ftz* are increased (ftz ↑) as the levels of *eve* are decreased (eve↓), very small percentages or no organisms survive. However, when the relative expression levels of *ftz* and *eve* are increased simultaneously (eve↑ ftz↑) the percentage of surviving larvae and adults are similar to that obtained with wild type embryos that were heat shocked. All numbers shown illustrate the homozygous phenotypes. Error bars represent standard deviation.

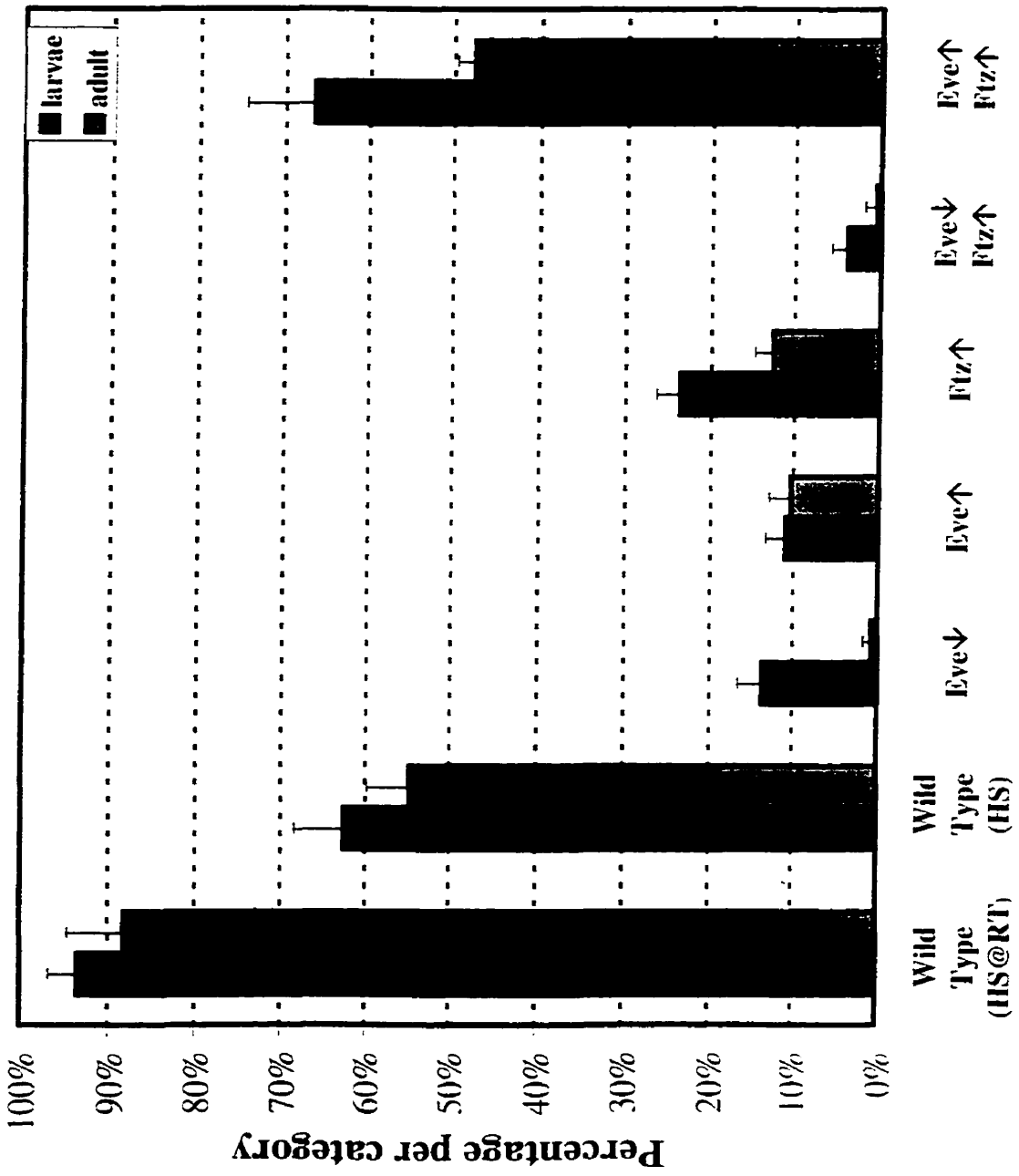
larvae
adult
100%
90%
80%
70%
60%
50%
40%
30%
20%
10%
0%
Percentage per category
Wild Type (HS@RT)
Wild Type (HS)
Eve↓
Eve↑
Ftz↑
Eve↓ Ftz↑
Eve↑ Ftz↑

was not affecting survival rates. With this treatment, 94% of embryos hatched and 88% eclosed as adults. However, following a 4-minute heat shock, 63% of the wild type embryos hatched and 55% survived to adulthood (Fig. 2.4). This provided a baseline for the effect of heat treatment on embryo survival. As expected, raising or lowering the levels of either gene in isolation dramatically lowered the number of embryos that hatched and the numbers of adult flies that eclosed (Fig. 2.4). When the levels of *eve* are lowered, 14% of the embryos hatched while only 1% eclosed as adults. Raising the level of *eve* results in 11% of the embryos hatched and 10% eclosed as adults. Additionally, raising the levels of *ftz* results in 24% of the embryos hatching and 13% eclosing as adults. These numbers were reduced even further when the levels of *eve* were reduced at the same time that levels of *ftz* were increased (Fig. 2.4). In this case only 4% of the embryos hatched and 1% of the adults eclosed. Unexpectedly, when the levels of *ftz* and *eve* were both increased at the same time, viability returned to near wild-type control levels, both for the number of embryos hatching and the number of adults eclosing (Fig. 2.4). Again, similar results were obtained when *ftz* and *eve* were both lowered at the same time (although viability was not as high due to non-equivalency of the temperature sensitive lines; data not shown). These results illustrates quite dramatically that it is the relative levels of *ftz* and *eve*, and not their absolute levels (within the limits tested), that define the width, identity, and function of alternate parasegments.

2. 5 Discussion

2.5.1 A new model for parasegment definition

Previous studies have shown that *ftz* and *eve* are the primary determinants of parasegmental boundaries and identities (even versus odd) (Lawrence et al., 1987; Lawrence and Johnston, 1989). Until quite recently, however, it was believed that the two genes perform these roles relatively late, at around the time of gastrulation (stage 6-7), and that high levels of expression coupled with sharp anterior stripe boundaries were crucial (Lawrence and Johnston, 1989). However, other studies have questioned whether high expression levels and sharp stripe boundaries are indeed important (Frasch and Levine, 1987; Frasch et al., 1988; Manoukian and Krause, 1992; Lawrence and Pick, 1998).

Based on the data presented above, I clearly show that when in the right proportions, the absolute levels of *ftz* and *eve* are not all that important for establishing parasegmental boundaries. Rather, it is their relative levels that are key. Furthermore, based upon the timing of the temperature shift and heat shock experiments, it appears that *ftz* and *eve* first define the positions of parasegmental borders prior to the completion of cellularization (stage 5 or earlier). At this time, *ftz* and *eve* protein levels can be envisioned in a bell-shaped distribution across each stripe, with the two gradients overlapping at their edges (Frasch and Levine, 1987; Ingham and Martinez Arias, 1992; SCH and HMK; data not shown). Altering *ftz* and *eve* expression to varying degrees demonstrates that the parasegment boundaries appear to occur at the point where the gradients

intersect, and where activity levels are equivalent (Fig. 2.5A). If the activity of one gene is raised while the other remains unchanged, or vice versa, these positions of equivalency move (Fig. 2.5B). The result is an alternating set of enlarged and narrowed parasegments. These shifts become more pronounced with greater changes in activity or when both gene activities change in opposite directions. However, if the activities of both genes are increased (Fig. 2.5C) or decreased (Fig. 2.5D) at the same time, the positions of equivalency do not change and parasegments remain equal in width. The transition from overlapping stripe boundaries to sharp non-overlapping boundaries may occur via a combination of autoregulatory and mutually antagonistic functions. For example, above a certain relative threshold level, FTZ autoregulation may win out over repression by EVE, and *ftz* expression rises to maximal levels. If below that relative threshold, then repression by EVE predominates over FTZ autoregulation and *ftz* expression is lost. The ability of FTZ and EVE to autoregulate and to mutually repress one another (directly or indirectly) has been well documented (Hiromi and Gehring, 1987; Frasch et al., 1988; Goto et al., 1989; Harding et al., 1989; Kellerman et al., 1990; Manoukian and Krause, 1992; Klingler and Gergen, 1993; Fujioka et al., 1995; Saulier-Le Drean et al., 1998; Nasiadka and Krause, 1999). For example, it has been shown that *eve* is able to autoregulate it's own expression by repressing the activity of repressors encoded by the *run*

Figure 2.5: A simplified model for the positioning of parasegmental borders by *ftz* and *eve* expression. Expression patterns of *ftz* and *eve* in late stage 5 embryos are indicated as sinusoidal waves. Parasegment borders, indicated by vertical lines, are formed at the points where *ftz* and *eve* levels are equivalent. In wild-type embryos (A) this results in evenly spaced borders. Panel B) shows the result predicted when *eve* levels are decreased or *ftz* levels are increased. Panel C) shows the result expected when the levels of both genes are simultaneously increased and panel D) shows the result expected when the levels of both genes is reduced.

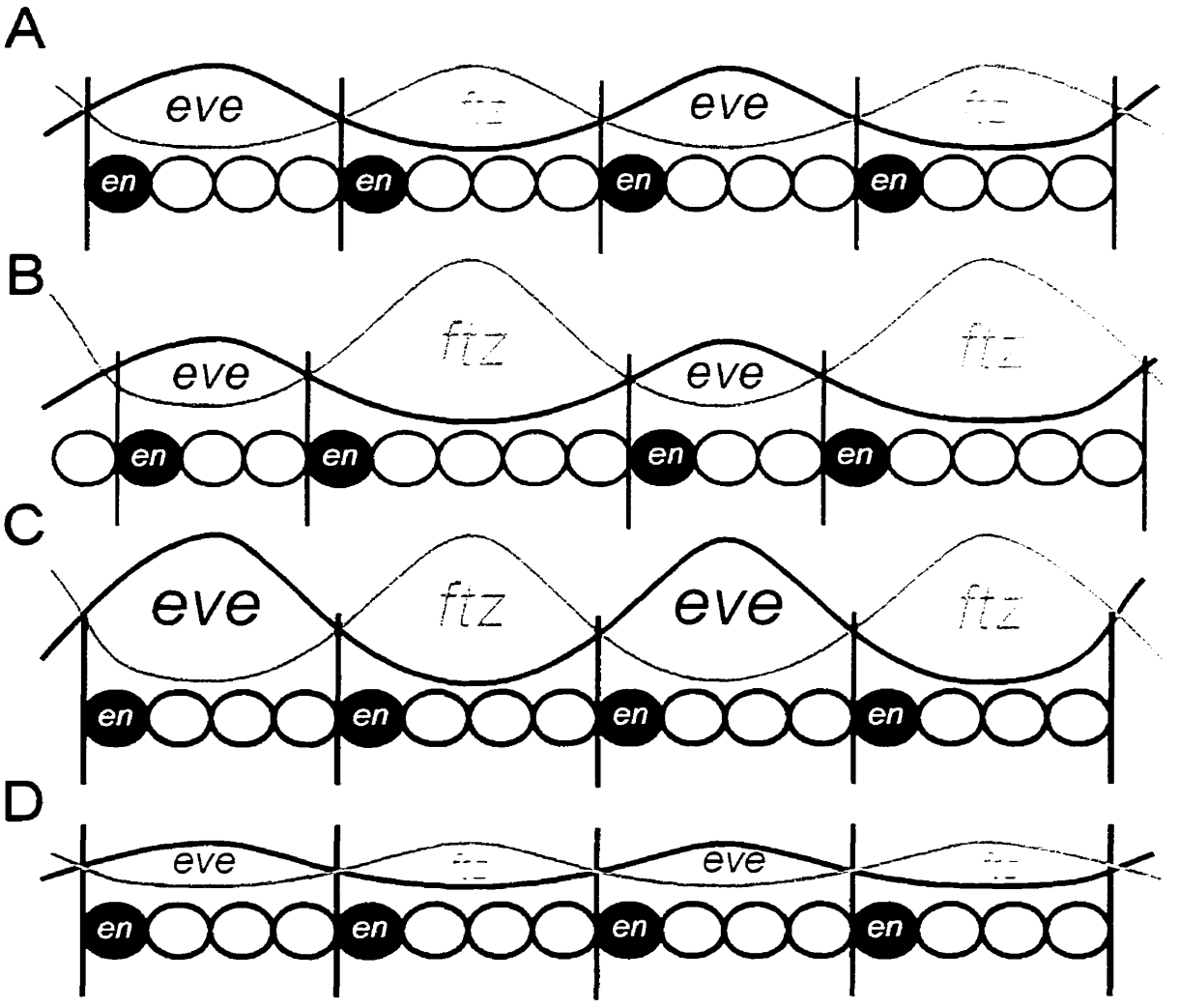
A
eve
ftz
eve
ftz
en
en
en
en
B
eve
ftz
eve
ftz
en
en
en
en
C
eve
ftz
eve
ftz
en
en
en
en
D
eve
eve
en
en
en
en

and *odd* genes (Figure 2.6; Manoukian and Krause, 1992; Saulier-Le Drean et al., 1998). *ftz* also directly autoregulates it's own expression (Hiromi et al., 1985; Hiromi and Gehring, 1987). This may also occur indirectly as *ftz* is able to directly activate *odd* which then activates *ftz* just prior to cellularization (Saulier-Le Drean et al., 1998; Nasiadka and Krause, 1999). During gastrulation EVE has been shown to directly repress *ftz* activity (Manoukian and Krause, 1992). Repression of *ftz* activity by EVE may also occur indirectly as EVE represses ODD (Manoukian and Krause, 1992), which prior to gastrulation is an activator of *ftz* (Saulier-Le Drean et al., 1998). On the other hand, FTZ represses *eve* activity indirectly by activating *odd* (Figure 2.6; Nasiadka and Krause, 1999). ODD is a direct repressor of *eve* expression (Saulier-Le Drean et al., 1998). These direct and indirect interactions explain how the positions of early *eve* and *ftz* stripe overlaps (prior to cellularization) are subsequently converted into sharp parasegment boundaries (see Figure 2.6). Once the borders of *ftz* and *eve* stripes are established, combinatorial interactions with other segmentation gene products then determine where downstream targets such as *en* and *wg* are activated or repressed. EN and WG then act to mark and maintain the parasegmental boundaries.

Figure 2.6: A summary model of the circuitry between EVE, FTZ and ODD that may be involved in the transition from overlapping *ftz* and *eve* stripe boundaries to non-overlapping boundaries. The interactions summarized in this figure occur at gastrulation. H represents high levels of eve expression and L represents low levels of eve expression.

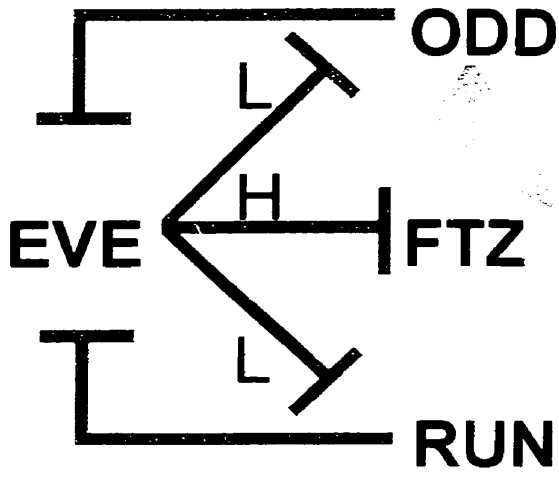
ODD
L
H
EVE
FTZ
L
RUN

CHAPTER 3: THE MECHANISM BY WHICH FTZ AND EVE PAIR-RULE PHENOTYPES ARE ESTABLISHED AND THE CONSEQUENCES OF ALTERING PARASEGMENTAL BORDER POSITION

This chapter comprises half of a similar report submitted to Development by Sarah C. Hughes and Henry M. Krause (2000)

3.1 Abstract

Previous studies have failed to determine how regions of an embryo are lost when segmentation gene activities are compromised. When the relative levels of *ftz* and *eve* are altered in the early embryo the positions of parasegmental boundaries are shifted, producing enlarged and reduced parasegments. The altered parasegments have only a limited ability to shift back to wild-type size. When boundaries are shifted by 30%, enlarged parasegments remain enlarged and reduced parasegments are lost. Loss of the reduced parasegments occurs in three steps; delamination of cells from the epithelial layer, apoptosis of the delaminated cells and finally apoptosis of inappropriate cells remaining at the surface. These processes have not been previously described. Retention of the enlarged parasegments correlates directly to the size of the *ftz* and *eve* mutant cuticles.

3.2 Introduction

A topic of some debate, and one that has not been properly explained is how *ftz* and *eve* pair-rule phenotypes are generated. Pair-rule phenotypes have been defined as the deletion of alternate, segment-wide regions (Nusslein-Volhard and Wieschaus, 1980). For example, *ftz* mutants were first described as a fusion of alternate segments resulting in half the number of double-wide segments (Wakimoto et al., 1984). In a subsequent study, Struhl (Struhl, 1985) describes *ftz* mutants as having lost segment-wide regions that correspond closely to parasegments. Also characterized in this study is a pair-rule

phenotype caused by ectopic expression of *ftz* (an "anti-*ftz*" phenotype). A *Drosophila* heat shock promoter (*hsp70*) was used to drive the expression of *ftz* throughout the entire embryo. As a result an anti-*ftz* phenotype or reciprocal *ftz* mutant pair-rule cuticle phenotype was obtained (Struhl, 1985). In *ftz* mutants, the odd-numbered abdominal segments derived from the even-numbered parasegments were lost (thus the regions retained were T1, T3, A2, A4, A6, A8; Wakimoto and Kaufman, 1981; Wakimoto et al., 1984). When *ftz* was expressed throughout the trunk region, the even-numbered abdominal segments derived from the odd-numbered parasegments were lost (thus the regions retained were T2, A1, A3, A5, and A7; Struhl, 1985). The regions deleted correspond to odd-numbered parasegmental compartments. The near reciprocal phenotypes observed suggested that both the regions of *ftz* expression and those lacking *ftz* expression were important in establishing the metameres early in embryogenesis and this would occur in combination with other pair-rule genes such as *eve*, *odd* and *prd* (Struhl, 1985). However, the deletions obtained in either *ftz* mutant or *HSFtz* embryos were not thought to be completely reciprocal. Certain regions at the anterior edge of odd-numbered parasegments appeared to be deleted in either case, whereas other regions at the posterior edges of the odd-numbered parasegments seemed not to be deleted in either of the *ftz* mutant or *HSFtz* embryos (Struhl, 1985). This suggested that the *ftz* and anti-*ftz* cuticle phenotypes did not arise from the deletion of alternate segment-wide regions. Despite this, the remaining parasegments are depicted as normal in width, and the resulting larvae about half the length of wild-type larvae.

Another interpretation of the pair-rule phenotype has been proposed based upon the analysis of a hypermorphic dominant *ftz* allele *Ultra-abdominal-like* (*Ual*), which produces a more stable *ftz* protein. The ftz^{Ual} phenotype was proposed to be a result of a slight widening of *ftz* stripes at blastoderm (Duncan, 1986). This ectopic *ftz* expression resulted in interference of the proper establishment of parasegmental boundaries producing *ftz*-dependent parasegments that were increased in width and *eve*-dependent parasegments that were reduced in width (Duncan, 1986). This produces a mixture of cells from adjacent parasegments into the enlarged parasegment, which were proposed to then express homeotic genes as they normally would to produce the end cuticular phenotype (Duncan, 1986). The reduced parasegments appeared to undergo pattern deletion (Duncan, 1986).

An third interpretation of the pair-rule phenotype has also been proposed based upon over-expression studies using a heat shock 70 promoter (*hsp70*). In this study *ftz* was again expressed throughout the embryo under the control of the *hsp70* gene promoter (*HSFtz*). It was suggested that while the outward appearance of cuticles from *HSFtz* embryos appear to be the reciprocal of *ftz* mutants, the metameric deletions are actually much the same (Ish-Horowicz and Gyurkovics, 1988). In *HSFtz* embryos, *ftz* stripes and even-numbered *en* stripes expand anteriorly by one cell (Ish-Horowicz and Gyurkovics, 1988). It was observed that these even-numbered (*ftz*-dependent) *en* stripes are unstable and decay by the end of germ band extension due indirectly to the repression of *wg* caused by the expanded expression of *ftz* (Ish-Horowicz and Gyurkovics, 1988;

Ish-Horowicz et al., 1989). These same *en* stripes were lost in *ftz* mutant embryos. Using *ftz*-lacZ constructs to mark regions where *ftz* had been expressed, it was suggested that FTZ expression was neither segmental nor parasegmental and as such the resulting metameric units were composed of fused parasegments (Ish-Horowicz and Gyurkovics, 1988). Thus, they postulated that the metameric organization of *ftz* mutants and *HSFtz* embryos are generated from the same fusion of alternate parasegments, but that the regions are given alternate parasegment identities by the differential expression of homeotic selector genes (Ish-Horowicz and Gyurkovics, 1988). These accounts are clearly inconsistent in their interpretation of what regions are retained within *ftz* pair-rule cuticles, and how this phenotype is obtained.

In terms of how alternate parasegmental regions are actually removed in a pair-rule mutant, it was proposed that the parasegmental regions lost in *ftz* mutant embryos were most likely removed by cell death (Martinez-Arias and Lawrence, 1985). As local cell death had been observed in some other segmentation mutants, it was suggested that a pair-rule phenotype could result from all cells mutant for a specific gene dying and leaving no descendants (Ingham et al., 1985; Martinez-Arias and Lawrence, 1985; White and Lehmann, 1986). However, in a follow-up study of cell death in *ftz* mutants, the numbers of dying cells are found to be higher in *ftz* mutant embryos (as compared to wild-type), but the dying cells are randomly distributed in the regions that normally form the even-numbered (*ftz*-dependent) parasegment (lost) as well as in the posterior regions of the odd-numbered (*eve*-dependent) parasegment (kept;

Magrassi and Lawrence, 1988). Again, this did not explain how alternate parasegmental regions are lost. This study hypothesized that failure to define the even-numbered (*ftz*-dependent) anterior parasegmental border may be the cause of this phenotype (Magrassi and Lawrence, 1988).

3.2.1 Parasegments as compartmental units

Another important property of parasegments, and one that is relevant to this study is that they are the first "compartments" to form within the embryo (Lawrence and Morata, 1994). Compartments are groups of cells that are defined in lineage and established by small groups of founder cells (Garcia-Bellido et al., 1973; Crick and Lawrence, 1975). Cells within adjoining compartments do not mix, most likely due to differential adhesion properties (Crick and Lawrence, 1975; Morata and Lawrence, 1977; Lumsden, 1990; Ingham and Martinez Arias, 1992; Dahmann and Basler, 1999). Consequently, compartment boundaries are generally straight. Compartments are further defined by unique gene expression patterns that respect their boundaries (Morata and Lawrence, 1977; Ingham and Martinez Arias, 1992; Lawrence and Morata, 1994). *Drosophila* parasegments fulfill each of these criteria.

Compartments are important spatial units of development, as they serve to maintain physical boundaries over long periods of time (Morata and Lawrence, 1975; Morata and Lawrence, 1977; Lawrence, 1997). Their straight borders also tend to serve as organizing centers, with diffusible morphogens secreted along the borders (Ingham and Martinez Arias, 1992; Heemskerk and DiNardo, 1994;

Lawrence and Struhl, 1996). The dependence of cells straddling the boundary on signals from the adjacent compartment also helps to maintain the borders. For parasegments, the major signaling molecules involved are Wingless (WG) and Hedgehog (HH; Bejsovec and Martinez Arias, 1991; Heemskerk and DiNardo, 1994; Lawrence et al., 1996; Alexandre et al., 1999). WG is secreted by the posterior-most cells of each parasegment and HH by the anterior-most cells of each parasegment (where *en* is expressed).

3.2.2 Proper establishment of compartment size is critical for patterning

Another property of compartments relevant to my work is that they appear able to modulate their sizes. If cells are inappropriately added or removed, there appears to be an inherent ability to sense and correct for these defects. For example, early grafting experiments using *Oncopeltus,* showed that removal of a narrow region approximately one quarter the size of a segment was often corrected during subsequent molts (Wright and Lawrence, 1981b). Similarly, small changes in parasegment size in *Drosophila*, achieved by genetic manipulation of the *bcd* gene can also be corrected. No matter whether the number of copies of *bcd* were increased or decreased, wild type larvae and adults were obtained (Frohnhofer and Nusslein-Volhard, 1986; Berleth et al., 1988; Driever and Nusslein-Volhard, 1988a; Driever and Nusslein-Volhard, 1988b). In the absence of correction pattern defects and abnormal development would result.

In this chapter, I address the consequences of altering the position of parasegmental boundaries. When the induced changes in parasegment width approach 30% or more, they cannot correct back to normal. Enlarged parasegments remain enlarged, while the reduced parasegments are lost during germ band retraction. The mechanisms by which this occurs were determined. Additionally, sizes of the enlarged parasegments correlate with the sizes of the remaining segments in *ftz* and *eve* mutant cuticles. These phenotypes appear to result from maintenance of the enlarged parasegments and loss of the reduced parasegments.

Pair-rule mutant cuticles produced when the expression levels of *ftz* or *eve* are altered early in embryogenesis (Fig. 2.1A-E), are on average 70% the length of wild type cuticles. Both the enlarged parasegments at mid-embryogenesis and the remaining segments in the pair-rule mutant cuticles are on average 1.3 times larger than the corresponding wild type segment. This does not correlate with the suggestion that pair-rule mutant cuticles are a result of a simple deletion of every other segment (Nusslein-Volhard and Wieschaus, 1980; Struhl, 1985), nor a fusion of alternate segments (Wakimoto et al., 1984; Ish-Horowicz and Gyurkovics, 1988). Thus, to explain the cuticle phenotypes and altered *en* patterns, one would predict that the pair-rule cuticle would result from the maintenance of enlarged parasegments and the loss of reduced parasegmental regions.

3.3 Materials and Methods

3.3.1 Drosophila stocks used

Stocks used for this study were previously described in Chapter 2.

3.3.2 Measurement of parasegmental widths

To clearly demarcate each cell, embryos of the appropriate age were hybridized with a digoxigenin-labeled *en* DNA probe (Saulier-Le Drean et al., 1998), visualized by NBT/BCIP (Saulier-Le Drean et al., 1998) and then counterstained with the DNA specific dye bis-benzamide (1:10000 dilution of a 5.0 mg/ml stock solution). The NBT/BCIP stain quenches the fluorescent bis-benzamide signal, clearly marking the *en* cells and the parasegment borders. Measurements of cell numbers and the distances in microns from one *en* stripe to the next were obtained using Northern Eclipse^{TM} image capture and analysis software (Empix Imaging, Mississauga, ON, Canada) and a Zeiss Axioplan 2E microscope. Measurements were obtained for parasegments 3, 4, 5, 6 along the ventral-lateral surface, four rows of cells above the ventral midline.

3.3.3 Cell death staining

This procedure was adapted from Abrams et al (Abrams et al., 1993). Embryos were suspended in equal volumes of heptane and a freshly prepared 10ug/ml solution of acridine orange (prepared in 1XPBS) for 5 minutes. Embryos were then transferred to a new scintillation vial and fixed as per common protocols (Lehmann and Tautz, 1994). Immunofluorescent staining was then carried out as described below.

3.3.4 Immunofluorescence and confocal microscopy

Embryos for immunofluorescence were collected and fixed as described above. Embryos were rinsed two times in methanol, then twice in PBTBB (1X PBS + 0.1% Tween 20 + 0.5% skim milk powder + 0.05% BSA). Blocking in PBTBB was carried out at room temperature for at least 2 hours. Primary antibodies [mouse α–*en* 4D9 (1:1000), mouse α–*wg* 4D4 (1:10; Developmental Hybridoma Bank), rabbit α–spectrin (1:1000; obtained from D. Branton)] were diluted in PBTBB and incubated with embryos overnight at 4°C. After washing, appropriate secondary antibodies [α-mouse CY3 (1:1000), α-mouse CY2 (1:1000), α-rabbit CY3 (1:1500); α-sheep CY3 (1:1000; obtained from Jackson ImmunoResearch Laboratories Inc.)] were diluted in PBTBB and incubated with the embryos for two hours. If two primary antibodies from the same species were used, one antibody was added first and then blocked with unconjugated sheep-α-mouse or sheep-α-rabbit antibodies (1:200; Jackson ImmunoResearch Laboratories Inc) as per manufacturer's instructions. After incubation with secondary antibodies, washes in PBTBB were carried out until background levels were sufficiently reduced. Embryos were resuspended in 2.5% DABCO (1,4-Diazabicyclo [2.2.2.] Octane) in glycerol, mounted on slides and observed using a Leica TCSNT confocal microscope.

3.4 Results

3.4.1 Consequences of improper establishment of parasegment size

In chapter 2, I showed that pair-rule phenotypes can occur even when 14 parasegments are initially present (Figure 2.1). To determine how alternate parasegments are lost, I monitored stripes of *en* expressing cells during later stages of embryogenesis. Figure 3.1 (panels A-F) shows that, in wild type embryos, an equivalent spacing between *en* stripes is seen during all stages tested. Panels on the right (F-J) show *en* stripes at equivalent stages in eve^{ID19} embryos. Here, the *ftz*-dependent parasegments are enlarged in width, and the *eve*-dependent parasegments are reduced in width (Fig. 3.1F-J). The reduced parasegments are retained through germ band retraction (Fig. 3.1H). However, by 12h AEL (stage 15) the reduced parasegments appear to have been lost (Fig. 3.1I) resulting in an embryo composed of seven segments. This correlates with the cuticle pattern observed in Fig. 2.1B. The fused *en* stripes, which are wider than normal at this stage, continue to resolve during later stages of development such that by 14h AEL (stage 16; Fig. 3.1J) they are only 1 to 2 cells wider than normal (Fig. 3.1E).

To quantitate the process of parasegment loss, the numbers of cells within specific parasegments were measured from 3 to 14h AEL. Figure 3.2 shows these measurements for parasegments 3, 4, 5, and 6 in wild type (Fig. 3.2 panels A, B), eve^{ID19} (Fig. 3.2 panels C, D), *HSFtz* (Fig. 3.2 panels E, F), and *HSEve* (Fig. 3.2 panels G, H) embryos. In wild type embryos, each parasegment contributed equally to the total number of cell number and total width of the four

Figure 3.1: Alteration in parasegment size is observed throughout the first half of embryogenesis, at which point the reduced parasegments appear to be extinguished. A) A wild type embryo at stage 8 with 14 evenly sized parasegments as marked by the expression of EN. Panel B, C and D illustrate the expression of EN in stage 12, stage 13, and stage 15 wild type embryos, respectively. The equivalent sizes of each parasegment are maintained through embryogenesis in the wild type embryos. The brace marks parasegment 5, an *eve*-dependent parasegment. When the relative levels of *ftz* and *eve* are changed, embryos composed of enlarged and reduced parasegments are observed. E) A stage 8 eve^{ID19} embryo is composed of enlarged *ftz*-dependent parasegments and reduced *eve*-dependent parasegments. The brace marks parasegment 5 that is an *eve*-dependent parasegment. F) In a stage 12 eve^{ID19} embryo or a stage 13 (G) A eve^{ID19} embryo, the reduced parasegments have not been further altered in size. However, in a stage 15 eve^{ID19} embryo (H) the reduced parasegments now appear to have been deleted. The embryo is now composed of seven parasegments only, as marked by the expression EN.

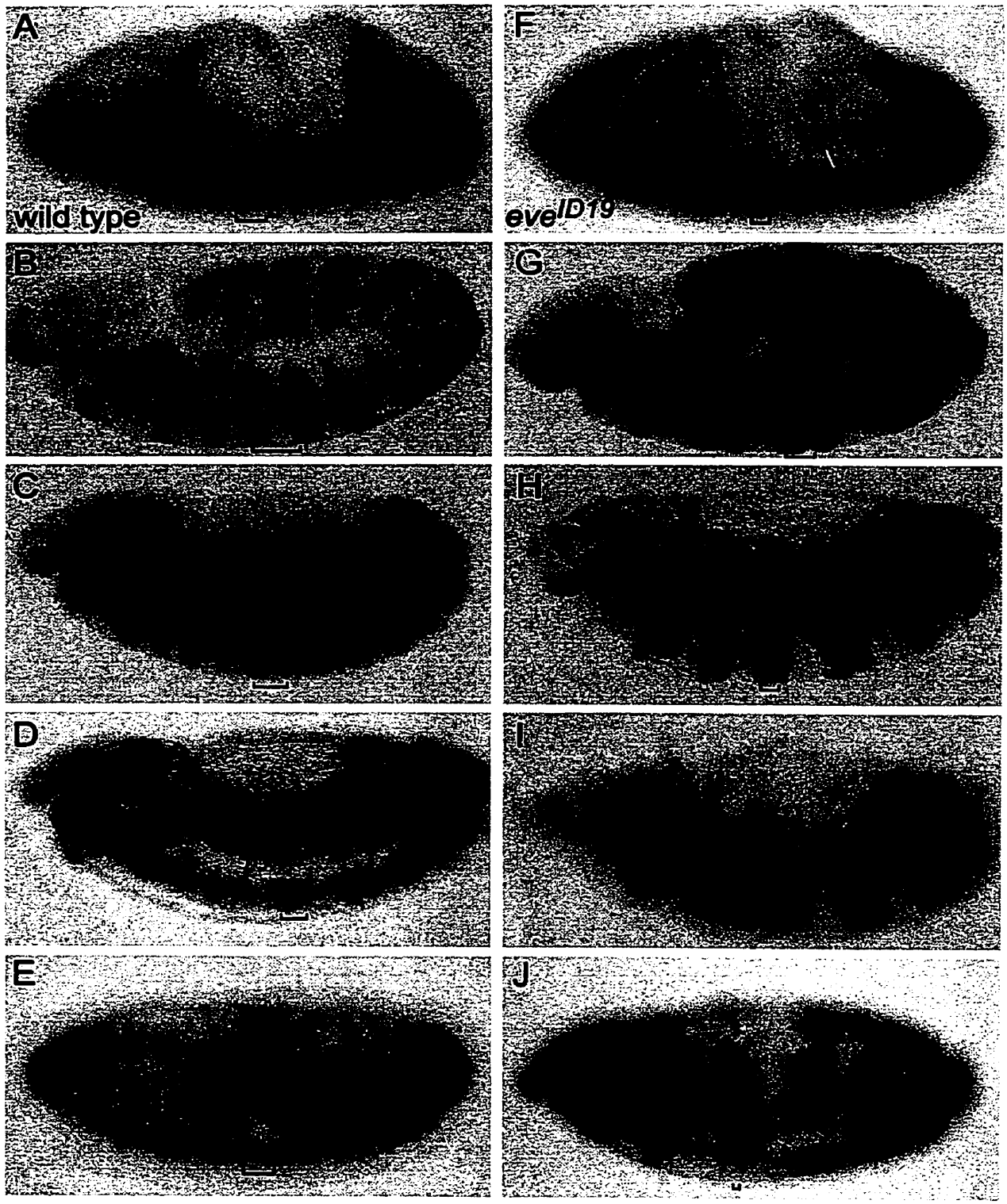
A
wild type
F
eve^ID19
B
G
C
H
D
I
E
J

Figure 3.2: Measurements of parasegmental width and cell number through embryogenesis. Stacked area graphs on the right represent the width of each parasegment (A, C, E, G) in microns, and on the left, the number of cells per parasegment (B, D, F, H). Each colour of the graph represents the contribution of a parasegment to the four parasegments counted. Wild type (A,B), *eve*^{ID19} (C,D), *HSFtz* (E,F) and *HSEve* (G,H) embryos were analyzed. The x-axis represents the time points during embryogenesis that embryos were fixed and analyzed. A total of 7348 parasegments were measured. Error bars represent standard deviation.

Measurement of parasegment width and cell number in 3 -14 hr embryos

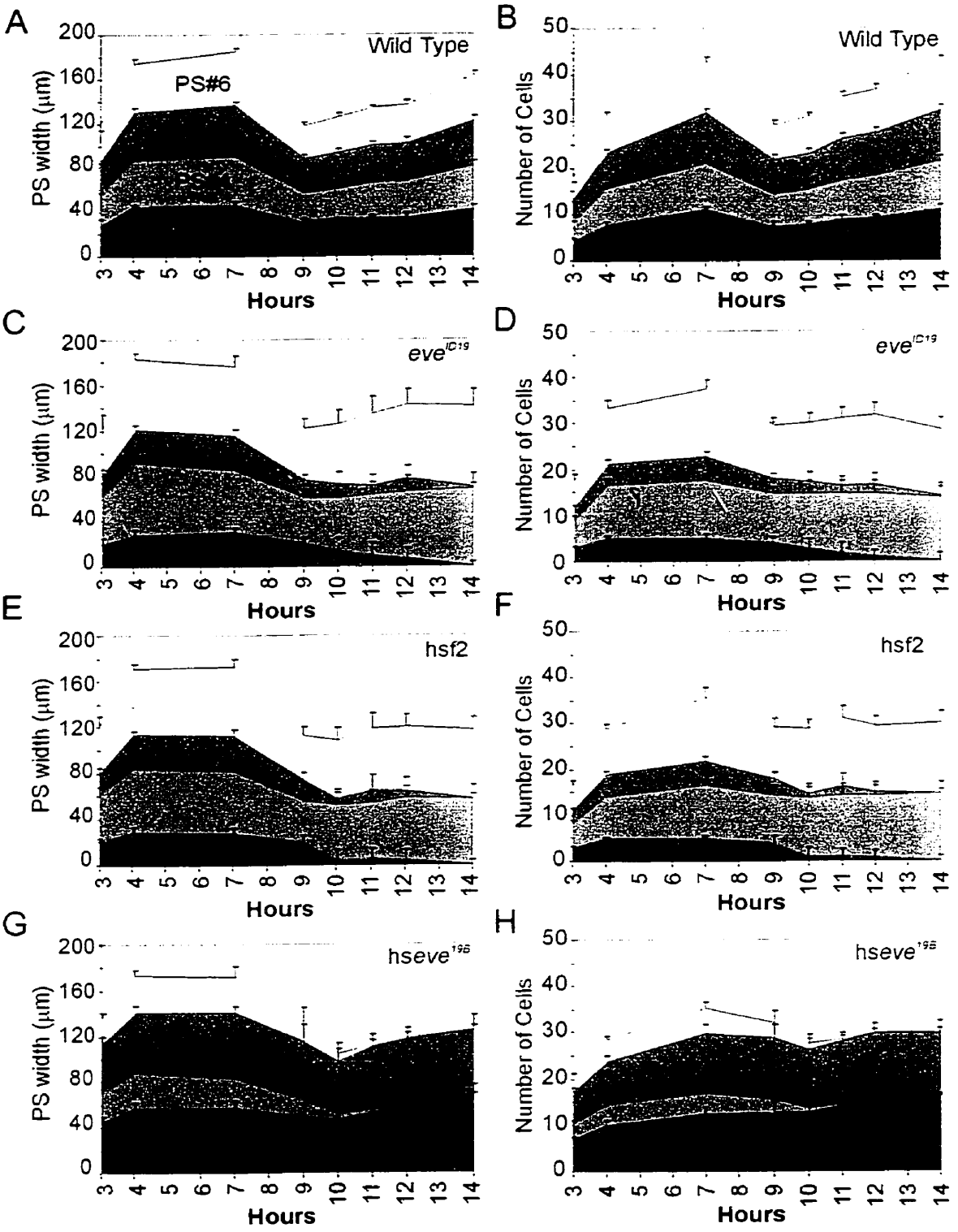

parasegments (Fig. 3.2A,B). In each of the mutant backgrounds, however, parasegments were already unequally spaced at 3-3.5h AEL (when *en* stripes initiate; stage 6-7; Fig. 3.2 D, F, G). The enlarged parasegments were on average 2.0 times wider than the reduced parasegments (about 1.4 times wider than wild type versus 0.6 times wild-type respectively). The widths of the enlarged parasegments are also about twice the width of the narrow parasegments in terms of cell number (6 versus 3; Fig. 3.2). However, the total width and number of cells in all four parasegments are equivalent to wild type, indicating that early changes in cell fate are responsible for these shifts in width. Approximately one in every four cells that normally make up the width of an odd-numbered parasegment are now recruited into an even-numbered parasegment in eve^{lD19} and *HSFtz* embryos (Fig. 3.2C-F). The opposite occurs in *HSEve* embryos (Fig. 3.2G,H).

In each of the mutant backgrounds, the narrow parasegments maintained a constant relative width until around 9h AEL (stage 12; Fig. 3.2). After this time, they decrease further in both width and cell number. By 14h AEL (stage 16), the reduced parasegments ceased to exist. The remaining enlarged parasegments, on the other hand, remain about 1.3-1.5 times wider and contain about 1.4 times as many cells as a normal parasegment. Overall, there is an average decrease of 35 microns (128 versus 163 microns) in parasegmental width and 13 cells (30 versus 43 cells) over the four parasegments in the mutants as compared to wild type (Fig. 3.2) at 14 h AEL. Taken together, these measurements illustrated that loss of the reduced parasegments is not due to changes in cell shape, size, or

identity. Alternative possibilities are that cells within the reduced parasegments die, fail to divide, or move out of the ectodermal layer, or a combination of all three. Cells in the enlarged parasegments, on the other hand, appear to differentiate and divide as normal. The overall patterns of the graphs throughout all developmental stages in wild type and in each mutant are quite similar, suggesting that the post blastoderm asynchronous rounds of mitosis (stage 8, 10, 11) are occurring normally. Additionally, the cell movements and re-intercalations associated with germ band elongation and retraction also appear to occur normally.

3.4.2 The role of cell death in parasegmental loss

To determine if cell death is responsible for loss of the reduced parasegments, acridine orange staining was used in conjunction with EN immunochemistry. Figure 3.3 (left hand panels; A-E) shows wild-type patterns of cell death at the relevant stages of embryogenesis. Normal apoptosis begins at 7 hours AEL (stage 11) and occurs in a fairly reproducible pattern that has been previously documented (Fig. 3.3A; Abrams et al., 1993; Pazdera et al., 1998). In the segmented regions of the embryo, the majority of cell death occurs between 9 and 11 hours AEL (stages 12-14; Fig. 3.3B-D) with 73% of cells dying within two to three cell widths of the segment border (Pazdera et al., 1998).

When the relative levels of *ftz* and *eve* are altered, a very different pattern of cell death is superimposed upon the normal pattern (Fig. 3.3, right hand panels; F-J). Increased levels of apoptosis do not appear to be induced at 7 hours AEL (stage 11) despite the earlier changes in

Figure 3.3: Overview of apoptotic patterns in wild type embryos (A, C, E, G, I) and in *eve*^{ID19} embryos (B, D, F, H, J). Embryos are double labeled with acridine orange marking apoptotic cells as yellow or green and the *en* expressing cells marked in red. Embryos were analyzed at stage 11 (A, B), stage 12 (C, D), stage 13 (E, F), stage 14 (G, H) and stage 15 (I, J). Higher numbers of apoptotic cells are observed in *eve*^{ID19} embryos. The arrowhead in (F) indicates a reduced parasegmental region in which very little apoptosis is observed. This is in contrast to the enlarged parasegments where a large number of apoptotic cells are apparent (F; arrow). Groups of apoptotic cells are apparent below the ectoderm at stage 14 and stage 15 (J; arrowhead).

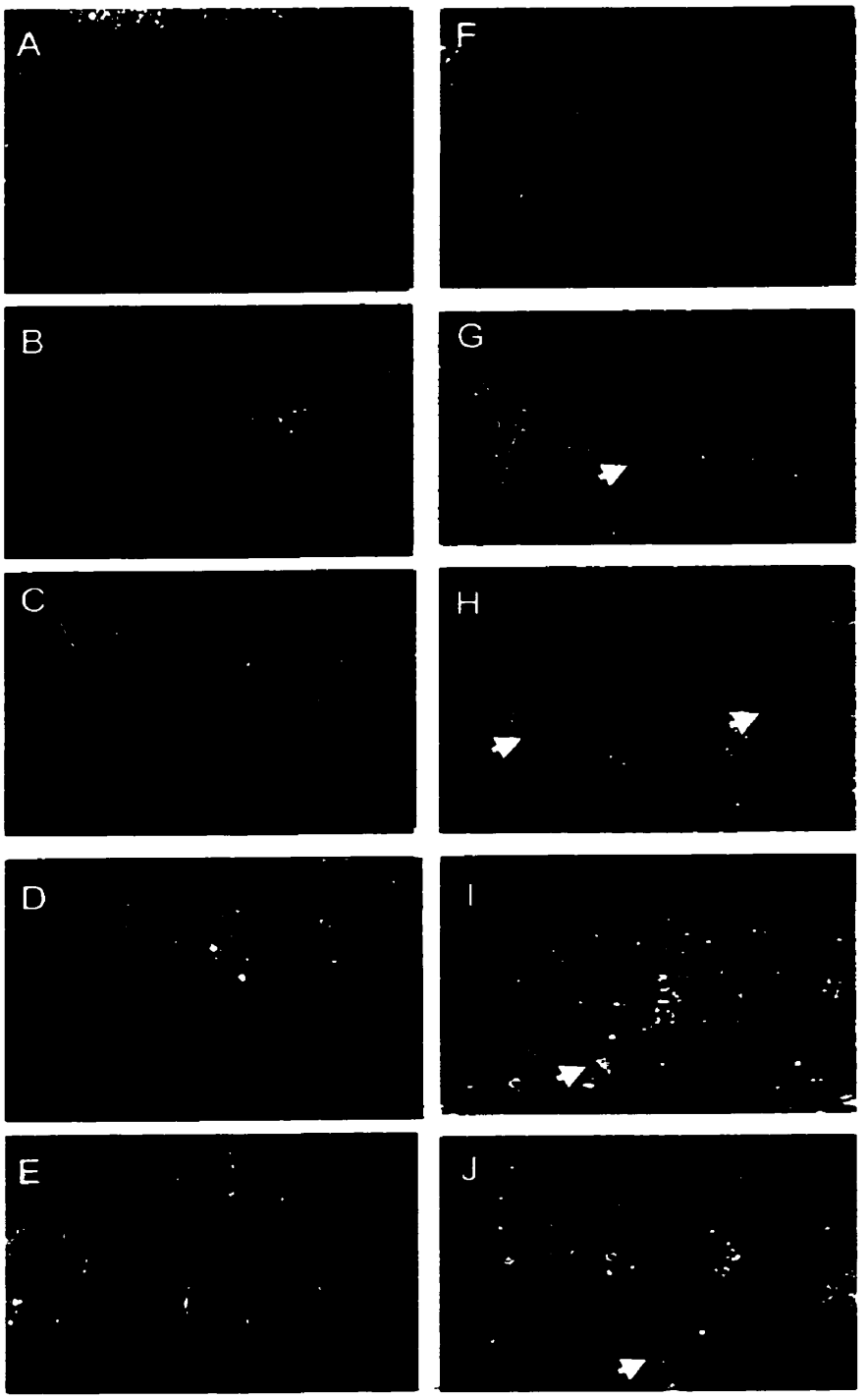
A
F
B
G
C
H
D
I
E
J

parasegment size (Fig. 3.4F). However, by 9 hours AEL (end of stage 12), higher than normal levels of cell death were observed (Fig. 3.3 compare B and G). Surprisingly, the dying cells were almost exclusively located in the enlarged parasegments with few, if any dying cells detected in the reduced parasegments (Fig. 3.3G, H; marked with arrow). Thus, both sets of parasegments appeared to be compensating for their abnormal widths by altering their rates of apoptosis. However, as clearly shown by the cell counts and cuticular phenotypes, these changes in apoptotic frequencies were not sufficient to correct for the changes in width introduced.

By 11 hours AEL (stage 14), levels of apoptosis within the ectodermal layer have decreased (Fig. 3.3I). However, clusters of dying cells begin to appear below the surface of the reduced parasegments (Fig. 3.3I; marked with arrow). These clusters increase in size and number at 12 hours AEL (stage 15; Fig. 3.3J arrow). At this time, dying cells also begin to co-localize with EN in the newly fused stripes (Fig. 3.3I, J). This continued until the fused EN stripes are reduced to a normal width (by approximately 14-15 hours AEL).

In order to more clearly determine whether cells are dying within or below the ectodermal layer, confocal sections perpendicular to the embryo surface were obtained. Figure 3.4 shows wild-type and *eve*^{ID19} embryos stained for EN (red), Wingless (WG; green) acridine orange (cell death; yellow) and α-Spectrin

Figure 3.4 Reduced parasegments are predominantly removed by delamination from the ectodermal surface. Embryos were triple-labeled and visualized by confocal microscopy to follow the fates of ectodermal cells. In all panels, ectodermal cell membranes are stained blue (α-Spectrin) and *en*-expressing cells are stained in red. WG is stained in green in panels A, C, E and G. Acridine orange-staining cells (yellow) are shown in panels B, D, F, and H. Wild-type embryos are shown on the left (A-D) and eve^{ID19} embryos on the right (E-H). The top four panels (A, B, E, F) are 9-9.5h AEL (stage 12) embryos and the bottom four panels (C, D, G, H) are 11-11.5h AEL (stage 14) embryos. The scale bar is equivalent to 5 microns.

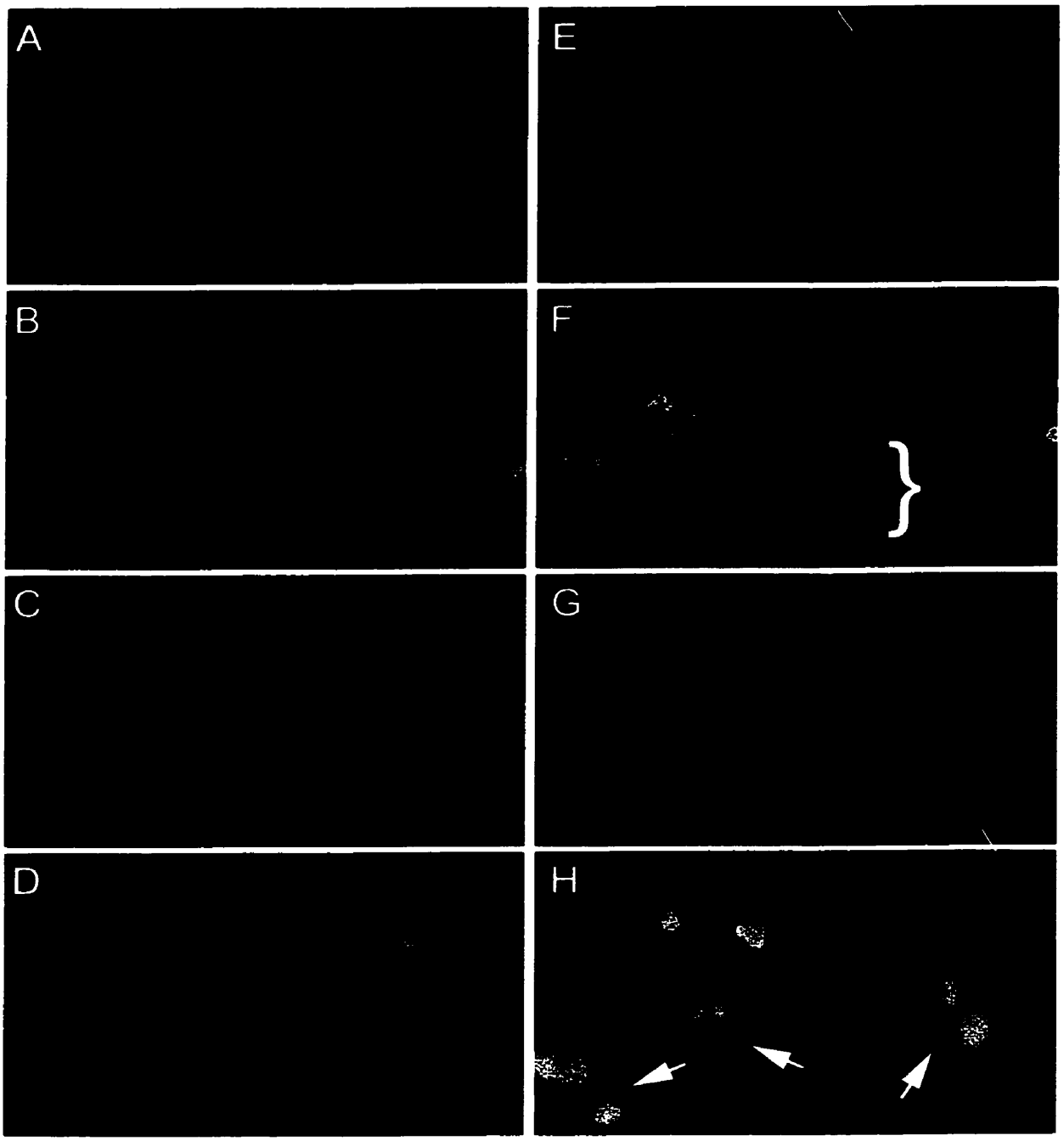
A
E
B
F
C
G
D
H

(ectodermal cell membranes; blue). As the borders of the reduced parasegments begin to fuse, cells staining for EN and WG begin to appear below the ectodermal surface (Fig. 3.4E,F,G). Cells derived from the middle regions of the reduced parasegments, which stain for α-Spectrin but not EN or WG, are also present below the ectodermal surface (brace in Fig. 3.4F), clearly showing that cells of the reduced parasegments were delaminating and moving interiorly. In contrast, delaminating cells were rarely observed below the ectodermal surface of wild-type or enlarged parasegments (Fig. 3.4A-D and Fig. 3.5A,C,D,F).

In the 9-9.5 hour AEL mutant embryos, individual acridine orange-staining cells are seen within or just below the ectoderm of enlarged parasegments (Fig. 3.4F). The cells that have delaminated from the surface of reduced parasegments, however, rarely stain with acridine orange until 11-11.5 hour AEL embryos (Fig. 3.4H). At this time, large clusters of dying cells begin to appear below the ectodermal surface (Fig. 3.4H). With time, these clusters move away from the sites of delamination and break apart. At about the same time, *en*-expressing cells in the fused stripes also begin to stain with acridine orange (Fig. 3.4H). They then move out of the ectoderm, eventually yielding stripes of EN that were normal 1-2 cells in width (see Fig. 3.1H). Within wild-type embryos, apoptotic cells were observed within the ectoderm and were most often observed near the *en*-expressing cells (Fig. 3.4B,D and Fig.3.5A,D)

In summary, the majority of cells in the reduced parasegments were lost via delamination from the ectodermal surface followed afterwards by cell death. The final resolution of the fused EN stripes to normal widths also occurs by cell

Figure 3.5 Confocal sections showing cell movement and apoptosis in reduced versus enlarged parasegments. Cell outlines are marked with α-spectrin (blue), segment boundaries by EN (red) and apoptotic cells are marked with acridine orange staining (yellow). Panels A-C represent 9-9.5h AEL (stage 12) embryos. A) wild type segment showing two EN stripes and a single apoptotic cell near the segment border. B) A reduced parasegment in an eve^{ID19} embryo showing a group of cells within an EN stripe that have delaminated from the ectoderm and undergone apoptosis. C) An enlarged parasegment in an eve^{ID19} embryo showing two EN stripes and several apoptotic cells in between. Panels D-F represent 11-11.5 h AEL (stage 14) embryos. D) Wild type segment with a single *en* stripe and apoptotic cell near the boundary. E) A reduced parasegment with an expanded EN stripe from which a cell has delaminated and undergo apoptosis. F) A enlarged parasegment in which apoptotic cells were located throughout.

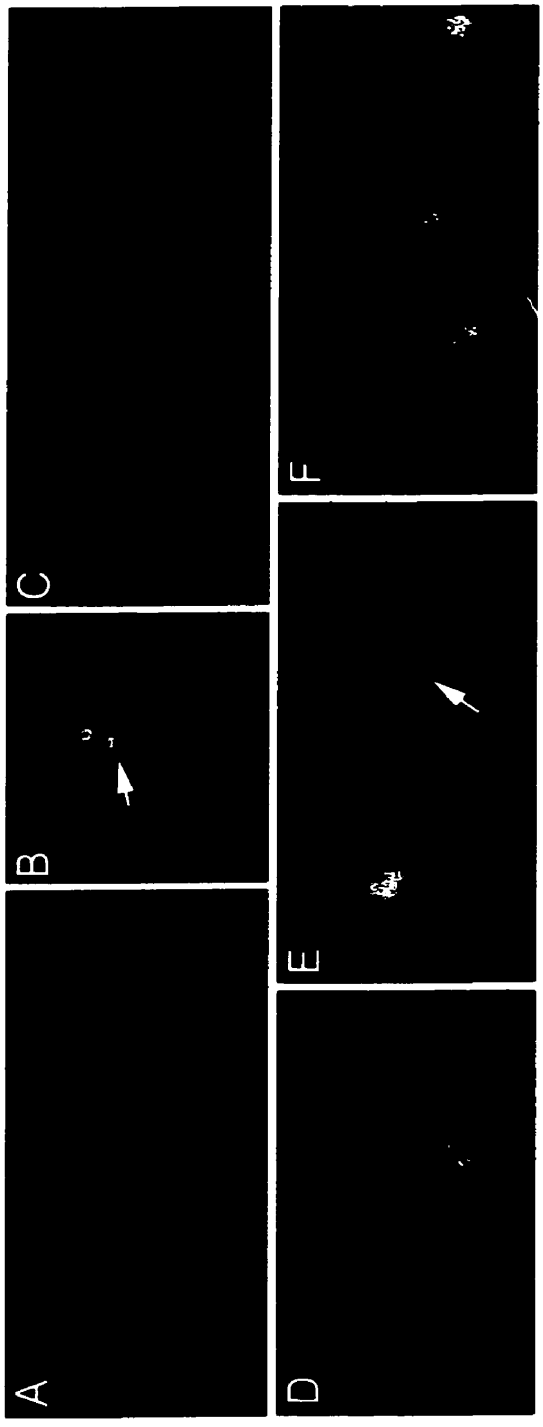
A
B
C
D
E
F

death, but this occurs within the ectodermal layer. In situ hybridization with probes to *reaper* (data not shown) confirmed that acridine orange stained cells do indeed represent cells that are dying via apoptosis, and that for the majority of cells in the reduced parasegment, this process does not appear to initiate until after the cells have delaminated.

3.5 Discussion

3.5.1 ftz and eve pair-rule phenotypes arise via novel mechanisms

As detailed in the introduction,a number of conflicting hypotheses to explain *ftz* and *eve* pair-rule phenotypes have been described. I show here that the remaining cuticle is not simply composed of every second parasegment, nor is it composed of double-wide or homeotically re-transformed segments. A relative decrease in *ftz* or *eve* activity causes a decrease in parasegment width and a corresponding expansion of adjacent parasegments. The smaller parasegments are lost (discussed further below) and the enlarged parasegments maintained. Efficient deletion of these parasegments occurs when reduced by 30% or more. Enlarged parasegments are rarely more than 1.4 - 1.5 fold times wider than normal parasegments, even when *ftz* or *eve* activities are lowered to negligible levels and alternate *en* stripes disappear. These enlarged widths represent the edges of the remaining stage 5 pair-rule gene stripes (*ftz* or *eve*). Further expansion of these stripes may be limited by the actions of other gap or pair-rule gene products. The resulting larva is composed of half the normal number of segments, but these are 1.3-1.5 times wider than normal segments, giving an overall length that is about 65-75% the length of a normal larva.

Although this model is consistent with all of the phenotypes described in this study, it simplifies the contributions made by other pair-rule genes. Some of these genes are necessary for *ftz* and *eve* function while others repress their functions or have complicating effects on FTZ and EVE target genes. For example, when *eve* is completely inactivated, stripes of *en* fail to appear despite

the presence of *ftz* (Carroll and Scott, 1986; Harding et al., 1986). This has been attributed to expansion of *odd-skipped* and *runt* stripes. Both genes encode repressors of *en* (Manoukian and Krause, 1993; Fujioka et al., 1995). Thus, other pair-rule genes also have important effects on parasegment size and stability, but these actions can be attributed to indirect effects on *ftz* or *eve* expression or on the regulation of FTZ and EVE target genes.

In this chapter I present an alternative model to explain the *ftz* and *eve* pair-rule phenotypes. Previous models relied upon analysis of the cuticular phenotypes of *HSFtz* embryos and hypermorphic *ftz* alleles in an attempt to describe the cause of the pair-rule phenotype. Struhl (Struhl, 1985) correctly suggested that pair-rule cuticles resulting from *HSFtz* embryos are nearly reciprocal of *ftz* mutants and result from roughly parasegmental deletions. These parasegmental deletions have been suggested to be a result of cell death (Martinez-Arias and Lawrence, 1985). Others suggested that the resultant phenotype is due to parasegmental instability because of expanded *ftz* expression in *HSFtz* embryos combined with a transformation in homeotic gene expression (Ish-Horowicz and Gyurkovics, 1988; Ish-Horowicz et al., 1989). These subsequent studies suggested that the pair-rule cuticle obtained from *HSFtz* and *ftz* mutant embryos are not reciprocal but actually contain the same cells (Ish-Horowicz and Gyurkovics, 1988; Ish-Horowicz et al., 1989). However, my work suggests that a very different mechanism; the resulting pair-rule cuticle phenotype is not due to a simple deletion of alternate regions or a homeotic transformation of one segment identity into another. Rather, the pair-rule

phenotypes are due to an initial change in parasegmental border position followed by loss of the reduced parasegments.

3.5.2 Parasegments have a limited ability to compensate for alterations in size

A number of studies have shown that compartments have a remarkable capacity to sense and compensate for changes in size. Such changes can be induced by injury, transplantation, irradiation, or genetic manipulation (Simpson and Morata, 1981; Wright and Lawrence, 1981b; Frohnhofer and Nusslein-Volhard, 1986; Berleth et al., 1988; Driever and Nusslein-Volhard, 1988a; Driever and Nusslein-Volhard, 1988b; Yasuda et al., 1991; Busturia and Lawrence, 1994; Namba et al., 1997). In the case of reductions in size, compensation is most often in the form of increased cellular proliferation or growth. For example, partial segmental grafts in *Oncopeltus* frequently result in the regeneration of complete segments (Wright and Lawrence, 1981b). Similarly, the removal of appropriate portions of *Drosophila* imaginal disks can be compensated for by re-growth (Bryant, 1975).

For tissues that have been increased in size, compensation is usually in the form of increased cell death (Pazdera et al., 1998). This has been observed, for example, in the head regions of *Drosophila* embryos following expansion induced by adding additional copies of the *bicoid* gene (Pazdera et al., 1998). Similarly, increased rates of cell death have been observed in the trunk of the embryo after the induction of additional rounds of cellular division (Li et al., 1999). In many of these cases, the compartment boundaries themselves may be instrumental in sensing compartment size and in determining whether changes in

rates of cell growth or cell death are required. In support of this possibility, cells in imaginal disks that are given a growth advantage, can grow at the expense of their neighboring cells but only until they reach the compartment border (Garcia-Bellido et al., 1973; Morata and Ripoll, 1975).

Our studies show that parasegmental compartments also appear to be able to sense their size and to make compensations for changes. However, their ability to compensate is relatively limited. The hypomorphic and hypermorphic alleles used here typically altered parasegmental widths by about 30%. Staining for cell death showed that there was an apparent attempt by both the reduced and enlarged parasegments to compensate by altering the frequencies of apoptotic events (Fig. 3.3). Dying cells were rarely seen in the ectoderm of reduced parasegments while higher than normal numbers were seen in the enlarged parasegments (Fig. 3.3G,H). However, these changes were insufficient to compensate for the changes in widths induced.

Changes in mitotic frequency, as a form of compensation, also did not occur. Once established, the ratio of the number of cells per mutant parasegment, as compared to wild-type segments, remained relatively constant until cells in the reduced segments began to delaminate (Fig. 3.2). This finding agrees with previous *bcd* gene dosage studies, which showed that segmental regions that had been reduced in size failed to compensate by increasing the number of cellular divisions (Busturia and Morata, 1988; Namba et al., 1997).

Although segments altered in size by increased *bicoid* gene copy number showed no changes in rates of mitosis, the induced changes in width were subtle

enough that many of these segments were able to recover (Frohnhofer and Nusslein-Volhard, 1986; Berleth et al., 1988; Driever and Nusslein-Volhard, 1988a; Driever and Nusslein-Volhard, 1988b). Our results and those of Pazdera et al., suggest that they were able to do so by reducing their rates of apoptosis (Pazdera et al., 1998). This appears to be sufficient to correct for reductions in width ranging as high as 20%. However, with changes in width of 30% or more, variations in apoptotic frequencies can no longer compensate.

Based on the response to altered parasegment borders, it appears that embryonic compartments can sense their size, but the mechanism by which they accomplish this is not clear. A possible sensing mechanism might involve signals that emanate from the parasegmental borders. For example, cells that are moved too close to the border, or alternatively too far away, may receive or fail to receive signals required for cell fate decisions. Another mechanism might involve the abilities of parasegments to initiate and maintain minimal or maximal numbers of cell fates within the narrow confines of their borders. For example, if four cell types were mutually required across the width of each parasegment, and there was sufficient space for only three, the viability or identities of the remaining three cells might be lost. This might be due to lost interactions or intercellular communication (perhaps emanating from compartment borders) between the remaining cells die to the lack of input from the missing cells. Increasing parasegment size, on the other hand, may separate cells from neighbors that provide necessary signals or contacts, prompting partial correction by programmed cell death.

The limited ability of narrow parasegments to return back to normal widths is probably due to the lack of a mitotic recovery mechanism and the limited number of excess cells that are initially present. The excess cells that are normally available are probably there to buffer against genetic and developmental inconsistencies such as modest changes in segmentation gene activities and variations in the numbers of cells that delaminate from the ectoderm to form other structures.

3.5.3 Why do reduced parasegments delaminate?

One of the novel and most intriguing findings of my study was the instability of reduced parasegments and the manner in which they were removed. This appeared to be a three-step process. The majority of reduced parasegment cells migrated out of the ectodermal layer. Next, they pinched off from the overlying ectoderm and initiated programmed cell death. The final clearing of remaining ectodermal cells was carried out by late and sporadic apoptotic events. Although the precise spatial and temporal details of this process varied somewhat between individual embryos and between different mutant backgrounds, the general trends and final consequences were the same.

The delamination of cells from the reduced parasegments occurred primarily during late stages of germ band retraction. This coincidence between reduced parasegment delamination and germ band retraction suggests the possibility that cellular movement and adhesion may play a prominent role in the process. During germ band retraction, cells within each parasegment change

shape and re-intercalate such that short but wide parasegments are converted into narrow but tall parasegments (Martinez Arias, 1993). Our cell counts show that, during this process, normal parasegments are reduced in width by almost half (from ~11 cells to 7; Fig. 3.2). In the reduced parasegments, the corresponding decrease results in a width of just 3 cells. This reduced width means fewer contacts between cells of the reduced parasegments and more contacts with cells of the enlarged parasegments. This may be akin to what happens with small clones of cells with anterior compartment identity are formed in the posterior compartment of imaginal disks (Lawrence, 1997). These cells tend to form spheres that delaminate from the disk surface. These events may be driven by an attempt to maximize the number of homologous adhesive cellular interactions. Alternatively, it could also be driven by repulsive forces between cells of adjacent compartment identity. Examples of this type of repulsion have been observed between transplants of cells taken from homologous or heterologous positions within alternate segments in the insect *Rhodnius* (Locke, 1967). Transplants from homologous regions (from the same position in two different segments) will completely mix and result in a normal pattern. However, transplants from heterologous regions will not mix and result in altered patterns. Additionally, cells taken from adjacent rhombomeres in the hindbrain of mammalian embryos will not mix, but form new borders in between the two populations of cells (Guthrie and Lumsden, 1991).

Molecules that provide differential adhesion have long been hypothesized to exist within and between different clonal compartments (Crick and Lawrence,

1975; Morata and Lawrence, 1977; Lumsden, 1990; Ingham and Martinez Arias, 1992). Their purpose would be to prevent the mixing of cells between compartments and to maintain straight boundaries between them. These boundaries, in turn, often serve as organizing centers (Meinhardt, 1983; Martinez Arias et al., 1988; Bejsovec and Martinez Arias, 1991; Heemskerk and DiNardo, 1994; Blair, 1995; Lawrence and Struhl, 1996). Evidence supporting a role for both types of cell-cell interaction molecules in compartment boundary establishment and maintenance is currently strongest for vertebrates. In support of differential adhesion molecules are mixing and transplantation experiments of rhombomeres, which show that cells of odd-numbered rhomdomeres prefer to associate with cells of their own identity rather than with cells of adjacent even-numbered identities (Guthrie and Lumsden, 1991). Experiments with rhombomeres also provide evidence for molecules that provide repulsion between cells of adjacent compartments (Klein, 1999; Mellitzer et al., 1999; Xu et al., 1999). Ephrin ligands and their counterpart Eph receptors are expressed on the surfaces of cells in adjacent rhombomeres (Klein, 1999). When cells that differentially express the two proteins are mixed they actively repel one another (Klein, 1999; Mellitzer et al., 1999; Xu et al., 1999).

Homologues of the *Drosophila* segmentation genes *hairy* and *engrailed* are involved in the segmental patterning of somites (Muller et al., 1996; Holland et al., 1997; Palmeirim et al., 1997). This suggests that rhombomeres and somites may share other properties in common with parasegments. For example, the molecules responsible for the differential adhesiveness of

rhombomeres and somites may have homologues that are expressed in parasegments. Conversely, rhombomeres and somites may share some of the compartmental properties described here.

CHAPTER 4: GENERAL DISCUSSION AND FUTURE EXPERIMENTS

4.1 General Summary

My thesis presents an analysis of the establishment and maintenance of parasegmental compartments and represents a basic characterization of the responsiveness of an embryo to changes in gene expression during early development. In previous experiments, the number of copies of the maternal gene *bcd* were increased or decreased to examine the consequences of changing compartment sizes by small amounts (on average, less than 15%). Initial experiments suggested that despite the changes in size compartments were able to correct themselves producing essentially wild type adults (Frohnhofer and Nusslein-Volhard, 1986; Berleth et al., 1988; Driever and Nusslein-Volhard, 1988a). Subsequent studies suggested that, depending on the extent of the alteration in compartment size (changes approaching 20%), various segmental defects or reduced viability are produced (Busturia and Lawrence, 1994; Namba et al., 1997). In this thesis, I alter the relative levels of the pair-rule genes *ftz* and *eve* to change the spacing between the parasegmental borders to a somewhat larger extent (on average 30%). In this case, rather than correcting back to wild type size, these larger changes led to parasegment loss.

My study also dissects the process of how a pair-rule mutant cuticle phenotype can be formed. Previously, it was proposed that the pair-rule phenotype was the result of a complete deletion of alternate segments coupled with widespread cell death (Nusslein-Volhard and Wieschaus, 1980). However, in *ftz* mutants large-scale cell death is not restricted to *ftz*-dependent

parasegments. Rather cell death is distributed randomly throughout the embryo (Magrassi and Lawrence, 1988). Alternatively, it was suggested that partial deletions of parasegments may be coupled with homeotic transformations, thus changing the identity of fused segmental regions to produce alternative pair-rule phenotypes (Ish-Horowicz and Gyurkovics, 1988). Although these studies suggested that portions of each parasegment are lost, there are conflicting results as to which parasegments are affected. Ish-Horowicz and Gyurkovics (1988) proposed that the majority of the region lost appears to be derived from the even-numbered parasegments, with the rest derived from the odd-numbered parasegments.

4.2 How do ftz and eve pair-rule phenotypes form?

In this thesis, I show that a pair-rule phenotype is produced by altering parasegment border position to an extent that is not correctable by the organism. I achieved this alteration by taking advantage of the powerful *Drosophila* genetic system such that expression levels of *ftz* and *eve* relative to wild type and to each other could be precisely modulated. In this way I could readily dissect the developmental processes that lead to the formation of a pair-rule phenotype. By altering the ratio of *ftz* and/or *eve* in small increments, one can correlate the precise relationship between changes in the positions of parasegmental boundaries and the production of a pair-rule phenotype.

In Chapter 2, I demonstrated that the relative levels of *ftz* and *eve* expression, prior to cellularization (stage 5), establish where the boundaries

between the parasegmental units will be formed. Either raising the expression level of ftz, or lowering the expression level of eve produced a similar cuticle phenotype in which the odd-numbered (*ftz*-dependent) abdominal segments were maintained. Conversely, by lowering the expression level of *ftz*, or raising that of *eve*, a cuticle phenotype in which the complementary set of even-numbered (*eve*-dependent) abdominal segments were maintained was produced. In all cases tested, where the relative ratio of *ftz* to *eve* expression are altered, only half the parasegments are present at the end of embryogenesis (Fig. 2.1). However, within the early embryo, all fourteen parasegments can be detected, albeit with altered sizes (Fig. 2.1). Even though the parasegments are altered in size, they still represent individual compartmental units as demonstrated by the expression of *en, ftz* and *eve* reporter genes, and the homeotic gene *Ubx* (Fig 2.2). To produce a pair-rule phenotype, changes in *ftz* or *eve* expression levels must occur early in embryogenesis prior to when *en* is being activated initially. By equivalently raising the levels of *ftz* and *eve* at the same time, embryos exhibited a wild type pattern of *en* stripes suggesting that parasegments are established correctly. Further, these embryos are also able to hatch and to pass through three larval stages and a pupal stage prior to eclosing as normal adults.

4.2.1 Proposed experiments

Although the additional levels of *ftz* or *eve* produced from heat shock transgenes is well below endogenous levels, it would be informative to obtain a

quantitative determination of the actual amount that *ftz* and *eve* expression is changed in order to alter boundary position. Previous studies have initially addressed EVE and FTZ levels (Fitzpatrick et al., 1992; Manoukian and Krause, 1992), but a more extensive analysis would be useful. FTZ and EVE protein levels could be quantified by Western blot analysis. The amount of FTZ and EVE protein could be measured against loading controls of *actin* or *tubulin*, which are expressed ubiquitously, using a phosphoimager. Alternatively, the amount of protein in wild type and mutant embryos could be compared by fluorescent staining which could be measured quantitatively by comparing fluorescence intensity.

The correlation between the levels of FTZ or EVE with the shifts in *en* stripe position and the severity of defects in the resulting cuticle phenotypes could also be determined. These experiments would also address the question of whether the parasegmental boundary positions are shifted continuously as the relative expression levels of *ftz* or *eve* change, or if is there a limit where other pair-rule gene expression may inhibit further shifting of position. A useful approach is to use incremental temperature shifts of eve^{ID19} or ftz^{54B} embryos, or to increase the durations of heat shock for *HSFtz* or *HSEve*. Initial experiments (data not shown) suggest that a very slight change in *ftz* or *eve* expression produces a moderately coupled *en* phenotype. For example, in *HSFtz* embryos, a heat shock of only 1 minute will produce embryos with slightly coupled *en* stripes (reduced parasegments are on average 19% narrower in width as

compared to normal parasegments at stage 9), but the majority of these embryos produce wild type cuticles. With a 2 minute heat shock, a larger number of embryos exhibited a coupled pattern (reduced parasegments are on average 31% narrower in width) and this correlates with an increase in the number of cuticles with defects. Most of these cuticles have partial fusions of denticle bands (80%) with a smaller number (20%) exhibiting complete pair-rule phenotypes. This appears to be on the margin between where parasegments can self-correct and cannot. Generally with a shift in compartment size of 30%, over 90% of the embryos exhibit a pair-rule phenotype. Differences between experiments in terms of aging of embryos and penetrance of heat shock may be a factor. Between 2 minutes and 6 minutes of heat shock, the number of embryos exhibiting a coupled *en* pattern does not change significantly. Additionally, the size of the enlarged and reduced parasegments also does not change significantly. However, as the extent of heat shock increases (greater than 6 minutes), the percentage of embryos exhibiting complete pair-rule phenotypes increases until there are equivalent numbers of partial and complete phenotypes. By 8 minutes of heat shock, the majority of embryos exhibit a pair-rule phenotype. It appears, however, that parasegment size can only be reduced to a certain width. This may suggest that the mechanism that responds to the relative levels of FTZ and EVE to establish parasegmental boundaries becomes saturated or unable to respond further at very high levels. These data are

preliminary and a more extensive analysis of tightly aged embryos is required.

4.3 How can the early expression patterns of ftz and eve generate sharp parasegmental boundaries?

How might the broad bell-shaped patterns of initial *ftz* and *eve* expression act to determine the distinct positions of the parasegmental boundaries? First, this may occur through FTZ and EVE levels being increased through autoregulation. Secondly, these boosted levels may then negatively regulate each other's expression (Kellerman et al., 1990; Manoukian and Krause, 1992; Klingler and Gergen, 1993).

4.3.1 FTZ and EVE autoregulation

It is known that FTZ and EVE are able to autoregulate their own expression (Hiromi et al., 1985; Hiromi and Gehring, 1987; Hoey and Levine, 1988). For example, a *ftz* autoregulatory element containing multiple FTZ binding sites has been isolated between –6 to –4 kb upstream of its transcriptional start site (Hiromi et al., 1985; Hiromi and Gehring, 1987; Pick et al., 1990; Schier and Gehring, 1992; Schier and Gehring, 1993). FTZ autoregulation is likely direct since mutation of FTZ binding sites within a minimal enhancer element disrupts autoregulation (Schier and Gehring, 1992). An autoregulatory sequence within the *eve* promoter is located approximately 5 kb upstream of the transcription start site (Goto et al., 1989; Jiang et al., 1991). There appear to be early- and

late-acting responsive elements within the *eve* promoter, where the early element responds to the activity of upstream gap genes to establish the broad expression pattern of *eve* (Goto et al., 1989). The late element responds to EVE itself as well as to the products of the other primary pair-rule genes *h* and *run* to refine the expression of *eve* stripes (Goto et al., 1989). Later autoregulation may occur during mid-cellularization (Goto et al., 1989). Later, *in vitro* studies determined that there are two binding sites for *eve* protein within the autoregulatory sequence located between –5.35 to –5.25 kb upstream of the transcriptional start site (Jiang et al., 1991). Additionally, three binding sites for nuclear factors were identified within this sequence, which appear to be required in combination with EVE for autoregulation (Jiang et al., 1991). However, these EVE binding sites may not be used, since kinetic experiments suggest that autoregulation is indirect via repression by EVE of the *eve* repressors, *run* and *odd* (Manoukian and Krause, 1992; Saulier-Le Drean et al., 1998).

4.3.2 Mutual repression of FTZ and EVE activity

The conversion from bell shaped gradients to sharp parasegmental borders may also occur through mutual repression of FTZ and EVE. The mutual repression occurs by a roundabout manner. For example, FTZ is known to directly activate *odd* expression, which then directly represses the activity of *eve*, which will in turn directly repress *ftz* (Saulier-Le Drean et al., 1998; Nasiadka and Krause, 1999). On the other hand EVE has

been shown to directly repress *ftz*, and *run* (Manoukian and Krause, 1992). RUN can activate *ftz* expression prior to gastrulation (Manoukian and Krause, 1992; Manoukian and Krause, 1993). EVE can also indirectly repress *ftz* by repressing *odd*, an activator of *ftz* (Manoukian and Krause, 1992; Saulier-Le Drean et al., 1998).

4.4 How do FTZ and EVE interactions occur at the molecular level?

As stated above, my work suggests that the positions of parasegmental boundaries are determined by sensitive measurement of the relative ratio of *ftz:eve* expression in the syncytial embryo. This measurement of the FTZ:EVE ratio could occur through a counting mechanism, such that equivalent amounts of FTZ and EVE within one nucleus in essence cancel each other out, and thus only the protein in excess is functionally active. This could occur either through a direct interaction between FTZ and EVE, competitive binding for specific target sites, or cross-regulation of each other's expression. FTZ and EVE are transcription factors that contain a homeodomain that binds DNA (Laughon and Scott, 1984; Desplan et al., 1988; Laughon et al., 1988). FTZ and EVE homeodomains are classified as members of the same family and *in vitro* recognize a similar consensus sequence, CAATTA (Desplan et al., 1988; Hoey and Levine, 1988).

FTZ and EVE could interact directly with each other forming a heterodimer, or alternately FTZ and EVE could bind to the same co-factor,

forming alternative protein complexes. Binding of a co-factor may be quite possible as both FTZ and EVE require co-factors for various functions including autoregulation or target gene regulation (Jiang et al., 1991; Copeland et al., 1996; Guichet et al., 1997). In either case when FTZ and EVE are both present in the same cell, the complexes would be balanced and thus inactive. However, any remaining FTZ or EVE, either as unbound protein or interacting with a permissive co-factor, would be active and thus FTZ-specific or EVE-specific functions would be initiated. The active protein would then bind its specific target promoter.

As an example, *en* is a direct target of FTZ with conserved binding sites for FTZ and its co-factor Ftz-F1 adjacent to one another within the *en* enhancer (Florence et al., 1997; Nasiadka and Krause, 1999). Both FTZ and FTZ-F1 are required for *en* activation (Florence et al., 1997; Guichet et al., 1997; Yu et al., 1997). In the cells at the anterior edge of the even-numbered parasegment in which slightly more FTZ than EVE is present, *en* is activated.

EVE probably does not act directly on *en* and may even affect other (as yet unknown) binding sites within the *en* enhancer (apart from the FTZ/FTZF1 binding sites). EVE may compete non-productively such that in the posterior cells of the *eve*-dependent parasegment, no *en* is activated. However, EVE may activate *en* indirectly in the anterior cells of the parasegment by repressing *run* and *odd* (Manoukian and Krause, 1992), which would then block the activities of other *en* regulatory

elements within the *en* enhancer. For example, in the anterior-most cells a combination of EVE and PRD activate *en* (Scott and O'Farrell, 1986; DiNardo and O'Farrell, 1987; Ingham et al., 1988). Additionaly, ODD and RUN repression marks the posterior and anterior boundaries of *en* expression as well as the expression of *prd* (Manoukian and Krause, 1993; Saulier-Le Drean et al., 1998). Thus, alternate elements within the *en* enhancer may be reponsive to *en* activators such as PRD, such that when EVE directly represses *run* and *odd,* PRD would be available to bind to a specific element and *en* activation could occur. The indirect and direct activities of EVE are deduced from kinetic analysis and the overlapping expression of these proteins. Direct repression of one gene by another occurs quickly (within 15-20 min or less) and this would be fast enough to allow activation of *en* indirectly by EVE.

Due to the early expression and interactions between FTZ, EVE, and ODD, much of the interplay between FTZ and EVE in establishing parasegmental boundaries may occur at the FTZ and ODD promoters (by FTZ and EVE). Other interactions via RUN would most likely be indirect effects on the activities of FTZ and EVE. Within the remaining cells of the parasegment that are not future boundary cells, interaction of active FTZ or EVE with other differentially expressed segmentation genes would further determine parasegment polarity and identity.

FTZ and EVE both repress *wg* expression and this probably occurs directly. WG is present within the most posterior cells as the expression of

ftz and *eve* resolves out of these cells. EVE may repress *wg* directly or this may occur through PRD (Manoukian and Krause, 1992). Additionally, FTZ may also repress *wg* via PRD (Copeland et al., 1996). In this way the expression of *wg* and *en* would be juxtaposed on either side of the parasegmental boundary.

Thus, by this model, when the relative expression level of one gene is increased or decreased, the amount of active protein present within a cell would change, thus affecting the specific target genes. The targets would be activated and the position of the parasegmental boundary would be correspondingly shifted. If only a small amount of active FTZ or EVE is present (or the other is absent or lower) this could be increased through autoregulation. Additionally, if FTZ and EVE are acting as mutual repressors or through a counting mechanism (equivalent levels of proteins would cancel each other out), increased expression through autoregulation together with repression of the lower expressed gene would convert the expression of overlapping gradients into sharp parasegmental boundaries.

It is also interesting to speculate that both EVE and FTZ may be acting in conjunction with histone deacetylases or histone acetyltransferases, which may regulate gene expression. For example, genetic studies show that mutants of the histone deacetylase Rpd3 reduce the repressive activity of EVE resulting in loss of the *ftz*-dependent *en* stripes (Mannervik and Levine, 1999). Additionally, nuclear receptors can

activate transcription via the recruitment of histone acetylases. This occurs with the cooperation of co-activators (Johnson and Turner, 1999). Drosophila Ftz-F1 is a nuclear receptor and is required along with FTZ to activate *en*. It has been speculated that FTZ may be a co-factor required for histone acetyltransferase recruitment (Guichet et al., 1997).

4.4.1 Proposed experiments

To determine if FTZ and EVE interact directly, affinity chromatography or Far-Western assays could be carried out. Alternatively co-immunoprecipitation experiments from embryo extracts could be performed. Mass spectrometric analysis of the components in the complexes isolated could then help determine if this interaction between FTZ and EVE was occurring directly or through a cofactor.

The idea that the relative levels of two proteins might directly determine patterning also stems from studies of other genes in *Drosophila*. Two genes expressed in imaginal discs, *Scalloped* (SD, a transcription factor) and *Vestigial* (VG, an activator) are each required for wing development. SD is required for VG function. These genes act coordinately, and altering the relative expression levels of either gene results in inhibition of wing formation (Simmonds et al., 1998). An excess of one protein is as detrimental as not enough of that same protein, and in either case, wing formation was inhibited. These two proteins interact

directly with one another to control the activation of genes required for wing development (Halder et al., 1998; Simmonds et al., 1998).

If FTZ and EVE are not interacting with each other (directly or through a cofactor), then competition for differential binding sites in target gene promoters may be occurring. As both FTZ and EVE belong to the same class of homeodomains, and recognize similar sequences, competition for binding sites may be occurring. Competition between two proteins to activate one another has been observed, *in vitro*, for the correct activation of the homeotic gene *Ubx* within parasegment 6. Within the *Ubx* promoter there are FTZ DNA binding sites that are adjacent to or overlap with Hunchback (HB) binding sites. HB is a repressor of Ubx activity. Competition between FTZ and HB proteins for these binding sites results in the formation of the sharp anterior boundary of *Ubx* expression (Muller and Bienz, 1992). Although not shown *in vivo*, the binding sites may not need to be overlapping due to quenching (HB could repress FTZ directly). It is likely that, within target gene promoters, binding sites for both FTZ and EVE are present (overlapping or not) that may have differential binding affinity for either protein, or for which FTZ and EVE may compete. As both FTZ and EVE recognize a similar target sequences *in vitro*, competition for binding sites may be possible. *In vivo*, co-factors may influence this type of regulation. Specific binding sites would need to be identified and then *in vitro* binding assays as well as *in vivo* tests carried out to determine if competition between FTZ and EVE is

occurring. It would be difficult to determine if competition is occurring *in vivo*, but this could be tested for example in Schneider cells (insect cells). In Schneider cells, FTZ can act as an activator and EVE as a repressor on target promoters (*en*; Han et al., 1989). By co-injection of FTZ and EVE into cells, the importance of the relative levels of each protein could be determined. If levels of FTZ or EVE were found to be relevant, competition between FTZ and EVE may occur *in vivo*.

4.5 How do other pair-rule genes influence parasegment size and borders?

When the relative levels of *ftz* or *eve* are altered, parasegment size is altered, however the effect of altering parasegment border position on the expression of other relevant pair-rule genes has been described less extensively (DiNardo and O'Farrell, 1987; Carroll and Vavra, 1989; Mullen and DiNardo, 1995). For example in *odd* null mutants, coupled *en* patterns much like those obtained in this study are observed. The *eve*-dependent parasegments are larger than normal, because ODD initially activates *ftz* and represses *eve* (Saulier-Le Drean et al., 1998). The even numbered *en* stripes in *odd* mutant embryos are much broader and split in two by 6 hrs AEL (DiNardo and O'Farrell, 1987). This produces a cuticle in which the odd-numbered denticle belts are missing and are replaced by very narrow denticle bands that are a result of a mirror image duplication of the remaining even-numbered *en* stripes (DiNardo and O'Farrell, 1987). *odd* expression is also required to ensure that *en* is

expressed only in the proper domain. Very early in development, FTZ is an activator of *odd* such that the expression of *ftz* and *odd* stripes are completely overlapping (Nasiadka and Krause, 1999). However, ODD and EVE repress each other, which would refine *ftz* expression and allow for the activation of *en* (Manoukian and Krause, 1992; Saulier-Le Drean et al., 1998). Hence, in HSFTZ embryos, *odd* expresion expands causing a reduction in the size of the *eve*-dependent parasegments. Conversely, in *ftz* mutants the opposite would occur and *eve*-dependent parasegments would increase in size. Whether or not *en* stripes are present may depend upon the overlap between *ftz* and *odd* and the repression of *odd* by EVE. Thus, although *odd* plays a major role in the positioning of the *en* stripes and parasegmental boundaries, much of this role is explained through indirect actions on both FTZ and EVE. The effects on FTZ and EVE in turn can be partially explained by their effects on *odd*. It would also be useful to determine more extensively the changes in expression of *prd*, *run*, and *slp* in embryos in which the relative levels of *ftz* and *eve* expression have been altered, and vice versa. Using a combination of genetics and heat shock kinetic experiments to determine direct and indirect regulatory relationships may reveal interactions that were previously missed.

4.6 Why are reduced parasegments lost?

There are two main explanations for the delamination of cells within the reduced parasegments from the ectodermal layer. First, altered segment polarity gene expression, including *wg*, *hh* and *nkd* may contribute to parasegment loss. The expression of these genes is important in maintaining parasegments and

parasegmental boundaries. Second, cells could be delaminating due to changes in adhesiveness between cells, or between enlarged and reduced parasegmental regions.

4.6.1 Changes in the expression of signaling molecules may result in loss of reduced parasegments

Local signals emanating from the cells at compartment boundaries play important roles both in establishing and maintaining the boundary, and also guide patterning across the parasegment (Baker, 1988; Martinez Arias et al., 1988; Bejsovec and Martinez Arias, 1991). Two such short-range signaling molecules within the embryonic ectoderm come from the *wg* expressing and *hedgehog* (*Hh*) expressing cells. I have demonstrated that within the reduced parasegments, the expression domains of *en* (cells producing the Hh signal) and *wg* are wider than normal (Fig. 3.4; data not shown). Within the reduced parasegments it is possible that improper signaling between a fewer number of cells may be occurring, resulting in cells losing their fate and delaminating from the ectoderm. There are also other segment-polarity genes expressed within a parasegment that are required to determine overall polarity and identity including *patched* (*ptc*) and *naked* (*nkd*; Bejsovec and Wieschaus, 1993; Mullen and DiNardo, 1995). Within the reduced parasegment, fewer cells are present to express these different genes, which may also contribute to cells losing their fate and delaminating. It would be informative to follow the expression patterns of other segment polarity genes such as *hh*, *ptc* and *nkd* in embryos where the levels of FTZ and EVE have been altered. Altered signaling between the cells of the

reduced parasegments could account for the loss of these cells. However, cell loss could also be occurring in conjunction with changes in adhesive properties between cells in the ectoderm of the mutant embryos.

4.6.2 Changes in adhesion may result in loss of the reduced parasegments

Cells of the reduced parasegments may become mesenchymal and move into the interior of the embryo because of changes in the adhesion between the cells of the parasegment, or between the cells of the enlarged and reduced parasegments. When cells are observed to delaminate, germ band retraction is also occurring, which could be placing new forces upon the reduced parasegments. During germ band retraction, the segments lengthen dorsal-ventrally and narrow anteriorly-posteriorly. This change, combined with the very reduced sizes of the alternate parasegments, could contribute to the delamination of those cells. To fully address these questions several lines of investigation could be followed.

In order to change cell shape or position, a change in intercellular adhesion would have to occur. The movement of cells out of the ectoderm could be a result of or influenced by such changes. Epithelial sheets are composed of tightly packed cells that have apical –basal polarity (Martinez Arias, 1993). Cell-cell adhesions between the epithelial cells are mediated through the adherens junctions or zonula adherens (Gumbiner, 1996). The adherens junctions allow cells to form a single epithelial layer, to establish and maintain polarity, to

maintain cell shape by organizing the actin cytoskeleton, and to localize cell-cell signaling pathways (Muller and Wieschaus, 1996; Oda et al., 1997).

In Drosophila, the adherens junctions contain DE-cadherin, Dα-catenin, and *Armadillo* (β-catenin), *crumbs*, *shotgun* (DE-cadherin), *stardust* and *bazooka* (Tepass et al., 1990; Knust et al., 1993; Peifer et al., 1993; Tepass et al., 1996; Oda et al., 1998). Together these molecules form a link between the cell membranes and the actin cytoskeleton. All components of the link must be maintained to preserve tissue integrity and in many cases are required for morphogenic movements (cell shape changes and cell movements) to occur (Oda et al., 1993; Peifer and Wieschaus, 1993; Oda et al., 1994; Grawe et al., 1996; Muller and Wieschaus, 1996; Miller and McClay, 1997; Oda et al., 1998). The *armadillo* (*arm*) protein is directly affected by *wg* signaling within the ectoderm (Hinck et al., 1994; Peifer et al., 1994; Siegfried et al., 1994; van Leeuwen et al., 1994). In older embryos where the compartment border positions have been shifted, the *wg* signaling gradient could be changed resulting in altered localization and expression of *arm* and perhaps adhesion between cells. A loss of integrity of the epithelial junctions, such as the adherens junctions, could result in cell shape changes that then disrupt the epithelial monolayer. These cells may then begin to exhibit mesenchymal features. For example, when *armadillo* is removed from embryos early in development, a normal cellular blastoderm is formed, but at gastrulation cells begin to lose adhesion with one another and undergo changes in shape and organization (Cox et al., 1996). The cells of the ectoderm begin to round up and become

mesenchymal (Cox et al., 1996). This has also been observed in the *Drosophila* ectoderm where the levels and expression patterns of cadherin change as cells change from an ectodermal fate to a mesodermal or neuronal fate (Oda et al., 1998).

Loss of expression of other proteins associated with adherens function (*bazooka* and *stardust*) could also result in cells converting from an epithelial fate to mesenchymal-like cells (Muller and Wieschaus, 1996). In vertebrate systems a down-regulation of cadherins has been associated with the invasiveness of tumour cells (Takeichi, 1991; Gumbiner, 1996). Thus, loss or alteration of signals emanating from the boundaries of reduced parasegmental regions may produce changes in adhesiveness between cells resulting in delamination of those cells.

4.6.3 Proposed experiments

Changes in the expression of components of the adherens junctions including *armadillo* (β-catenin), Dα *–catenin, crumbs*, *shotgun* (DE-cadherin), *stardust* and *bazooka* could be analyzed throughout development (up to stage 16) using fluorescent in situ hybridization or fluorescent antibody studies. Alternately, or in conjunction, quantitative Western blot analyses for each of the proteins at the various stages could also be carried out. Again, any changes in expression could be quantified against the ubiquitously expressed proteins *actin* or *tubulin*. In this manner, subtle changes in expression may be detected that are not apparent by confocal analysis, or alternately confirm those from the

confocal analysis. Within the reduced parasegments, one might expect to observe either an increase or decrease in the expression of the various components of the adherens junctions. Not all components of the adherens junctions would be expected to change in expression equivalently. If adhesion is lost between cells resulting in their delamination, a decrease or loss of expression of adhesion proteins might be expected. This may be akin to instances in which small clones of cells with anterior compartment identity are formed in the posterior compartment of imaginal disks (Lawrence, 1997). These cells tend to form spheres that delaminate from the disk surface. These events may be driven by an attempt to maximize the number of homologous adhesive cellular interactions.

Another approach to determine the role of the various adhesion molecules in delamination is to remove expression of the various components at different time points throughout development using temperature sensitive alleles of various genes in *ftz* and *eve* mutants. For example, the $arm^{H8.6}$ allele of *armadillo* is a temperature-sensitive hypomorphic allele. Removal of $arm^{H8.6}$ very early in development, results in cells of the ectoderm of the gastrulating embryo becoming multi-layered, similar to the movement of cells within the reduced parasegments of the late-stage *ftz* and *eve* mutants (Cox et al., 1996). Within the enlarged or reduced parasegments, removing the adhesion components at subsequent time points may cause delamination of cells to occur at an earlier time point. In addition, cells of the reduced parasegment may delaminate as a whole group simultaneously as opposed to a more random fashion. Novel

phenotypes and changes in expression resulting from over-expression assays in which the various adhesion molecules are placed under the control of a heat shock promoter or in the UAS/GAL4 system that ectopically expressed the protein (Brand and Dormand, 1995) could also be analyzed. For example, overexpression of DE-cadherin (or other components of the adherens junctions) may prevent cells of the reduced parasegments from delaminating, if the loss of adhesion is a key factor in this process.

The observation that cells delaminate concurrently with germ band retraction suggests that perhaps it is this morphogenic process that initiates the delamination process (Fig. 3.2 and Fig. 3.4). Cell shape changes may only be associated with germ band retraction and other forces are unknown (Martinez Arias, 1993). It would be interesting to observe the effect of altering parasegment size in mutant genetic backgrounds in which embryos do not undergo germband retraction. Mutants that could be analyzed include genes such as *hindsight*, *tail-up* or *u-shaped* (Frank and Rushlow, 1996; Yip et al., 1997). Using confocal analysis of cells within the reduced and enlarged parasegments, any changes in the delamination of cells would be followed. If germ band retraction is prevented, then delamination of reduced parasegment cells should fail to occur. However, if germ band retraction has no effect on this process, then one would expect cells within these regions to delaminate normally.

Other morphological movements that occur during development could also provide the force causing the smaller parasegments to delaminate. For example,

the formation of the deep segmental furrows (beginning at stage 11) could force reduced parasegments to be internalized. In stage 13 to 16 embryos in which *ftz* or *eve* is altered, extra furrows are often formed alongside normal segment furrows. However, initial formation of segmental furrows is not well understood. Although they are characterized as the point at which body musculature attaches to the body wall (at approximately 14 hrs AEL), this does not occur until well after the beginning of internalization of the reduced parasegmental regions. In fact, by 14 hrs AEL the reduced parasegments have already been completely internalized. Nevertheless, changes in cell intercalation during germ band extension within a very reduced parasegment together with formation of the segmental furrow could result in the movement of the region into the interior of the embryo. Thus, the role of the segment furrows, and the elucidation of mechanisms of normal furrow formation require further investigation.

4.7 Role of apoptosis in loss of the reduced parasegments

Another avenue of investigation that should be pursued is the role of apoptosis in the reduced parasegments. It appears that the enlarged parasegments undergo increased apoptosis to attempt to correct to wild type size, whereas the reduced parasegments undergo very little or no apoptosis (Fig. 3.3). Increased apoptotic rates in enlarged segments are also observed in embryos in which extra copies of *bcd* increase the size of head structures (Pazdera et al., 1998). If the *ftz* and *eve* alleles were placed in a genetic background which blocked apoptosis, one would expect to see even larger

embryos as the excess cells within the enlarged parasegments would not be reduced in size and thus would most likely be larger than 1.4 times wild type size. Even though the internalized reduced parasegments would not die, embryo size would not be changed by this alone. The deletion (H99), which removes the genes, *hid grim*, and *rpr* (required for apoptosis) is viable as a heterozygote. When a combination of H99 and increased *bcd* gene copy number was tested, the head regions remained enlarged and did not correct back to wild type size (Bangs and White, 2000). Thus, in embryos in which the expression of *ftz* or *eve* has been altered, enlarged parasegments would be increased in size but no effect on delamination would be expected if apoptosis is only occurring after the cells leave the ectoderm (Fig. 3.4, 3.5). However, the widened *en* stripes present after the reduced parasegment delaminates may not resolve back to wild type size since apoptosis within these ectodermal stripes appears to be required subsequent to delamination of the reduced parasegment.

4.8 Possible correlations between Drosophila and other metameric organisms

The existence of molecules that provide differential adhesion within and between compartments has been hypothesized for many years (Crick and Lawrence, 1975; Morata and Lawrence, 1977; Lumsden, 1990; Ingham and Martinez Arias, 1992). Their purpose would be to prevent the mixing of cells between alternate compartments and to maintain straight boundaries between them. As discussed previously the strongest evidence for a role of molecules in

compartment boundary establishment and maintenance is found in vertebrates. Rhombomere mixing and transplantation experiments show that cells of odd-numbered rhomdomeres prefer to associate with cells of their own identity rather than with cells of adjacent even-numbered identity (Guthrie and Lumsden, 1991). For example, when cells of alternate rhombomeres (odd and even) are placed adjacent to each other, new boundaries are formed suggesting that differences in cell adhesive properties may be present (Guthrie and Lumsden, 1991). Eph-receptors and their membrane bound ligands, ephrins, are expressed in complementary rhombomeres and have been shown to be required for boundary formation. Bi-directional signaling between adjacent cells expressing either Eph-receptor tyrosine kinase or it's ephrin ligand plays a role in the establishment of rhombomere boundaries, by restricting cell intermingling between segments (Klein, 1999). Bi-directional signaling between the ephrins and Eph-receptors may act as repulsive forces, which cause cells to sort out. Alternatively, these molecules may interact in combination with various cell-adhesion molecules to maintain the integrity of a compartment once the cells have been sorted.

A search of the completed Drosophila genome sequence (Adams et al., 2000) reveals a single ephrin-like molecule and Eph-receptor located close to another on the fourth chromosome (1024-C5 and 1026-C1, respectively). Each gene has been has been cloned and sequenced, but there are no known mutant alleles. The Eph-receptor has been isolated from an imaginal disc library and it is expressed within the compartment boundary of wing discs (Shibata and Bryant, 1998). As the complete expression patterns of ephrin and Eph-receptor

are unknown, it would be interesting to determine their spatial and temporal expression patterns, and to determine whether or not they are expressed within alternate parasegments during development. Over-expression studies, or the generation of mutants, would then be useful to determine their roles within embryogenesis. Additionally, if Eph-receptor is expressed within the compartment boundary in imaginal discs (later stages of development), is there any expression of ephrin in this same region, perhaps on alternate sides of the compartment boundary? If so, do these molecules play a similar role to that observed in the rhombomeres of mammalian embryos?

Further support for conservation of mechanisms and molecules in compartmentalization derives from the vertebrate homologues of the *Drosophila* segmentation genes *hairy* and *engrailed*, which are involved in the segmental patterning of somites (Muller et al., 1996; Holland et al., 1997; Palmeirim et al., 1997). These homologues include the zebrafish *her1* gene, the avian *c-hairy1* (both orthologues of the pair-rule gene *hairy*) gene and the amphioxous *engrailed* gene (Muller et al., 1996; Holland et al., 1997; Palmeirim et al., 1997). Both vertebrate *hairy* genes are expressed in stripes in the presomitic mesoderm, a pair-rule type pattern. This pattern suggests that *c-hairy1* and her1 play roles in mesoderm segmentation and somite development in vertebrates (Palmeirim et al., 1997; Takke and Campos-Ortega, 1999). Amphioxus is the closest living invertebrate relative of the vertebrates. Early in development amphioxus *en* is expressed as metameric stripes along the anteroposterior axis in the posterior

portion of each newly formed segment, a pattern that strongly resembles that of *Drosophila en* (Holland et al., 1997).

Hox genes in vertebrates, as in invertebrates (homeotic genes), provide positional identity and Hox gene expression is delimited by rhombomere boundaries. Thus, given the similarities in expression and/or function of compartment-specific genes across evolution, the mechanisms that allow parasegments to respond to changes in size may also be conserved in vertebrates. Conversely, molecules that are responsible for the differential adhesiveness of rhombomeres and somites may also have homologues that are expressed in parasegments.

Appendix 1

This appendix was published as a short communication in BioTechniques:

Hughes, S.C., B. Saulier-Le Drean, I. Livne-Bar and H.M. Krause. 1996. Fluoresence In Situ Hybridization in Whole-Mount Drosophila Embryos. BioTechniques 20(5):748-749.

S.C.H. established the technique and determined the original condition with the initial probes *en*, *wg* and *ftz*.

B.S.L.D. helped to establish some of the proper conditions and tested some probes on whole-mount embryos.

I.L.B. carried out the *wg* in situ and performed the confocal microscopy.

Fluorescence In Situ Hybridization in Whole-Mount *Drosophila* Embryos

In situ hybridization within whole-mount *Drosophila* embryos was made routine approximately six years ago by the introduction of digoxigenin-labeled probes (Tautz and Pfeifle, 1989). However, methods of digoxigenin detection have been handicapped by a requirement for alkaline phosphatase-conjugated secondary antibodies. A fluorescence in situ hybridization (FISH) technique for whole-mount embryos would provide a number of advantages over existing technology. For example, conjugated fluorescent molecules do not diffuse as do the products of the alkaline phosphatase reaction, giving higher resolution staining (Harlow and LAne, 1988). The use of fluorescent probes also allows the use of laser scanning confocal microscopy (LSCM). In addition to providing better resolution than conventional microscopes, LSCM also facilitates resolution of internal signals, optical sectioning of the embryo in different planes and reconstruction of sections into three-dimensional images. Overlaps in gene expression patterns observed in double-labeling experiments would also become more distinct, since overlaps generate novel colours. Paddock et al. (Paddock et al., 1993) have demonstrated the power of double-protein labeling in whole-mount embryos using fluorescent probes and LSCM. With FISH, the same approach could be used to monitor overlaps in patterns of mRNA, or mRNA and protein.

We describe here a protocol for FISH in whole-mount embryos using a fluorescein-tagged RNA probe. The RNA probe, in turn, is detected with anti-fluorescein antibodies, and fluorescein isothiocyanate (FITC)-conjugated

secondary antibodies. Signals generated were strong and worked with four of five probes tested. The fluorescein in the RNA probe itself does not contribute to the signal. Thus other secondary antibody-conjugated fluorochromes, such as rhodamine or cyanine, could also be used to advantage. Figure 1A shows *wingless (wg)* gene transcripts detected by FISH and low magnification LSCM. Figure 1B is a higher magnification LSCM section of the embryo surface showing asymmetric subcellular distribution of the *wg* transcripts. Note the punctate nature of the signal (not detectable by enzymatic detection) and the nascent transcripts in the nucleus.

Fluorescein-12-UTP (Boehringer Mannheim, Laval, Quebec, Canada)-labeled RNA probes were synthesized essentially as directed by the manufacturer. Briefly, the 20-μL reaction contains 1μg linearized template DNA, 2μL 10X reaction buffer (0.4 mM Tris-HCL, pH 8.0, 60 mM $MgCl_2$; dithiothreitol [DTT]; 20 mM spermidine; 100 mM NaCl, and 1 U/μL RNase inhibitor), 2μL 10X NTPs (10 mM each of ATP, GTP, CTP, 6.5 mM UTP, and 3.5 mM fluorescein-12-UTP [a manufacturer premade mix is available; Boehringer Mannheim]) and 1μL 20 U/μL T3 or T7 RNA polymerase (Boehringer Mannheim). Approximately 5-10 μg of product was obtained following a 2-h incubation at 37°C with probes ranging from 1.5 to 3kb in size. Template was removed by treating with 1 μL DNAase (1000 U/ml; Boehringer Mannheim) for 15 min at 37°C followed by heating for 15 min at 65°C. Partial degradation of the probe was observed following this step. Further degradation mediated by incubation in carbonate buffer (Lehmann and Tautz, 1994) was found to be unnecessary, and in fact

decreased probe activity. Ethanol precipitation was achieved using 2 µL of 4M LiCl (or 2M final concentration of ammonium acetate) and 60 µL of ethanol, and then resuspended in 100µL of distilled water.

Embryos were prepared according to Lehmann and Tautz (Lehmann and Tautz, 1994). Paraformaldehyde (4%) was found to be essential for fixation. Embryos fixed with formaldehyde, even EM-grade (5%; JBS-Chem, Pointe Claire-Dorval, Quebec, Canada) tended to fall apart.

Probe (0.5-1.0µL) was diluted in 100µL of hybridization buffer (HYB: 50% formamide, 5X SSC, 100µg/ml heparin, 100µg/ml sonicated salmon sperm DNA, 0.1% Tween-20), denatured for 3 min at 80°C and added to 25-50µL of settled embryos. Hybridization was carried out at 56°C for a minimum of 16 h. Successive post-hybridization washes (20 min each) were performed at 56°C using 250 µl each: HYB; 3:1 HYB:PBT (PBT is 1X PBS + 0.1% Tween-20); 1:1 HYB:PBT; 1:3 HYB:PBT, PBT. Embryos sticking to the tube sides or cap were pelleted by 5- to 10- s spins at 1500 rpm (2000X g) in a centrifuge. After a final rinse in PBT, embryos were incubated with a monoclonal anti-fluorescein antibody (1/5000 in PBT; Boehringer Mannheim) for 1.5-2 h. Primary antibody was then detected using a donkey anti-mouse-FITC antibody (1/50, whole antibody; Jackson IRL, West Grove, PA, USA, or 1/25, Amersham, Oakville, Ont., Canada). After washing, embryos were mounted in 70% glycerol containing 2% DABCO (Sigma, St. Louis, Mo., USA). Images were captured using either a Sony XC275 CCD camera and Northern Exposure software (Empix Imaging, Mississauga, Ontario, Canada), or a Zeiss laser confocal

microscope (Carl Zeiss, Thornwood, NY, USA). Figures were compiled using Adobe Photoshop 3.0 (Adobe Systems Incorporated, Mountain View, CA, USA).

This procedure should also be suitable for fluorescent mRNA/protein double-labeling experiments. The conditions used here for embryo fixation and hybridization are the same as those used previously for double labeling using enzyme-conjugated secondary antibodies (Mullen and DiNardo, 1995). Double-FISH labeling, on the other hand, will require the development of a second type of labeled probe, suitable for FISH. Thus far, combinations of digoxigenin-labeled DNA or RNA probes used together with sheep anti-digoxigenin antibodies (Boehringer Mannheim) and anti-sheep fluorescein or rhodamine-conjugated secondary antibodies (Amersham) have not worked in our hands. However, other sources and combinations of antibodies and the use of biotin-labeled probes have yet to be tested. In the meantime, double-mRNA labeling should be possible using a combination of FISH and conventional digoxigenin RNA probe detection. The fluorescent and bright-field images could be superimposed photographically or digitally. Where overlaps occur, the fluorescent signals would be partially quenched.

Figure 1. Fluorescent *in situ* detection of *wg* transcripts in whole-mount embryos. A) Low magnification LSCM detection of *wg* RNA in a stage 9 (germ band extended) embryo. Note the sharpness of the stripes. B) High magnification LSCM image showing *wg* mRNA subcellular localization in a stage 5 (cellular blastoderm) embryo. A monolayer of cells at the embryo surface is seen in cross-section with the epidermal surface up. The section is through the posterior-most *wg* stripe. Nascent sites of transcription within the nucleus are designated by arrows (as observed previously by (Shermoen and O'Farrell, 1991).

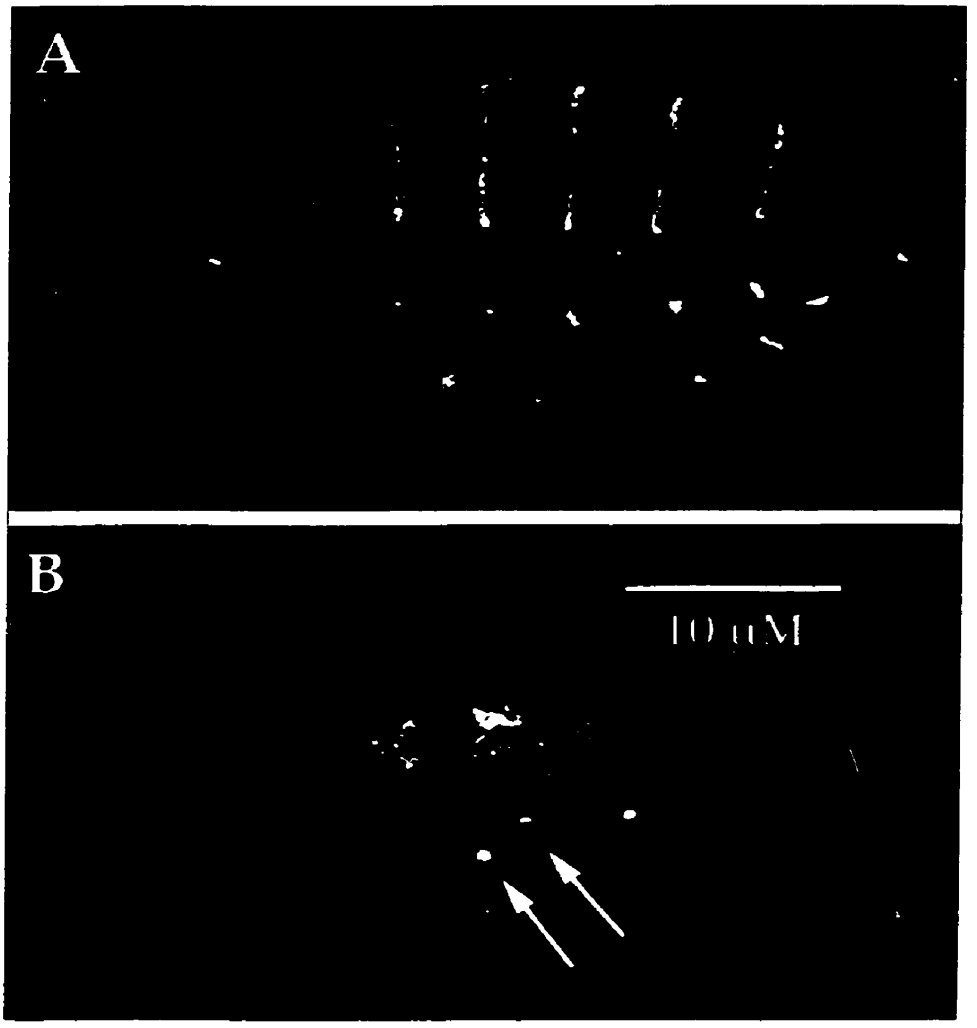
A
B
10 μM

Appendix 2

This appendix was published as a short communication in BioTehniques: Hughes, S.C. and H.M. Krause. 1998. Double labeling with fluorescence in situ hybridization in *Drosophila* whole-mount embryos. *BioTechniques* 24:530-532.

S.CH. developed the techniques and tested all probes and conditions.
H.K. helped to develop staining with digoxigenin labeled probes

Double labeling with FISH in *Drosophila* whole-mount embryos

Previously, we described a technique for fluorescence *in-situ* hybridization (FISH) in whole-mount *Drosophila* embryos using fluorescein labeled RNA probes (Hughes et al., 1996). This technique provides several advantages over conventional alkaline phosphatase based detection methods. For example, a fluorescent label is non-diffusable and so allows higher resolution imaging. Furthermore, it allows the use of confocal and deconvolution microscopy, which can take advantage of this enhanced resolution and at the same time penetrate deeply into the sample to give three dimensional information.

Another potential advantage of fluorescent detection methods is the possibility to generate double-labeled samples where relative overlaps between two or more expression patterns can be resolved at the cellular and sub-cellular levels. Our previous method allowed for the detection of only one transcript. Here we describe modifications of our protocol, which allow simultaneous detection of two different transcripts. We also describe a variation which combines whole-mount FISH with fluorescent antibody staining.

Double FISH was achieved using a combination of fluorescein and digoxigenin tagged RNA probes. The probes were detected by incubating first with anti-fluorescein and anti-digoxigenin antibodies and subsequently with the corresponding non cross-reacting fluorescently tagged secondary antibodies. Several probes were tested with equally successful results. Strong signals were detected using conventional fluorescent microscopy.

RNA probes were made using T7 (Boehringer Mannheim, Laval, QC, Canada; Cat No. 881 767) or T3 (Boehringer Mannheim, Laval, QC, Canada; Cat No. 103 163) RNA polymerases essentially as described in the manufacturers specification sheet. Enzyme buffers (10X) provided with the polymerases were used. Flourescein-12-UTP and digoxigenin-12-UTP ribonucleotides were obtained as premixed 10X cocktails containing appropriate concentrations of unlabeled ribonucleotides (Fluorescein RNA labeling Mix, Cat No. 1685 619; DIG RNA labeling Mix, Cat No. 1277 073; Boehringer Mannheim). Before use, template DNA must be cut to completion and carefully phenol/chloroform, and chloroform extracted and then ethanol precipitated prior to use. RNAse free reagents are recommended but are not essential if care is used in preparation of the template and assembly of the transcription reactions. To eliminate possible RNAse contamination, 1μL RNAse inhibitor (RNAguard Cat No. 27-0815-01; Pharmacia Biotech, 500 Morgan Blvd., Baie d'Urfe, QC, Canada; 1 U/μl) was added to each 25 μL transcription reaction. Following the transcription reaction (at 37°C for 2 hr), the labeled probes were precipitated by the addition of 1 μl 0.5M EDTA, 2.5 μl 4M LiCl, and 75 μL absolute ethanol. The resulting pellet was washed with 500 μL cold 70% ethanol and resuspended in 100 μL RNAse-free H_2O. Figure 1 shows the products of two transcription reactions resolved on a 0.8% agarose gel and stained with ethidium bromide. Degradation of the probe by carbonate buffer treatment (Lehmann and Tautz, 1994) was found to be not only unnecessary but usually detrimental.

Embryos were prepared essentially as described by Lehmann and Tautz (Lehmann and Tautz, 1994) using 4% formaldehyde. A 40% stock formaldehyde solution can be prepared prior to embryo fixation as follows. Paraformaldehyde (0.92 g) is added to a glass test tube along with 2.5 mL H_20 and 35 µL 1N NaOH. The mixture is heated at 90-100°C until the paraformaldehyde is fully in solution. Fixation was performed in scintillation vials containing 8 mL heptane, 2.25 mL 1X PBS and 0.25 mL 40% formaldehyde. The mixture is intermittently swirled for 20 minutes, and then the embryos are drawn off in heptane taking care not to transfer any of the lower aqueous phase, and transferred to a 1.5 mL microfuge tube. The volume is then adjusted to 0.5 mL heptane and 0.5 mL methanol and shaken vigorously for 30 seconds to devitillinize the embryos. Most of the embryos should sink to the bottom. As much of the methanol as possible is removed along with most of the heptane and then the step is repeated. Finally, embryos are washed three times with methanol and then stored if necessary in methanol at -20°C. The remaining post fixation and protease steps are as described in (Tautz and Pfeifle, 1989) using freshly prepared formaldehyde.

Concentrations of probes and antibodies should be worked out empirically for different probes and antibody preparations. The following conditions worked

Figure 1. An ethidium bromide stained DNA agarose gel showing the products of two transcription reactions. Lane 1: 0.5 µg *Eco*R1 digested *engrailed* template DNA (pBSen). Lane 2: 3 µl digoxigenin labeled *engrailed* probe. Lane 3: 4 µl fluorescein labeled *fushi tarazu* probe. Lane 4 0.5 µg *Hin*dIII digested *fushi tarazu* template DNA (pGEMF 4). Arrows indicate the positions of full-length probes. Note that the probes appear to be intact and that the majority of unincorporated nucleotides have been removed.

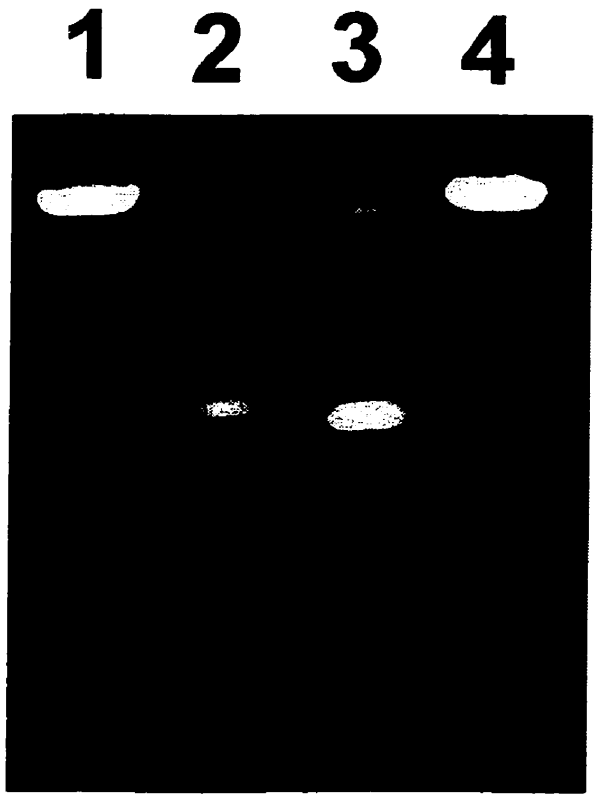
1 2 3 4

best for us. Probe (0.5 to 1 µl) was added to 100 µl RNA hybridization buffer (HYB: 50% formamide, 5X standard saline citrate [SSC], 100 µg/ml heparin, 100 µg/ml sonicated salmon sperm DNA and 0.1% Tween 20) and heated to 80°C for 3 minutes, cooled on ice and then added to approximately 25 µl (settled volume) prehybridized (1-2 hr in HYB at 56°C) embryos. Hybridizations were carried out at 56°C for 12 to 16 hours. Successive post-hybridization washes (30 minutes each) were carried out at 58°C using 400 µl each: HYB; 3:1 HYB:PBT (PBT = 1X PBS + 0.1% Tween 20); 1:1 HYB:PBT; 1:3 HYB:PBT; and PBT. Embryos were rinsed once more in PBTB (PBT + 0.5% skim milk powder). Use of skim milk powder appears to reduce background significantly. Pre-incubating the secondary antibodies with unhybridized embryos can also reduce background, but was not found to be essential.

Hybridized RNA probes were detected by incubating the embryos in a combination of a mouse monoclonal anti-fluorescein antibody (1/2000 dilution of a 0.1 mg/ml solution; Boehringer Mannheim, Laval, QC, Canada; Cat No. 1426 3320) and a sheep anti-digoxigenin antibody (1/1000 dilution of a 0.2 mg/ml solution; Boehringer Mannheim, Laval, QC, Canada; Cat No. 1333 089) in PBTB for 2 hours at 25°C. Following this, embryos were washed with four changes of PBTB over the course of 2 hours. Primary antibodies were then detected by incubating the embryos in a combination of goat anti-mouse antibodies conjugated to CY2 (1/2000 dilution of a 1 mg/ml solution; Jackson ImmunoResearch Laboratories, Inc., West Grove, PA, USA; Cat No. 115-226-052) and donkey anti-sheep antibodies conjugated to CY3 (1/2000 dilution of a 1

mg/ml solution; Jackson ImmunoResearch Laboratories, Inc., West Grove, PA, USA; Cat No. 713-166-147) in PBTB for 1.5 hours at 25°C. After washing once more in PBTB for 1-2 hours, the embryos were mounted in 70% glycerol containing 2% DABCO (Sigma Chemicals, St. Louis, MO, USA). Embryos were viewed using a Zeiss Axioplan 2E microscope (Carl Zeiss, Thornwood, NY, USA) and images captured using a Princeton Systems Micromax CCD camera (Princeton Instruments, Trenton, NJ, USA) and Northern Eclipse™ software (Empix Imaging, Mississauga, ON, Canada). Figures were compiled using Adobe Photoshop™ 4.0.1 (Adobe Systems, Mountain View, CA, USA).

Figure 2A shows an example of a whole-mount embryo double-labeled with a fluorescein labeled *fushi tarazu* (*ftz*) and a digoxigenin labeled *wingless* (*wg*) probe. Several other combinations of differentially labeled probes were tested including a fluorescein labeled *ftz* probe together with a digoxigenin labeled *engrailed* (*en*) probe, a fluorescein labeled *wg* probe together with a digoxigenin labeled *en* probe and a fluorescein labeled *wg* probe together with a digoxigenin labeled *wg* probe. All combinations worked equally well (data not shown).

We also tested whether this type of FISH was compatible with immunofluorescence-based protein detection. Figure 2B shows an embryo that was labeled for *wg* mRNA (red) and *en* protein (green). The mRNA probe preparation, hybridization and post-hybridization washes were carried out as described for the double in-situ protocol above, except that a shorter proteinase K treatment (half the time) was used to reduce degradation of protein epitopes.

Figure 2. Double labeled embryos. A) Low magnification (x20) detection of *fushi tarazu* mRNA (green) and *wingless* mRNA (red) in a stage 7 embryo. B) Same magnification of a whole mount embryo double labeled for *wingless* mRNA (red) and *engrailed* protein (green) in a stage 10 embryo.

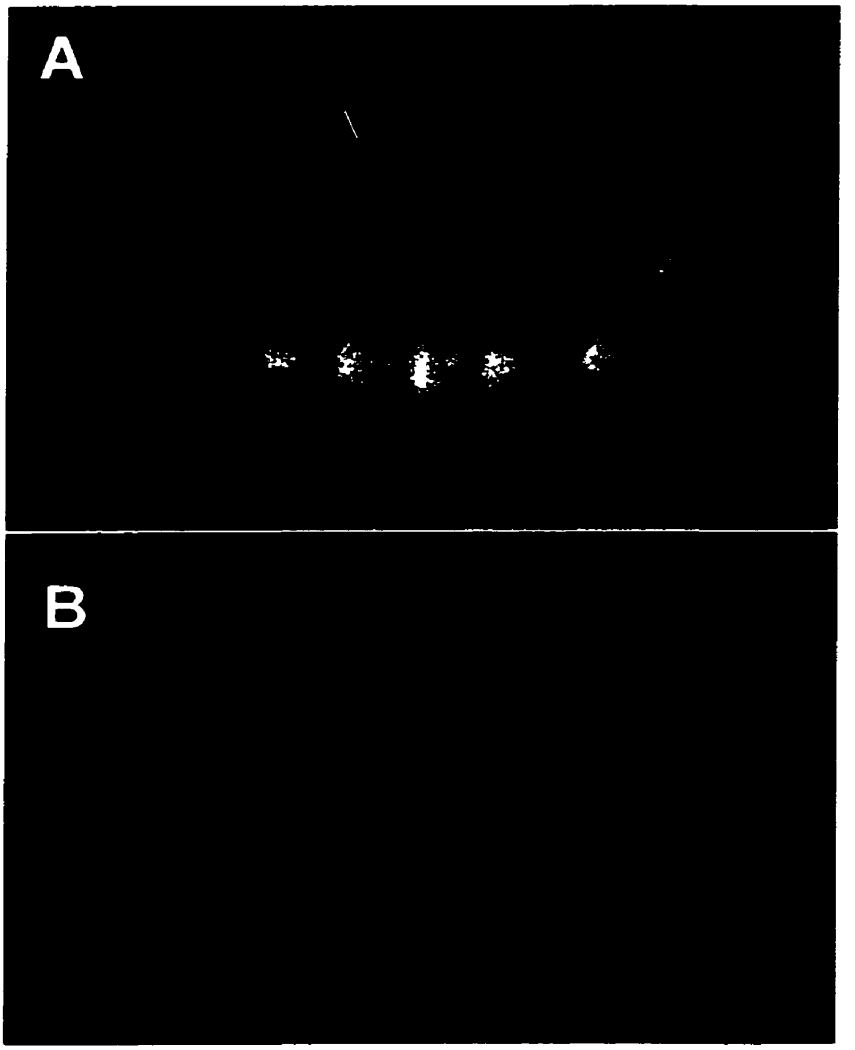
A
B

Appendix 3

This appendix was published as chapter 5 in *Methods in Molecular Biology*, vol. 122: *Confocal Microscopy Methods and Protocols*. 1999. Edited by: S. Paddock. Humana Press Inc., Totowa, N.J. pgs 93-101.

Single and Double FISH protocols for *Drosophila.*

Sarah C. Hughes and Henry M. Krause

This appendix contains a summary of the techniques established by S.C.H.

1. Introduction

In situ hybridization within whole-mount *Drosophila* tissues was made routine with the introduction of digoxigenin labeled probes and alkaline phosphatase based detection methods (Tautz and Pfeifle, 1989). However, this method of detection until recently has been limited by the required use of alkaline phosphatase conjugated secondary antibodies and chromogenic substrates. The use of alkaline phosphatase substrates and their diffuable products limits the resolution of staining, particularly in thick tissues and deep within the embryo. Without additional probes, double-labeling and interpretation of results is also very difficult.

In this chapter we describe techniques for fluorescent in situ hybridization (FISH) in *Drosophila* tissues. Unlike the products of the alkaline phosphatase reaction, a fluorescent signal is non-diffusable and thus allows higher resolution microscopy (Harlow and LAne, 1988). Resolution and sensitivity of probe detection are enhanced even further when coupled with laser scanning confocal microscopy (LSCM), or devolution microscopy. Other advantages include the ability to reconstruct three-dimensional images and to peer deep within the specimen. If more than one probe is available, the ability to assess overlaps in patterns of expression is also enhanced (Paddock et al., 1993). In addition to the increased resolution, overlaps show up as easily discerned novel colours (e.g. red + green = yellow). With LSCM, one can also tell if transcripts do or do not co-localize at the subcellular level.

This chapter describes how to generate multiple probes for double hybridization. Also described are variations of the protocol that allow simultaneous detection of transcripts and proteins and for use of these detection techniques in whole embryos as well as dissected tissues. Underlying the described detection methods is the use of non-radioactive RNA probes and fluorescently conjugated secondary antibodies. Probes labeled with digoxigenin or fluorescein work equally well. Primary antibodies against these molecules are available from Boehringer Mannheim, as are reagents and kits for making the labeled RNA probes. Non-cross-reacting secondary antibodies, conjugated to cyanine fluorocromoes, are then used to bind the primary antibodies.
The strength of the signals generated by this procedure, relative to standard chromogenic detection techniques, depends upon the equipment used for detection. We find that the intensities of fluorescent and chromogenic signals are similar when developed using the same RNA probe, and as detected on our Zeiss Axioplan 2E microscope. However, when detected by LSCM, the FISH approach is much more sensitive and gives far greater resolution.

2. Materials

2.1 *RNA Probe Preparation*

1. 1.5 ml Microcentrifuge tubes, autoclaved.
2. RNAse free Diethyl Polycarbonate (DEPC) treated or double-distilled water.

3. 5X T7/T3 transcription optimized buffer (Promega, Madison WI, USA; Cat No. P1181)
4. T7 or T3 RNA Polymerase (Promega, Madison WI, USA: Cat Nos. P2075, P2083; 1000 U).
5. Fluorescein RNA labeling Mix (Boehringer Mannheim; Cat No. 1685 619).
6. Digoxigenin RNA labeling Mix (Boehringer Mannheim; Cat No. 1277 073).
7. RNAguard (Pharmacia; Cat No 27-0815-01)
8. 0.5 M EDTA.
9. 4M Lithium chloride.
10. Absolute ethanol.
11. Cold 70% ethanol wash

2.2 *Initial Embryo Fixation*

1. Chlorine bleach; diluted 1:1 with water.
2. 40% formaldehyde solution (prepared fresh from paraformaldehyde as described below).
3. 10X Phosphate-buffered saline (PBS) solution.
4. Heptane.
5. Methanol.
6. 20-ml disposable glass scintillation vials (Fisher).
7. 1.5-ml microcentrifuge tubes, autoclaved.

2.3 *Post-Fixation and Hybridization of Whole-mount Embryos*

1. PBT solution: 1X PBS plus 0.1% Tween-20.
2. 40% formaldehyde solution prepared that day.
3. 20mg/ml Proteinase K (Sigma; dissolve in sterile H_2O, divide into 50-µl aliquots and stored at -20°C) .
4. 2mg/ml glycine in PBS.
5. RNA hybridization solution: 50% formamide, 5X SSC, 100 µg/ml heparin, 100 µg/ml sonicated salmon sperm DNA and 0.1% Tween 20). Filter through a 20 micron filter and store at -20°C in aliquots (stable for at least 6-12 months).
6. Hot block or water bath at 80°C.
7. Water bath at 56°C.

2.4 *Post-Hybridization Washes and Development of the FISH signal*

1. RNA Hybridization buffer.
2. PBT solution: 1XPBS, 0.1% Tween-20.
3. PBTB solution: 1XPBS, 0.1% Tween-20 and 0.5% milk powder.
4. Mouse monoclonal anti-fluorescein antibody (IgG: 1/2000 dilution of a 0.1 mg/ml solution [see Notes 2 and 3]; Boehringer Mannheim, Laval, QC, Canada; Cat No. 1426 3320).
5. Sheep anti-digoxigenin antibody (IgG; 1/1000 dilution of a 0.2 mg/ml solution; Boehringer Mannheim, Laval, QC, Canada; Cat No. 1333 089).
6. Goat anti-mouse antibody conjugated to CY2 [$F(ab')_2$ fragment of IgG (H+L) 1/2000 dilution of a 1 mg/ml solution; Jackson ImmunoResearch Laboratories Inc., West Grove, PA, USA; Cat No. 115-226-052].

7. Donkey anti-sheep antibody conjugated to CY3 [$F(ab')_2$ fragment of IgG (H+L); 1/2000 dilution of a 1mg/ml solution; Jackson ImmunoResearch Laboratories Inc., West Grove. PA, USA; Cat No. 713-166-147].
8. Embryo mountant: 70% glycerol, 2% DABCO (1,4-Diazabicyclo [2.2.2.] Octane; Sigma, USA; Cat No. D-2522).
9. Microscope slides.
10. Coverslips (22 X 50 mm).
11. Fluorescence (Zeiss Axioplan 2) and/or LSC microscope (Zeiss).

3. Methods

3.1 *RNA Probe Preparation*

1. To prepare run-off transcripts, the plasmid template is first linearized to completion (see Note 1) with the appropriate restriction enzyme, and then the enzyme is removed by careful phenol and then chloroform extractions. After removal of all chloroform (heating to 65°C for 15 min helps), precipitate the DNA by adding NaAcetate (pH 5.2) to 0.3M, 3 vol of ethanol, and cooling to -70°C for 20 min. Centrifuge 10 min in a cold microcentrifuge and wash with cold 70% ethanol. We generally prepare 5-10 μg linearized template, resuspended in 20 μl RNAse-free water.

2. RNA probes are prepared as described by Boehringer Mannheim on their digoxigenin and fluorescein RNA labeling spec sheets. On ice add 1 μg of linearized template DNA (3-5kb), 2μl fluorescein or digoxigenin RNA

labeling mix, 4 µl 5X transcription buffer (supplied with the RNA polymerase: 0.4M Tris-HCl, pH 8.0; 60 mM $MgCl_2$, 100 mM dithiothreitol, 20 mM spermidine), 1µl RNAse inhibitor (1 U/µl) and sterile, RNAse-free water to make the final reaction volume equal to 18 µl. Add 2 µl of the appropriate RNA polymerase (T7 or T3), mix well, and incubate at 37°C for 2 hours.

3. Following the transcription reaction (see Note 2), the labeled probe is precipitated by addition of 1 µl of 0.5M EDTA, 2.5 µl 4M LiCl, and 75 µl absolute ethanol. Chill to -70°C, centrifuge, and wash the pellet as described above. After drying, resuspend the pellet in 100 µl RNAse-free water (see Note 3). Check the probe by loading and running 4-5µl on a conventional agarose gel (~1%). The run-off transcript should easily be detected by ethidium bromide staining (Hughes and Krause, 1998). Probe should be stored at -20°C. Several freeze-thaw cycles on ice do not impair probe activity.

3.2 Initial Embryo Fixation

1. Prepare 40% formaldehyde stock solution just prior to embryo dechorionation (see Note 4). Dissolve 0.92 gm paraformaldehyde in 2.5 ml of water containing 35 µl 1N KOH. Heat the mixture at 80°C until dissolved.
2. Collect and rinse the embryos in water.

3. Dechorionate the collected embryos in a 1:1 mixture of chlorine bleach and water for approximately 90 s. When dechorionated, the embryos will either float to the surface of the bleach solution or stick to the sides of the collection basket. Embryos should be rinsed immediately, as over-dechorionation is apparently detrimental. Rinse the collection basket with plenty of water. Fast flowing tap water can help dechorionate partially dechorionated embryos. An optional rinse with 0.7% NaCl, 0.03% Triton X-100 is helpful for removing residual bleach and for washing embryos down from the side of the basket.

4. Transfer the embryos to a 20-ml glass scintillation vial (see Note 5) containing a two phase mixture of 8 ml heptane, 2.5 ml 1XPBS and 250µl of 40% formaldehyde. Shake for 20 minutes.

5. Using a 1ml pipetteman, draw up embryos (which are at the interphase), taking care not to suck up any of the lower aqueous phase (see Note 6). Transfer to a 1.5 ml microfuge tube containing 0.5 ml heptane and 0.5 ml methanol for devitilinization. Shake vigorously until the majority of the embryos sink the bottom (about 30 s). Carefully remove about 75% of the heptane and methanol and replace with 1ml methanol. Shake once more. All or most embryos should have now sunk to the bottom of the tube. Remove all liquid along with any embryos at the interphase, and then rinse 2-3 times with methanol. Embryos can be stored in methanol at -20°C for several months.

3.3 Post-Fixation and Hybridization of Whole-mount Embryos

The following steps are optimized for ~ 50 µl settled embryos in a 1.5 ml microfuge tube.

1. Rinse the embryos once in methanol.
2. Rinse the embryos twice in PBT (1XPBS, 0.1% Tween 20).
3. Post-fix the embryos for 20 minutes in 0.5ml PBT containing 50 µl freshly prepared 40% formaldehyde. Place tubes on a rocking platform to ensure even fixation.
4. Rinse embryos 3X in PBT. Washes should be approximately 2 min in duration.
5. Add approximately 0.5ml PBT containing 50 µg/ml of nondigested proteinase K. Incubate for ~1 to 1.5 min (see Note 7). Mix by drawing up some of the solution with a pipetteman and gently jetting the embryos back into suspension. Repeat once, allow embryos to settle and then remove the solution at least 30 s before the end of the incubation period.
6. Stop the proteinase K digestion by immediately adding 1ml of PBT containing 2mg/ml glycine. After about 2 min, remove and rinse for another 2 min in the same solution.
7. Rinse embryos twice in PBT to remove the glycine.
8. Post-fix the embryos once again (as in step 3) for 20 minutes in PBT containing 4% formaldehyde.

9. Wash the embryos extensively in PBT to remove all traces of fixative.

10. Rinse the embryos in 1ml of 50% PBT, 50% RNA hybridization solution. Replace the mixture with 100% hybridization solution and pre-hybridize the embryos at 56°C for a minimum of 2 hours. If required, embryos can be stored overnight at –20°C in the HYB solution prior to the 2-h heating step.

11. After pre-hybridization, place the embryos in a sterilized 0.5 ml microfuge tube, remove prehybridization solution and add probe. Optimal probe concentration needs to be determined empirically but generally 1 µl probe in 100 µl RNA hybridization solution works well. Diluted probe is heated to 80°C for 3 minutes, cooled briefly on ice and then added to the embryos.

12. Hybridizations are carried out at 56°C for 12 to 16 hours. Mix embryos 2-3 times during the course of the incubation, either by quickly inverting the tube, or by using a pipetteman to gently jet the embryos into suspension.

3.4 Post-Hybridization Washes and Development of the FISH signal

1. Remove any hybridization solution and embryos from the upper walls and cap of the microfuge tube by spinning the tube for ~ 10 seconds at 1,500rpm in a microcentrifuge.

2. Remove the probe solution and rinse the embryos once with 400 µl pre-warmed hybridization buffer. Add another 400 µl pre-warmed hybridization buffer, this time incubating at 56°C for 20-30 min. Invert tube several times during the course of the wash.

3. Wash embryos for another 20-30 min with a 1:1 mix of hybridization buffer and PBT and then with four 5 min washes of PBT. All washes should be done with preheated solutions at 56°C.
4. Cool to room temperature and incubate for 10 min in 400 µl PBTB (1X PBS, 0.1% Tween 20, 0.5% milk powder). The use of milk powder in this and subsequent steps helps to reduce background.
5. Hybridized RNA probes are detected by first incubating the embryos with the appropriate primary antibodies diluted in PBTB. For double-labeling, both anti-digoxigenin and anti-fluorescein antibodies are added. Dilutions (see Note 8) that were optimal in our hands are given in the Materials section, but batches may vary, as may optimal activity given the many variations that exist in a particular laboratory's reagents, equipment, and methodology. Incubate with primary antibodies for 2 h (optionally overnight at 4°C), with constant mixing on a rocking platform or rotating mixer.
6. Wash for 1-2 hr (optionally overnight) with four or five changes of PBTB.
7. Add the appropriate (see Note 9) secondary antibody(s) diluted in PBTB, and incubate with constant mixing for 2 h. Carry out this step and all subsequent steps in dim light with tubes covered or wrapped in foil.
8. Wash for 2 h with four or five changes of PBTB and then finally with PBT.
9. Resuspend embryos in DABCO-containing mountant. Allow the embryos to settle to the bottom of the tube (1-3 h or overnight at 4°C) before resuspending and mounting.

10. Transfer the embryos to a clean slide in ~ 80 μl mountant and covered with a 25 X 50 mm coverslip. Seal the edges with nail polish. Slides can be stored for weeks at 4°C in the dark. Background levels will often decrease over the first few days.
11. Embryos can be viewed by either conventional fluorescence microscopy, LSCM, or deconvolution microscopy. Basic LSCM techniques are discussed elsewhere in this book. An example of double FISH labeling of a *Drosophila* embryo is shown in Fig. 1A.

3.5 RNA-Protein Double-labeling

1. Collect and fix embryos as described above for FISH, with the exception of the Proteinase-K step. The Proteinase-K concentration may have to be lowered to preserve integrity of protein epitopes (see Note 7).
2. After performing the hybridization and washes, as described, add the primary antibody for the protein of interest, along with the anti-fluorescein or anti-digoxigenin antibody. To obtain non-cross-reacting signals, the protein-specific antibody must have been raised in a host other than the host(s) used for the probe-specific antibodies (i.e., not mouse or sheep).
3. After primary antibody incubation and washes, the primary antibodies are detected using appropriate secondary antibodies (see Note 9). Wash and mount as with single or double FISH staining. With careful choice of antibodies, triple-staining a combination of transcript and protein targets is possible. However, secondary antibodies conjugated to CY5 are

necessary (Paddock et al., 1993), as are the microscope excitation and detection components required for visualization.

3.6 Performing FISH on Dissected Tissues

1. Dissect tissues such as imaginal disks or salivary glands in PBS. Dissected tissues can be stored briefly (up to 30 min) on ice in a microfuge tube containing PBS while collecting enough tissues for analysis.
2. Remove the PBS and add 50 µl 10X PBS, 325 µl water, 500 µl heptane and 125 µl 40% formaldehyde (freshly prepared as described above). Shake gently for 45 s.
3. Remove the heptane and most of the fixative, and replace with PBT containing 4% formaldehyde. Continue fixation for another 20 min with gentle mixing.
4. Wash 4X with PBT and proceed to the proteinase K and subsequent steps, as described above for embryos. Use the appropriate reagents for single or double FISH, or FISH/protein double labeling in dissected imaginal disks. Figure 1B shows an example of FISH/antibody double labeling in dissected imaginal disks.

Fig. 1. (A) shows the trunk region of a cellular blastoderm embryo with *wg* transcripts detected on the left (CY3 channel) and *ftz* transcripts on the right (CY2 channel). (B) A wing imaginal disk with wingless transcripts detected on the left (CY3) and engrailed protein detected on the right (CY2).

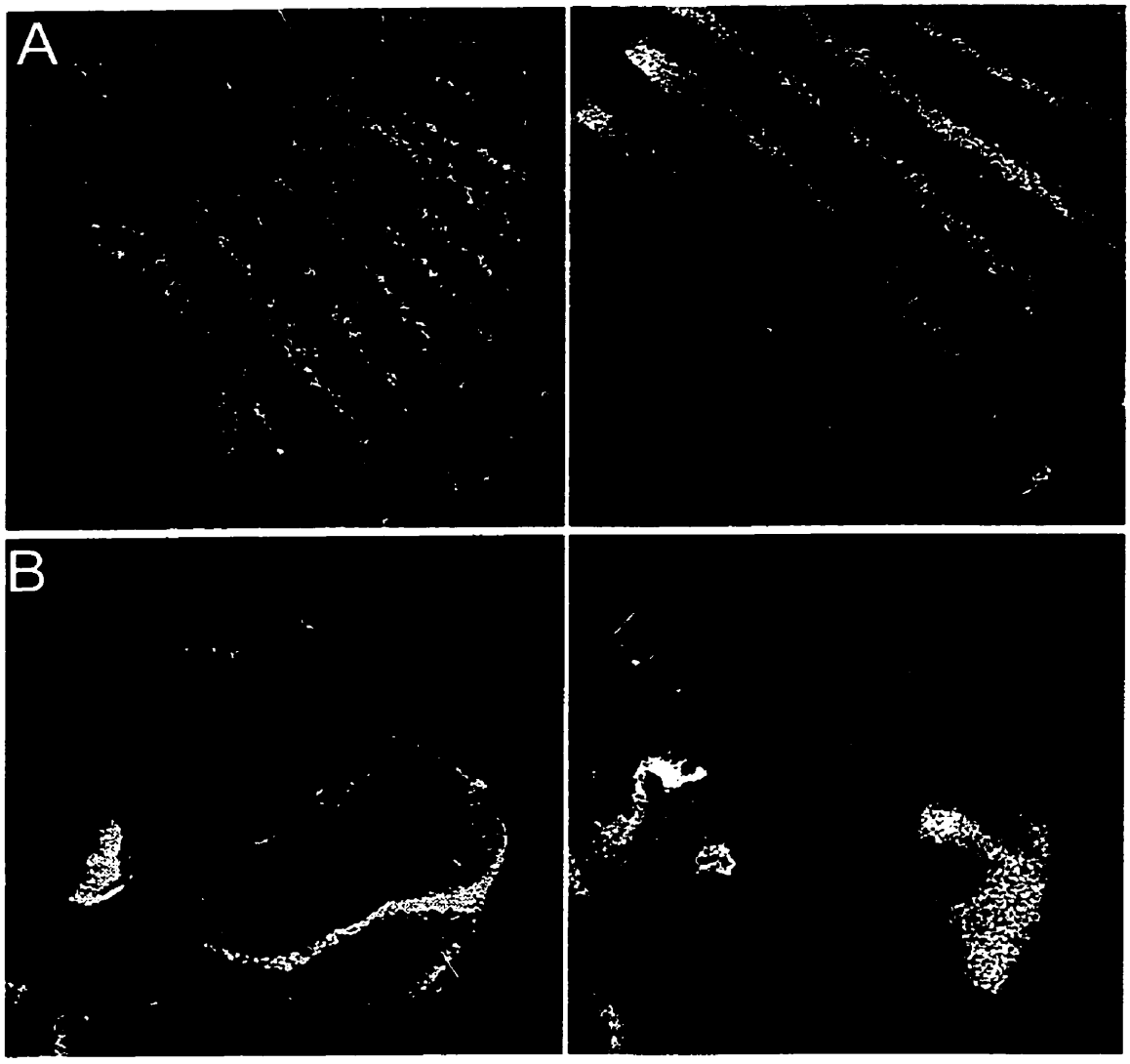
A
B

4. Notes

1. Template DNA should be chosen and linearized such that run-off transcripts correspond to unique portions of the gene's coding region. So far, we've found that run-off transcripts ranging from about 0.4 to 1kb work well as probes. Cutting to completion generally takes 2-4hr, and should be confirmed by agarose gel electrophoresis.
2. Removal of template with DNaseI subsequent to the transcription reaction was found to be unnecessary. Precipitation of the probe with LiCl removes most unincorporated nucleotides.
3. Previous protocols (e.g. (Lehmann and Tautz, 1994)) used carbonate degradation to reduce the size of probe RNA. In our hands this was found to be unnecessary and in fact was usually detrimental.
4. Freshly prepared formaldehyde appears to be required with the high temperatures used for RNA hybridization. Commercially prepared formaldehyde solutions, even ultrapure, generally yield ruptured embryos.
5. Vessel sizes used here are optimized for small collections (<250 µl settled embryos). For greater collection sizes, larger vessels should be used, keeping approximately to the same relative ratios. 50 ml Falcon tubes work well for fixing and devitillinizing settled embryo volumes from ~ 0.25 to 2 ml. Care should be used as some tubes or plastics appear to interfere with fixation and devitillinazation (e.g., Sarstedt polystyrene tubes).

6. Aqueous solution interferes with the efficiency of the subsequent devitillinzation step. This has likely occurred if the devitillinization solution is cloudy and less than 80% of embryos have moved from the interphase to the bottom of the tube. Care should be taken to minimize uptake of the lower aqueous phase when drawing up embryos from the fixative into the pipette tip. Quite often, if this occurs, the phases will separate in the tip, and the lower aqueous phase can be returned to the scintillation vial. If transfer of aqueous solution has already occurred, the devitillinaztion step can be repeated as necessary by removing as much heptane and methanol as possible, replacing with fresh heptane and methanol and shaking again.

7. The extent of proteinase K digestion is a very important consideration. In general, proteinase K digestion enhances probe accessibility and hence the strength of the signal. However, over-digestion results in poor embryo morphology and ruptured embryos. Also, when double-labeling for proteins, proteinase K digestion can destroy the epitope. This can be remedied by lowering the working concentration of proteinase K as required. In fact, some in situ probes work very well with little or no proteinase K digestion. Newly prepared proteinase K stock solutions should be tested at several dilutions and/or digestion times. Prepare a 20 mg/ml stock of proteinase K by dissolving in sterile water and storing at -20°C in 20- 50 µl aliquots. Repeated freeze-thaws appear to increase the activity of the enzyme.

8. The antibodies used here come lyophilized. For uniformity and convenience, we resuspend the powders in 50% glycerol and then aliquot and store at -70°C. One of the aliquots can be kept at -20°C for convenience (does not freeze and is relatively stable).

9. Antibodies described here have been chosen with usefulness in double-labeling in mind. The primary antibodies are whole IgGs raised in different hosts. Similarly, secondary antibodies are selected so that they are unlikely to cross react with the second primary antibody or with each other. Jackson laboratories, from which the recommended secondary antibodies were obtained, provide information, suggestions and many products that make choosing and obtaining the appropriate antibodies relatively easy. Secondary antibodies most suitable for multiple-labeling are designated "ML". These are generally comprised of the $F(ab')_2$ portion of IgG antibodies that recognize both heavy and light (H and L) chains of their target antibodies. ML antibodies are also preabsorbed against multiple host sera. For this reason, and because the antibodies contain light sensitive molecules, we do not bother to preabsorb them against embryos. However, if background is obtained, this may help. Cyanine-conjugated secondaries were chosen because of their strong emission spectra and resistance to photo-bleaching. That latter is particularly important with the high energy lasers used for LSCM.

References:

Abrams, J. M., White, K., Fessler, L. I. and Steller, H. (1993). Programmed cell death during Drosophila embryogenesis. *Development* 117, 29-43.

Adams, M. D. Celniker, S. E. Holt, R. A. Evans, C. A. Gocayne, J. D. Amanatides, P. G. Scherer, S. E. Li, P. W. Hoskins, R. A. Galle, R. F. et al. (2000). The genome sequence of Drosophila melanogaster. *Science* 287, 2185-2195.

Akam, M. (1987). The molecular basis for metameric pattern in the Drosophila embryo. *Development* 1, 1-22.

Alexandre, C., Lecourtois, M. and Vincent, J. (1999). Wingless and Hedgehog pattern Drosophila denticle belts by regulating the production of short-range signals. *Development* 126, 5689-5698.

Baker, N. E. (1987). Molecular cloning of sequences from *wingless*, a segment polarity gene in *Drosophila*: The spatial distribution of a transcript in embryos. *EMBO* 6, 1765-1773.

Baker, N. E. (1988). Embryonic and imaginal requirements for wingless, a segment-polarity gene in Drosophila. *Dev Biol* 125, 96-108.

Bangs, P. and White, K. (2000). Regulation and execution of apoptosis during Drosophila development [In Process Citation]. *Dev Dyn* 218, 68-79.

Bashirullah, A., Cooperstock, R. L. and Lipshitz, H. D. (1998). RNA localization in development. *Annu Rev Biochem* 67, 335-394.

Baumgartner, S. and Noll, M. (1990). Network of interactions among pair-rule genes regulating paired expression during primordial segmentation of Drosophila. *Mech Dev* 33, 1-18.

Bejsovec, A. and Martinez Arias, A. (1991). Roles of wingless in patterning the larval epidermis of Drosophila. *Development* 2, 471-485.

Bejsovec, A. and Wieschaus, E. (1993). Segment polarity gene interactions modulate epidermal patterning in Drosophila embryos. *Development* 2, 501-517.

Berleth, T., Burri, M., Thoma, G., Bopp, D., Richstein, S., Frigerio, G., Noll, M. and Nusslein-Volhard, C. (1988). The role of localization of bicoid RNA in organizing the anterior pattern of the Drosophila embryo. *Embo J* 7, 1749-1756.

Binari, R. and Perrimon, N. (1994). Stripe-specific regulation of pair-rule genes by hopscotch, a putative Jak family tyrosine kinase in Drosophila. *Genes Dev* 8, 300-312.

Blair, S. S. (1995). Compartments and appendage development in Drosophila. *Bioessays* 4, 299-309.

Bohn, H. (1974). Extent and properties of the regeneration field in the larval legs of cockroaches (leucophea maderae). III. Origin of the tissues and determination of symmetry properties in the regernates. *J. Embryol. Exp. Morph.* 32, 81-98.

Brand, A. H. and Dormand, E. L. (1995). The GAL4 system as a tool for unravelling the mysteries of the Drosophila nervous system. *Current Opinion in Neurobiology* 5, 572-578.

Bryant, P. J. (1975). Pattern formation in the imaginal wing disc of Drosophila melanogaster: fate map, regeneration and duplication. *J Exp Zool* 193, 49-77.

Busturia, A. and Lawrence, P. A. (1994). Regulation of cell number in Drosophila. *Nature* 370, 561-563.

Busturia, A. and Morata, G. (1988). Ectopic expression of homeotic genes caused by the elimination of the Polycomb gene in Drosophila imaginal epidermis. *Development* 4, 713-720.

Cabrera, C. V., Alonso, M. C., Johnston, P., Phillips, R. G. and Lawrence, P. A. (1987). Phenocopies induced with antisense RNA identify the wingless gene. *Cell* 50, 659-663.

Cadigan, K. M., Grossniklaus, U. and Gehring, W. J. (1994). Localized expression of sloppy paired protein maintains the polarity of Drosophila parasegments. *Genes Dev* 8, 899-913.

Campos-Ortega, J. A. and Hartenstein, V. (1985). The embryonic development of *Drosophila melanogaster*. Berlin: Springer-Verlag.

Carroll, S. B., DiNardo, S., PH, O. F., White, R. A. and Scott, M. P. (1988a). Temporal and spatial relationships between segmentation and homeotic gene expression in Drosophila embryos: distributions of the fushi tarazu, engrailed, Sex combs reduced, Antennapedia, and Ultrabithorax proteins. *Genes & Development* 3, 350-360.

Carroll, S. B., Laughon, A. and Thalley, B. S. (1988b). Expression, function, and regulation of the hairy segmentation protein in the Drosophila embryo. *Genes & Development* 7, 883-890.

Carroll, S. B. and Scott, M. P. (1985). Localization of the fushi tarazu protein during Drosophila embryogenesis. *Cell* 1, 47-57.

Carroll, S. B. and Scott, M. P. (1986). Zygotically active genes that affect the spatial expression of the fushi tarazu segmentation gene during early Drosophila embryogenesis. *Cell* 45, 113-126.

Carroll, S. B. and Vavra, S. H. (1989). The zygotic control of Drosophila pair-rule gene expression. *Development* 3, 673-683.

Cohen, S. M. and Jurgens, G. (1990). Mediation of Drosophila head development by gap-like segmentation genes [see comments]. *Nature* 346, 482-485.

Cooperstock, R. L. and Lipshitz, H. D. (1997). Control of mRNA stability and translation during Drosophila development. *Semin Cell Dev Biol* 8, 541-549.

Copeland, J. W., Nasiadka, A., Dietrich, B. H. and Krause, H. M. (1996). Patterning of the Drosophila embryo by a homeodomain-deleted Ftz polypeptide. *Nature* 6561, 162-165.

Cox, R. T., Kirkpatrick, C. and Peifer, M. (1996). Armadillo is required for adherens junction assembly, cell polarity, and morphogenesis during Drosophila embryogenesis. *J Cell Biol* 134, 133-148.

Crick, F. H. and Lawrence, P. A. (1975). Compartments and polyclones in insect development. *Science* 189, 340-347.

Dahmann, C. and Basler, K. (1999). Compartment boundaries: at the edge of development [In Process Citation]. *Trends Genet* 15, 320-326.

Dearolf, C. R., Topol, J. and Parker, C. S. (1989a). The caudal gene product is a direct activator of fushi tarazu transcription during Drosophila embryogenesis. *Nature* 6240, 340-343.

Dearolf, C. R., Topol, J. and Parker, C. S. (1989b). Transcriptional control of Drosophila fushi tarazu zebra stripe expression. *Genes & Development* 3, 384-398.

Desplan, C., Theis, J. and P., O'Farrell. (1988). The sequence specificity of homeodomain-DNA interaction. *Cell* 7, 1081-1090.

DiNardo, S., Kuner, J. M., Theis, J. and O'Farrell, P. H. (1985). Development of embryonic pattern in D. melanogaster as revealed by accumulation of the nuclear engrailed protein. *Cell* 43, 59-69.

DiNardo, S. and O'Farrell, P. H. (1987). Establishment and refinement of segmental pattern in the Drosophila embryo: spatial control of engrailed expression by pair-rule genes. *Genes Dev* 1, 1212-1225.

DiNardo, S., Sher, E., Heemskerk-Jongens, J., Kassis, J. A. and PH, O. F. (1988). Two-tiered regulation of spatially patterned engrailed gene expression during Drosophila embryogenesis. *Nature* 6165, 604-609.

Doe, C. Q., Smouse, D. and Goodman, C. S. (1988). Control of neuronal fate by the Drosophila segmentation gene even-skipped. *Nature* 6171, 376-378.

Dougan, S. and DiNardo, S. (1992). Drosophila wingless generates cell type diversity among engrailed expressing cells. *Nature* 6402, 347-350.

Driever, W. and Nusslein-Volhard, C. (1988a). The bicoid protein determines position in the Drosophila embryo in a concentration-dependent manner. *Cell* 54, 95-104.

Driever, W. and Nusslein-Volhard, C. (1988b). A gradient of bicoid protein in Drosophila embryos. *Cell* 54, 83-93.

Dubnau, J. and Struhl, G. (1996). RNA recognition and translational regulation by a homeodomain protein [see comments] [published erratum appears in Nature 1997 Aug 14;388(6643):697]. *Nature* 379, 694-699.

Duncan, I. (1986). Control of bithorax complex functions by the segmentation gene fushi tarazu of D. melanogaster. *Cell* 47, 297-309.

Duncan, I. (1996). How do single homeotic genes control multiple segment identities? *Bioessays* 18, 91-94.

Edgar, B. A., Kiehle, C. P. and Schubiger, G. (1986a). Cell cycle control by the nucleo-cytoplasmic ratio in early Drosophila development. *Cell* 44, 365-372.

Edgar, B. A., Odell, G. M. and Schubiger, G. (1987). Cytoarchitecture and the patterning of fushi tarazu expression in the Drosophila blastoderm. *Genes Dev* 1, 1226-1237.

Edgar, B. A. and P., O'Farrell. (1989). Genetic control of cell division patterns in the Drosophila embryo. *Cell* 1, 177-187.

Edgar, B. A., Weir, M. P., Schubiger, G. and Kornberg, T. (1986b). Repression and turnover pattern fushi tarazu RNA in the early Drosophila embryo. *Cell* 47, 747-754.

Eldon, E. D. and Pirrotta, V. (1991). Interactions of the Drosophila gap gene *giant* with maternal and zygotic pattern-forming genes. *Development* 111, 367-378.

Fitzpatrick, V. D., Percival-Smith, A., Ingles, C. J. and Krause, H. M. (1992). Homeodomain-independent activity of the fushi tarazu polypeptide in Drosophila embryos. *Nature* 6370, 610-612.

Fjose, A., McGinnis, W. J. and Gehring, W. J. (1985). Isolation of a homoeo box-containing gene from the engrailed region of Drosophila and the spatial distribution of its transcripts. *Nature* 313, 284-289.

Florence, B., Guichet, A., Ephrussi, A. and Laughon, A. (1997). Ftz-F1 is a cofactor in Ftz activation of the Drosophila engrailed gene. *Development* 4, 839-847.

Foe, V. E. and Alberts, B. M. (1983). Studies of nuclear and cytoplasmic behaviour during the five mitotic cycles that precede gastrulation in Drosophila embryogenesis. *J Cell Sci* 61, 31-70.

Frank, L. H. and Rushlow, C. (1996). A group of genes required for maintenance of the amnioserosa tissue in Drosophila. *Development* 122, 1343-1352.

Frasch, M. and Levine, M. (1987). Complementary patterns of even-skipped and fushi tarazu expression involve their differential regulation by a common set of segmentation genes in Drosophila. *Genes & Development* 9, 981-995.

Frasch, M., Warrior, R., Tugwood, J. and Levine, M. (1988). Molecular analysis of even-skipped mutants in Drosophila development. *Genes & Development* 12B, 1824-1838.

Frigerio, G., Burri, M., Bopp, D., Baumgartner, S. and Noll, M. (1986). Structure of the segmentation gene paired and the Drosophila PRD gene set as part of a gene network. *Cell* 47, 735-746.

Frohnhofer, H. G. and Nusslein-Volhard, C. (1986). Organization of the anterior pattern in the *Drosophila* embryo by the maternal gene *bicoid*. *Nature* 324, 120-125.

Fujioka, M., Emi-Sarker, Y., Yusibova, G. L., Goto, T. and Jaynes, J. B. (1999). Analysis of an even-skipped rescue transgene reveals both composite and discrete neuronal and early blastoderm enhancers, and multi-stripe positioning by gap gene repressor gradients. *Development* 126, 2527-2538.

Fujioka, M., Jaynes, J. B. and Goto, T. (1995). Early even-skipped stripes act as morphogenetic gradients at the single cell level to establish engrailed expression. *Development* 12, 4371-4382.

Fujioka, M., Miskiewicz, P., Raj, L., Gulledge, A. A., Weir, M. and Goto, T. (1996a). Drosophila Paired regulates late even-skipped expression through a composite binding site for the paired domain and the homeodomain. *Development* 122, 2697-2707.

Fujioka, M., Yusibova, G. L., Sackerson, C. M., Tillib, S., Mazo, A., Satake, M. and Goto, T. (1996b). Runt domain partner proteins enhance DNA binding

and transcriptional repression in cultured Drosophila cells. *Genes to Cells* 8, 741-754.

Garcia-Bellido, A., Ripoll, P. and Morata, G. (1973). Developmental compartmentalisation of the wing disk of Drosophila. *Nat New Biol* 245, 251-253.

Gorfinkiel, N., Sanchez, L. and Guerrero, I. (1999). Drosophila terminalia as an appendage-like structure. *Mech Dev* 86, 113-123.

Goto, S. and Hayashi, S. (1997). Cell migration within the embryonic limb primordium of *Drosophila* as revealed by a novel fluorescence method to visualize mRNA and protein. *Dev Genes Evol* 207, 194-198.

Goto, T., Macdonald, P. and Maniatis, T. (1989). Early and late periodic patterns of even skipped expression are controlled by distinct regulatory elements that respond to different spatial cues. *Cell* 3, 413-422.

Grawe, F., Wodarz, A., Lee, B., Knust, E. and Skaer, H. (1996). The Drosophila genes crumbs and stardust are involved in the biogenesis of adherens junctions. *Development* 122, 951-959.

Gritzan, U., Hatini, V. and DiNardo, S. (1999). Mutual antagonism between signals secreted by adjacent Wingless and Engrailed cells leads to specification of complementary regions of the Drosophila parasegment. *Development* 126, 4107-4115.

Guichet, A., Copeland, J. W., Erdelyi, M., Hlousek, D., Zavorszky, P., Ho, J., Brown, S., Percival-Smith, A., Krause, H. M. and Ephrussi, A. (1997). The nuclear receptor homologue Ftz-F1 and the homeodomain protein Ftz are mutually dependent cofactors. *Nature* 6616, 548-552.

Gumbiner, B. M. (1996). Cell adhesion: the molecular basis of tissue architecture and morphogenesis. *Cell* 84, 345-357.

Guthrie, S. and Lumsden, A. (1991). Formation and regeneration of rhombomere boundaries in the developing chick hindbrain. *Development* 112, 221-229.

Hafen, E., Kuroiwa, A. and Gehring, W. J. (1984). Spatial distribution of transcripts from the segmentation gene fushi tarazu during Drosophila embryonic development. *Cell* 37, 833-841.

Halder, G., Polaczyk, P., Kraus, M. E., Hudson, A., Kim, J., Laughon, A. and Carroll, S. (1998). The Vestigial and Scalloped proteins act together to directly regulate wing-specific gene expression in Drosophila. *Genes Dev* 12, 3900-3909.

Hammerschmidt, M., Brook, A. and McMahon, A. P. (1997). The world according to hedgehog. *Trends Genet* 13, 14-21.

Han, K., Levine, M. S. and Manley, J. L. (1989). Synergistic activation and repression of transcription by Drosophila homeobox proteins. *Cell* 56, 573-583.

Harding, K., Hoey, T., Warrior, R. and Levine, M. (1989). Autoregulatory and gap gene response elements of the even-skipped promoter of Drosophila. *EMBO Journal* 4, 1205-1212.

Harding, K., Rushlow, C., Doyle, H. J., Hoey, T. and Levine, M. (1986). Cross-regulatory interactions among pair-rule genes in Drosophila. *Science* 4767, 953-959.

Harlow, E. and LAne, D. (1988). Antibodies. A Laboratory Manual: Cold Spring Harbor Laboratory.

Hartenstein, V. and Campos-Ortega, J. A. (1985). Fate-mapping in wild-type *Drosophila melanogaster. Roux's Arch Dev Biol* 194, 181-195.

Hayes, P. H., Sato, T. and Denell, R. E. (1984). Homoeosis in Drosophila: the ultrabithorax larval syndrome. *Proc Natl Acad Sci U S A* 81, 545-549.

Heemskerk, J. and DiNardo, S. (1994). Drosophila hedgehog acts as a morphogen in cellular patterning. *Cell* 76, 449-460.

Heemskerk, J., DiNardo, S., Kostriken, R. and PH, O. F. (1991). Multiple modes of engrailed regulation in the progression towards cell fate determination. *Nature* 6334, 404-410.

Hinck, L., Nelson, W. J. and Papkoff, J. (1994). Wnt-1 modulates cell-cell adhesion in mammalian cells by stabilizing beta-catenin binding to the cell adhesion protein cadherin. *Journal of Cell Biology* 5, 729-741.

Hiromi, Y. and Gehring, W. J. (1987). Regulation and function of the Drosophila segmentation gene fushi tarazu. *Cell* 50, 963-974.

Hiromi, Y., Kuroiwa, A. and Gehring, W. J. (1985). Control elements of the Drosophila segmentation gene fushi tarazu. *Cell* 43, 603-613.

Hoey, T. and Levine, M. (1988). Divergent homeo box proteins recognize similar DNA sequences in Drosophila. *Nature* 6167, 858-861.

Holland, L. Z., Kene, M., Williams, N. A. and Holland, N. D. (1997). Sequence and embryonic expression of the amphioxus engrailed gene (AmphiEn): the metameric pattern of transcription resembles that of its segment-polarity homolog in Drosophila. *Development* 9, 1723-1732.

Hooper, K. L., Parkhurst, S. M. and Ish-Horowicz, D. (1989). Spatial control of hairy protein expression during embryogenesis. *Development* 3, 489-504.

Howard, K. and Ingham, P. (1986). Regulatory interactions between the segmentation genes fushi tarazu, hairy, and engrailed in the Drosophila blastoderm. *Cell* 6, 949-957.

Howard, K. R. and Struhl, G. (1990). Decoding positional information: regulation of the pair-rule gene hairy. *Development* 110, 1223-1231.

Hughes, S. C. and Krause, H. M. (1998). Double labeling with fluorescence in situ hybridization in Drosophila whole-mount embryos. *Biotechniques* 24, 530-532.

Hughes, S. C., Saulier-Le Drean, B., Livne-Bar, I. and Krause, H. M. (1996). Fluorescence in situ hybridization in whole-mount Drosophila embryos. *Biotechniques* 20, 748-750.

Ingham, P. and Gergen, P. (1988). Interactions between the pari-rule genes *runt*, *hairy*, *even-skipped*, and *fushi-tarazu* and the establishment of periodic pattern in the *Drosophila* embryo. *Development Supplement* 104, 51-60.

Ingham, P. W. (1993). Localized hedgehog activity controls spatial limits of wingless transcription in the Drosophila embryo. *Nature* 6455, 560-562.

Ingham, P. W., Baker, N. E. and Martinez-Arias, A. (1988). Regulation of segment polarity genes in the Drosophila blastoderm by fushi tarazu and even skipped. *Nature* 331, 73-75.

Ingham, P. W., Howard, K. R. and Ish-Horowicz, D. (1985). Transcription pattern of the *Drosophila* segmentation gene *hairy*. *Nature* 318, 439-445.

Ingham, P. W. and Martinez Arias, A. (1992). Boundaries and fields in early embryos. *Cell* 68, 221-235.

Ingham, P. W. and Martinez-Arias, A. (1986). The correct activation of Antennapedia and bithorax complex genes requires the fushi tarazu gene. *Nature* 6097, 592-597.

Irish, V. F., Martinez-Arias, A. and Akam, M. (1989). Spatial regulation of the Antennapedia and Ultrabithorax homeotic genes during Drosophila early development. *Embo J* 8, 1527-1537.

Irvine, K. D. and Wieschaus, E. (1994). Cell intercalation during Drosophila germband extension and its regulation by pair-rule segmentation genes. *Development* 120, 827-841.

Ish-Horowicz, D. and Gyurkovics, H. (1988). Ectopic segmentation gene expression and metameric regulation in *Drosophila*. *Development Supplement* 104, 67-73.

Ish-Horowicz, D. and Pinchin, S. M. (1987). Pattern abnormaiities induced by ectopic expression of the Drosophila gene hairy are associated with repression of ftz transcription. *Cell* 3, 405-415.

Ish-Horowicz, D., Pinchin, S. M., Ingham, P. W. and Gyurkovics, H. G. (1989). Autocatalytic ftz activation and metameric instability induced by ectopic ftz expression. *Cell* 57, 223-232.

Jiang, J., Hoey, T. and Levine, M. (1991). Autoregulation of a segmentation gene in Drosophila: combinatorial interaction of the even-skipped homeo box protein with a distal enhancer element. *Genes & Development* 2, 265-277.

Johnson, C. A. and Turner, B. M. (1999). Histone deacetylases: complex transducers of nuclear signals. *Semin Cell Dev Biol* 10, 179-188.

Jurgens, G., Wiechaus, E., Nusslein-Volhard, C. and Kluding, H. (1984). Mutations affecting the pattern of larval cuticle in *Drosophila melanogaster* II. Zygotic loci on the third chromosome. *Roux's Arch Dev Biol* 1984, 283-295.

Kania, M. A., Bonner, A. S., Duffy, J. B. and Gergen, J. P. (1990). The Drosophila segmentation gene runt encodes a novel nuclear regulatory protein that is also expressed in the developing nervous system. *Genes & Development* 10, 1701-1713.

Karr, T. L. and Kornberg, T. B. (1989). fushi tarazu protein expression in the cellular blastoderm of Drosophila detected using a novel imaging technique. *Development* 106, 95-103.

Kellerman, K. A., Mattson, D. M. and Duncan, I. (1990). Mutations affecting the stability of the fushi tarazu protein of Drosophila. *Genes & Development* 11, 1936-1950.

Kilchherr, F., Baumgartner, S., Bopp, D., Frei, E. and Noll, M. (1986). Isolation of the *paired* gene of *Drosophila* and its spatial expression during early embryogenesis. *Nature* 321, 493-500.

Klein, R. (1999). Bidirectional signals establish boundaries. *Curr Biol* 9, R691-R694.

Klingler, M. and Gergen, J. P. (1993). Regulation of runt transcription by Drosophila segmentation genes. *Mech Dev* 43, 3-19.

Knust, E., Tepass, U. and Wodarz, A. (1993). crumbs and stardust, two genes of Drosophila required for the development of epithelial cell polarity. *Development Supplement* 261-268.

Kornberg, T., Siden, I., O'Farrell, P. and Simon, M. (1985). The engrailed locus of Drosophila: in situ localization of transcripts reveals compartment-specific expression. *Cell* 40, 45-53.

Krause, H. M., Klemenz, R. and Gehring, W. J. (1988). Expression, modification, and localization of the fushi tarazu protein in Drosophila embryos. *Genes & Development* 8, 1021-1036.

Kraut, R. and Levine, M. (1991). Spatial regulation of the gap gene *giant* during *Drosophila* development. *Development* 111, 601-609.

Laughon, A., Howell, W. and Scott, M. P. (1988). The interaction of proteins encoded by Drosophila homeotic and segmentation genes with specific DNA sequences. *Development* 104, 75-83.

Laughon, A. and Scott, M. P. (1984). Sequence of a Drosophila segmentation gene: protein structure homology with DNA-binding proteins. *Nature* 310, 25-31.

Lawrence, P. A. (1966). Development and determination of hairs and bristles in the milkweed bug, Oncopeltus fasciatus (Lygaeidae, Hemiptera). *J Cell Sci* 1, 475-498.

Lawrence, P. A. (1971). The organization of the insect segment. *Symp Soc Exp Biol* 25, 379-390.

Lawrence, P. A. (1973a). A clonal analysis of segment development in Oncopeltus (Hemiptera). *J Embryol Exp Morphol* 30, 681-699.

Lawrence, P. A. (1973b). Maintenance of boundaries between developing organs in insects. *Nat New Biol* 242, 31-32.

Lawrence, P. A. (1981). The cellular basis of segmentation in insect. *Cell* 26, 3-10.

Lawrence, P. A. (1988). The present status of the parasegment. *Development Supplement* 104, 61-65.

Lawrence, P. A. (1992). The Making of a Fly: The Genetics of Animal Design: Oxford: Blackwell Scietific Publications.

Lawrence, P. A. (1997). Developmental biology. Straight and wiggly affinities. *Nature* 389, 546-547.

Lawrence, P. A. and Green, S. M. (1975). The anatomy of a compartment border. *J. Cell Science* 65, 373-382.

Lawrence, P. A. and Johnston, P. (1989). Pattern formation in the Drosophila embryo: allocation of cells to parasegments by even-skipped and fushi tarazu. *Development* 4, 761-767.

Lawrence, P. A., Johnston, P., Macdonald, P. and Struhl, G. (1987). Borders of parasegments in Drosophila embryos are delimited by the fushi tarazu and even-skipped genes. *Nature* 328, 440-442.

Lawrence, P. A. and Morata, G. (1994). Homeobox genes: their function in Drosophila segmentation and pattern formation. *Cell* 78, 181-189.

Lawrence, P. A. and Pick, L. (1998). How does the fushi tarazu gene activate engrailed in the Drosophila embryo? *Dev Genet* 23, 28-34.

Lawrence, P. A., Sanson, B. and Vincent, J. P. (1996). Compartments, wingless and engrailed: patterning the ventral epidermis of Drosophila embryos. *Development* 122, 4095-4103.

Lawrence, P. A. and Struhl, G. (1996). Morphogens, compartments, and pattern: lessons from drosophila? *Cell* 85, 951-961.

Lee, J. J., von Kessler, D. P., Parks, S. and Beachy, P. A. (1992). Secretion and localized transcription suggest a role in positional signaling for products of the segmentation gene hedgehog. *Cell* 1, 33-50.

Lehmann, R. and Tautz, D. (1994). *In Situ* Hybridizations to RNA. New York: Academic Press.

Lewis, E. (1978). A gene complex controlling segmentation in *Drosophila*. *Nature* 276, 565-570.

Li, Q. J., Pazdera, T. M. and Minden, J. S. (1999). Drosophila embryonic pattern repair: how embryos respond to cyclin E- induced ectopic division. *Development* 126, 2299-2307.

Locke, M. (1967). The development of patterns in the integument of insects. *Adv. Morphogenesis* 6, 33-88.

Lumsden, A. (1990). The cellular basis of segmentation in the developing hindbrain. *Trends Neurosci* 13, 329-335.

Lumsden, A. (1991). Cell lineage restrictions in the chick embryo hindbrain. *Philos Trans R Soc Lond B Biol Sci* 331, 281-286.

Lumsden, A. and Guthrie, S. (1991). Alternating patterns of cell surface properties and neural crest cell migration during segmentation of the chick hindbrain. *Development* Suppl, 9-15.

Macdonald, P. M., Ingham, P. and Struhl, G. (1986). Isolation, structure, and expression of even-skipped: a second pair- rule gene of Drosophila containing a homeo box. *Cell* 47, 721-734.

Macdonald, P. M. and Struhl, G. (1986). A molecular gradient in early Drosophila embryos and its role in specifying the body pattern. *Nature* 324, 537-545.

Macdonald, P. M. and Struhl, G. (1988). cis-acting sequences responsible for anterior localization of bicoid mRNA in Drosophila embryos. *Nature* 336, 595-598.

Magrassi, L. and Lawrence, P. A. (1988). The pattern of cell death in fushi tarazu, a segmentation gene of Drosophila. *Development* 3, 447-451.

Mannervik, M. and Levine, M. (1999). The Rpd3 histone deacetylase is required for segmentation of the Drosophila embryo. *Proc Natl Acad Sci U S A* 96, 6797-6801.

Manoukian, A. S. and Krause, H. M. (1992). Concentration-dependent activities of the even-skipped protein in Drosophila embryos. *Genes & Development* 9, 1740-1751.

Manoukian, A. S. and Krause, H. M. (1993). Control of segmental asymmetry in Drosophila embryos. *Development* 118, 785-796.

Martinez Arias, A. (1989). A cellular basis for pattern formation in the insect epidermis. *Trends Genet* 5, 262-267.

Martinez Arias, A. (1993). Development and Patterning of Larval Epidermis of *Drosophila*. In *The Development of Drosophila melanogaster*, vol. Volume 1 (ed. M. Bate and A. Martinez Arias), pp. 517-608: Cold Spring Harbor Laboratory Press.

Martinez Arias, A., Baker, N. E. and Ingham, P. W. (1988). Role of segment polarity genes in the definition and maintenance of cell states in the Drosophila embryo. *Development* 1, 157-170.

Martinez-Arias, A. and Lawrence, P. A. (1985). Parasegments and compartments in the Drosophila embryo. *Nature* 313, 639-642.

McGinnis, W. and Krumlauf, R. (1992). Homeobox genes and axial patterning. *Cell* 68, 283-302.

Meinhardt, H. (1977). A model of pattern formation in insect embryogenesis. *Journal of Cell Science* 23, 177-189.

Meinhardt, H. (1983). Cell determination boundaries as organizing regions for secondary embryonic fields. *Dev Biol* 96, 375-385.

Mellitzer, G., Xu, Q. and Wilkinson, D. G. (1999). Eph receptors and ephrins restrict cell intermingling and communication. *Nature* 400, 77-81.

Miller, J. R. and McClay, D. R. (1997). Changes in the pattern of adherens junction-associated beta-catenin accompany morphogenesis in the sea urchin embryo. *Dev Biol* 192, 310-322.

Minana, F. J. and Garcia-Bellido, A. (1982). Preblastoderm mosaics of mutants of the bithorax-complex. *Wilhelm Roux's Arch. devl Biol.* 191, 331-334.

Mlodzik, M. and Gehring, W. J. (1987). Expression of the caudal gene in the germ line of Drosophila: formation of an RNA and protein gradient during early embryogenesis. *Cell* 48, 465-478.

Morata, G. (1993). Homeotic genes of Drosophila. *Curr Opin Genet Dev* 3, 606-614.

Morata, G. and Kerridge, S. (1981). Sequential functions of the bithorax complex of Drosophila. *Nature* 290, 778-781.

Morata, G. and Lawrence, P. A. (1975). Control of compartment development by the engrailed gene in Drosophila. *Nature* 5510, 614-617.

Morata, G. and Lawrence, P. A. (1977). Homoeotic genes, compartments and cell determination in Drosophila. *Nature* 265, 211-216.

Morata, G. and Ripoll, P. (1975). Minutes: mutants of drosophila autonomously affecting cell division rate. *Developmental Biology* 2, 211-221.

Morrissey, D., Askew, D., Raj, L. and Weir, M. (1991). Functional dissection of the paired segmentation gene in Drosophila embryos. *Genes & Development* 9, 1684-1696.

Mullen, J. R. and DiNardo, S. (1995). Establishing parasegments in Drosophila embryos: roles of the odd-skipped and naked genes. *Developmental Biology* 1, 295-308.

Muller, H. A. and Wieschaus, E. (1996). armadillo, bazooka, and stardust are critical for early stages in formation of the zonula adherens and maintenance of the polarized blastoderm epithelium in Drosophila. *J Cell Biol* 134, 149-163.

Muller, J. and Bienz, M. (1992). Sharp anterior boundary of homeotic gene expression conferred by the fushi tarazu protein. *EMBO Journal* 10, 3653-3661.

Muller, M., v. Weizsacker, E. and Campos-Ortega, J. A. (1996). Expression domains of a zebrafish homologue of the Drosophila pair-rule gene hairy correspond to primordia of alternating somites. *Development* 122, 2071-2078.

Namba, R., Pazdera, T. M., Cerrone, R. L. and Minden, J. S. (1997). Drosophila embryonic pattern repair: how embryos respond to bicoid dosage alteration. *Development* 124, 1393-1403.

Nasiadka, A. and Krause, H. M. (1999). Kinetic analysis of segmentation gene interactions in drosophila embryos [In Process Citation]. *Development* 126, 1515-1526.

Noordermeer, J., Johnston, P., Rijsewijk, F., Nusse, R. and Lawrence, P. A. (1992). The consequences of ubiquitous expression of the wingless gene in the Drosophila embryo. *Development* 116, 711-719.

Nusslein-Volhard, C., Frohnhofer, H. G. and Lehmann, R. (1987). Determination of anteroposterior polarity in Drosophila. *Science* 238, 1675-1681.

Nusslein-Volhard, C., Kluding, H. and Jurgens, G. (1985). Genes affecting the segmental subdivision of the Drosophila embryo. *Cold Spring Harb Symp Quant Biol* 50, 145-154.

Nusslein-Volhard, C., Wiechaus, E. and Kluding, H. (1984). Mutations affecting the pattern of the larval cuticle in *Drosophila melanogaster*

I. Zygotic loci on the second chromosome. *Roux's Arch Dev Biol* 193, 267-282.

Nusslein-Volhard, C. and Wieschaus, E. (1980). Mutations affecting segment number and polarity in Drosophila. *Nature* 287, 795-801.

Oda, H., Tsukita, S. and Takeichi, M. (1998). Dynamic behavior of the cadherin-based cell-cell adhesion system during drosophila gastrulation [In Process Citation]. *Dev Biol* 203, 435-450.

Oda, H., Uemura, T., Harada, Y., Iwai, Y. and Takeichi, M. (1994). A Drosophila homolog of cadherin associated with armadillo and essential for embryonic cell-cell adhesion. *Dev Biol* 165, 716-726.

Oda, H., Uemura, T., Shiomi, K., Nagafuchi, A., Tsukita, S. and Takeichi, M. (1993). Identification of a Drosophila homologue of alpha-catenin and its association with the armadillo protein. *J Cell Biol* 121, 1133-1140.

Oda, H., Uemura, T. and Takeichi, M. (1997). Phenotypic analysis of null mutants for DE-cadherin and Armadillo in Drosophila ovaries reveals distinct aspects of their functions in cell adhesion and cytoskeletal organization. *Genes Cells* 2, 29-40.

Paddock, S. W., Langeland, J. A., DeVries, P. J. and Carroll, S. B. (1993). Three-color immunofluorescence imaging of Drosophila embryos by laser scanning confocal microscopy. *Biotechniques* 14, 42-48.

Palmeirim, I., Henrique, D., Ish-Horowicz, D. and Pourquie, O. (1997). Avian hairy gene expression identifies a molecular clock linked to vertebrate segmentation and somitogenesis. *Cell* 91, 639-648.

Pankratz, M. J. and Jackle, H. (1990). Making stripes in the Drosophila embryo. *Trends Genet* 6, 287-292.

Parkhurst, S. M. and Ish-Horowicz, D. (1991). Mis-regulating segmentation gene expression in Drosophila. *Development* 4, 1121-1135.

Patel, N. H., Kornberg, T. B. and Goodman, C. S. (1989). Expression of engrailed during segmentation in grasshopper and crayfish. *Development* 107, 201-212.

Pazdera, T. M., Janardhan, P. and Minden, J. S. (1998). Patterned epidermal cell death in wild-type and segment polarity mutant Drosophila embryos. *Development* 125, 3427-3436.

Peifer, M. and Bejsovec, A. (1992). Knowing your neighbors: Cell interactions determine intrasegmental patterning in *Drosophila*. *Trends in Genetics* 8, 243-249.

Peifer, M., Orsulic, S., Sweeton, D. and Wieschaus, E. (1993). A role for the Drosophila segment polarity gene armadillo in cell adhesion and cytoskeletal integrity during oogenesis. *Development* 118, 1191-1207.

Peifer, M., Sweeton, D., Casey, M. and Wieschaus, E. (1994). wingless signal and Zeste-white 3 kinase trigger opposing changes in the intracellular distribution of armadillo. *Development* 2, 369-380.

Peifer, M. and Wieschaus, E. (1993). The product of the Drosophila melanogaster segment polarity gene armadillo is highly conserved in sequence and expression in the housefly Musca domestica. *J Mol Evol* 36, 224-233.

Pick, L., Schier, A., Affolter, M., Schmidt-Glenewinkel, T. and Gehring, W. J. (1990). Analysis of the ftz upstream element: germ layer-specific enhancers are independently autoregulated. *Genes Dev* 4, 1224-1239.

Poole, S. J. and Kornberg, T. B. (1988). Modifying expression of the engrailed gene of Drosophila melanogaster. *Development* 104, 85-93.

Riedl, A. and Jacobs-Lorena, M. (1996). Determinants of Drosophila fushi tarazu mRNA instability. *Molecular & Cellular Biology* 6, 3047-3053.

Rijsewijk, F., Schuermann, M., Wagenaar, E., Parren, P., Weigel, D. and Nusse, R. (1987). The Drosophila homolog of the mouse mammary oncogene int-1 is identical to the segment polarity gene wingless. *Cell* 50, 649-657.

Roberts, D. B. (1986). Dosophila: a practical approach: Oxford: IRL Press.

Saulier-Le Drean, B., Nasiadka, A., Dong, J. and Krause, H. M. (1998). Dynamic changes in the functions of Odd-skipped during early *Drosophila* embryogenensis. *Development* 125, 4851-4861.

Schier, A. F. and Gehring, W. J. (1992). Direct homeodomain-DNA interaction in the autoregulation of the fushi tarazu gene. *Nature* 6372, 804-807.

Schier, A. F. and Gehring, W. J. (1993). Functional specificity of the homeodomain protein fushi tarazu: the role of DNA-binding specificity in vivo. *Proceedings of the National Academy of Sciences of the United States of America* 4, 1450-1454.

Schupbach, T. and Wiechaus, E. (1986). Maternal-effect mutations altering the anterior-posterior pattern of the *Drosophila* embryo. *Roux's Arch Dev Biol* 195, 302-317.

Scott, M. P. and O'Farrell, P. H. (1986). Spatial programming of gene expression in early Drosophila embryogenesis. *Annu Rev Cell Biol* 2, 49-80.

Shermoen, A. W. and O'Farrell, P. H. (1991). Progression of the cell cycle through mitosis leads to abortion of nascent transcripts. *Cell* 67, 303-310.

Shibata, T. and Bryant, P. J. (1998). Identification of Drosophila eph-type tyrosine kinase and its function in imaginal disc development. In *A. Dros. Rs. Conf. 39 162C*, (Washington, D.C).

Siegfried, E., Wilder, E. L. and Perrimon, N. (1994). Components of wingless signalling in Drosophila. *Nature* 6458, 76-80.

Simmonds, A. J., Liu, X., Soanes, K. H., Krause, H. M., Irvine, K. D. and Bell, J. B. (1998). Molecular interactions between Vestigial and Scalloped promote wing formation in Drosophila. *Genes Dev* 12, 3815-3820.

Simon, J. (1995). Locking in stable states of gene expression: transcriptional control during Drosophila development. *Curr Opin Cell Biol* 7, 376-385.

Simpson, P. and Morata, G. (1981). Differential mitotic rates and patterns of growth in compartments in the Drosophila wing. *Developmental Biology* 2, 299-308.

Small, S., Blair, A. and Levine, M. (1992). Regulation of even-skipped stripe 2 in the Drosophila embryo. *EMBO Journal* 11, 4047-4057.

Small, S., Blair, A. and Levine, M. (1996). Regulation of two pair-rule stripes by a single enhancer in the Drosophila embryo. *Dev Biol* 175, 314-324.

Small, S., Kraut, R., Hoey, T., Warrior, R. and Levine, M. (1991). Transcriptional regulation of a pair-rule stripe in Drosophila. *Genes & Development* 5, 827-839.

St Johnston, D. and Nusslein-Volhard, C. (1992). The origin of pattern and polarity in the Drosophila embryo. *Cell* 68, 201-219.

Stanojevic, D., Hoey, T. and Levine, M. (1989). Sequence-specific DNA-binding activities of the gap proteins encoded by hunchback and Kruppel in Drosophila. *Nature* 6240, 331-335.

Struhl, G. (1982). Genes controlling segmental specification in the Drosophila thorax. *Proc Natl Acad Sci U S A* 79, 7380-7384.

Struhl, G. (1984). Spitting the bithorax complex of *Drosophila*. *Nature* 308, 454-457.

Struhl, G. (1985). Near-reciprocal phenotypes caused by inactivation or indiscriminate expression of the Drosophila segmentation gene ftz. *Nature* 318, 677-680.

Struhl, G. (1989). Differing strategies for organizing anterior and posterior body pattern in Drosophila embryos. *Nature* 338, 741-744.

Struhl, G. and Basler, K. (1993). Organizing activity of wingless protein in Drosophila. *Cell* 72, 527-540.

Stumpf, H. (1966). Mechanisms by which cells estimate their location within the body. *Nature* 212, 430-431.

Takeichi, M. (1991). Cadherin cell adhesion receptors as a morphogenetic regulator. *Science* 251, 1451-1455.

Takke, C. and Campos-Ortega, J. A. (1999). her1, a zebrafish pair-rule like gene, acts downstream of notch signalling to control somite development. *Development* 126, 3005-3014.

Tautz, D. and Pfeifle, C. (1989). A non-radioactive in situ hybridization method for the localization of specific RNAs in Drosophila embryos reveals translational control of the segmentation gene hunchback. *Chromosoma* 98, 81-85.

Tepass, U., Gruszynski-DeFeo, E., Haag, T. A., Omatyar, L., Torok, T. and Hartenstein, V. (1996). shotgun encodes Drosophila E-cadherin and is preferentially required during cell rearrangement in the neurectoderm and other morphogenetically active epithelia. *Genes Dev* 10, 672-685.

Tepass, U., Theres, C. and Knust, E. (1990). crumbs encodes an Egf-like protein expressed on apical membranes of Drosophila epithelial cells and required for organization of epithelia. *Cell* 5, 787-799.

Tremml, G. and Bienz, M. (1989). An essential role of even-skipped for homeotic gene expression in the Drosophila visceral mesoderm. *EMBO Journal* 9, 2687-2693.

Tsai, C. and Gergen, P. (1995). Pair-rule expression of the Drosophila fushi tarazu gene: a nuclear receptor response element mediates the opposing regulatory effects of runt and hairy. *Development* 2, 453-462.

Turner, F. R. and Mahowald, A. P. (1976). Scanning electron microscopy of *Drosophila* embryogenesis. I. The structure of the egg envelopes and the formation of the cellular blastoderm. *Developmental Biology* 50, 95-108.

Turner, F. R. and Mahowald, A. P. (1977). Scanning electron microscopy of Drosophila melanogaster embryogenesis. II. Gastrulation and segmentation. *Dev Biol* 57, 403-416.

van Leeuwen, F., Samos, C. H. and Nusse, R. (1994). Biological activity of soluble wingless protein in cultured Drosophila imaginal disc cells. *Nature* 6469, 342-344.

Vincent, J. P. and O'Farrell, P. H. (1992). The state of engrailed expression is not clonally transmitted during early Drosophila development. *Cell* 68, 923-931.

Wakimoto, B. T. and Kaufman, T. C. (1981). Analysis of larval segmentation in lethal genotypes associated with the antennapedia gene complex in Drosophila melanogaster. *Dev Biol* 81, 51-64.

Wakimoto, B. T., Turner, F. R. and Kaufman, T. C. (1984). Defects in embryogenesis in mutants associated with the antennapedia gene complex of Drosophila melanogaster. *Dev Biol* 102, 147-172.

Warrior, R. and Levine, M. (1990). Dose-dependent regulation of pair-rule stripes by gap proteins and the initiation of segment polarity. *Development* 3, 759-767.

Weiner, A. J., Scott, M. P. and Kaufman, T. C. (1984). A molecular analysis of fushi tarazu, a gene in Drosophila melanogaster that encodes a product affecting embryonic segment number and cell fate. *Cell* 37, 843-851.

White, R. A. and Lehmann, R. (1986). A gap gene, hunchback, regulates the spatial expression of Ultrabithorax. *Cell* 47, 311-321.

Wiechaus, E., Nusslein-Volhard, C. and Jurgens, G. (1984). Mutations affecting the pattern of larval cuticle in *Drosophila melanogaster* III. Zygotic loci on the X-chromosome and fourth chromosome. *Roux's Arch Dev Biol* 193, 296-307.

Wilkins, A. S. and Gubb, D. (1991). Pattern formation in the embryo and imaginal discs of Drosophila: what are the links? *Developmental Biology* 1, 1-12.

Wolpert, L. (1969). Positional information and the spatial pattern of cellular differentiation. *J Theor Biol* 25, 1-47.

Wolpert, L. (1989). Positional information revisited. *Development* 107, 3-12.

Wolpert, L. (1996). One hundred years of positional information. *Trends Genet* 12, 359-364.

Wright, D. A. and Lawrence, P. A. (1981a). Regeneration of segment boundaries in oncopeltus: cell lineage. *Dev Biol* 85, 328-333.

Wright, D. A. and Lawrence, P. A. (1981b). Regeneration of the segment boundary in Oncopeltus. *Dev Biol* 85, 317-327.

Wu, X., Vakani, R. and Small, S. (1998). Two distinct mechanisms for differential positioning of gene expression borders involving the Drosophila gap protein giant. *Development* 125, 3765-3774.

Xu, Q., Mellitzer, G., Robinson, V. and Wilkinson, D. G. (1999). In vivo cell sorting in complementary segmental domains mediated by Eph receptors and ephrins. *Nature* 399, 267-271.

Yan, R., Small, S., Desplan, C., Dearolf, C. R. and Darnell, J. E., Jr. (1996). Identification of a Stat gene that functions in Drosophila development. *Cell* 3, 421-430.

Yasuda, G. K., Baker, J. and Schubiger, G. (1991). Temporal regulation of gene expression in the blastoderm Drosophila embryo. *Genes Dev* 5, 1800-1812.

Yip, M. L., Lamka, M. L. and Lipshitz, H. D. (1997). Control of germ-band retraction in Drosophila by the zinc-finger protein HINDSIGHT. *Development* 124, 2129-2141.

Yu, Y., Li, W., Su, K., Yussa, M., Han, W., Perrimon, N. and Pick, L. (1997). The nuclear hormone receptor Ftz-F1 is a cofactor for the Drosophila homeodomain protein Ftz. *Nature* 6616, 552-555.

Yu, Y. and Pick, L. (1995). Non-periodic cues generate seven ftz stripes in the Drosophila embryo. *Mech Dev* 50, 163-175.

Zecca, M., Basler, K. and Struhl, G. (1996). Direct and long-range action of a wingless morphogen gradient. *Cell* 87, 833-844.

Zisch, A. H., Stallcup, W. B., Chong, L. D., Dahlin-Huppe, K., Voshol, J., Schachner, M. and Pasquale, E. B. (1997). Tyrosine phosphorylation of L1 family adhesion molecules: implication of the Eph kinase Cek5. *J Neurosci Res* 47, 655-665.